The *FYN-TRAF3IP2* gene fusion drives oncogenic NF-κB signaling in peripheral T cell lymphoma

Christine S. Kim

Submitted in partial fulfillment of the
requirements for the degree of
Doctor of Philosophy
under the Executive Committee
of the Graduate School of Arts and Sciences

COLUMBIA UNIVERSITY

2020

ABSTRACT

The *FYN-TRAF3IP2* gene fusion drives

oncogenic NF-κB signaling in peripheral T cell lymphoma

Christine S. Kim

Angioimmunoblastic T cell lymphoma (AITL) and peripheral T cell lymphoma not-otherwise-specified (PTCL, NOS) have poor prognosis and lack actionable targets for directed therapies in most cases. Here we report the identification of *FYN-TRAF3IP2* as a novel highly recurrent oncogenic gene fusion in AITL and PTCL, NOS tumors. Mechanistically, FYN-TRAF3IP2 triggers aberrant NF-κB activity by engaging TRAF6 downstream of T cell receptor signaling. Moreover, *FYN-TRAF3IP2* expression in hematopoietic progenitors induces NF-κB-driven T cell transformation in mice and cooperates with loss of the Tet2 tumor suppressor in PTCL development. Therapeutically, abrogation of NF-κB signaling in *FYN-TRAF3IP2*-induced tumors via IκB kinase inhibitors delivers strong anti-lymphoma effects *in vitro* and *in vivo*. These results formally demonstrate an oncogenic role for *FYN-TRAF3IP2* and NF-κB signaling in the pathogenesis of PTCL.

Table of Contents

List of Figures

List of Tables

Acknowledgements

The past four years have been truly special in many ways. I would not have been where I am today without the support and guidance of so many people.

First and foremost, I have been extremely fortunate to have Dr. Adolfo Ferrando as my thesis advisor and a mentor. Thank you for providing a wonderful learning environment, thank you for your dedicated mentorship and undying enthusiasm for science, thank you for pushing me to think bigger and be bolder, and above all, thank you for believing in me even when I had self-doubts.

I am incredibly grateful to Dr. Teresa Palomero for her thoughtful guidance and encouragement when I needed them the most. Thank you for your invaluable insights as I navigated the world of peripheral T cell lymphoma and the path to become a better scientist, as well as in wedding planning, marriage, and motherhood.

Thank you to my thesis committee Dr. Laura Pasqualucci, Dr. Shan Zha, and Dr. Swarnali Acharyya for their continued support and inputs over the years as well as Dr. Riccardo Dalla-Favera for participating in my thesis defense.

I have to thank the members of the Ferrando lab, both past and present. I cannot imagine a better group of people to learn from and work with. My graduate work would not have been possible without their expertise, collegiality and patience. Thank you so much for your technical support, scientific discussions, and most importantly, kind friendship. You made lab life enjoyable with silly jokes, passionate (but sometimes very weird) takes on food, and late-night laughs.

Thank you to MD/PhD and CMBS program leadership for their commitment to students. I sincerely appreciate all the opportunities provided through this program. I'd be remiss if I did not thank the enormous amount of administrative support, in particular Zaia Sivo, Jeffrey Brandt, Kate Matthews, and Becky Spurr.

Lastly, I would never have achieved any of this without the love and support from my family and friends. I especially would like to thank the incredible group of women who have shaped me over the past thirty years. Thank you, Mom, for your dedication and strength. I love you and I am so proud to be your daughter. Thank you, Grandmother, for raising me with all the care and kindness in the world. Spending winter nights watching TV with you on the 'ondol (heated stone)' floor is one of my dearest childhood memories. I wish I could see you more often. To my little sister, Nakyung, thank you for being the best sister anyone can ever ask for. I am blessed to have someone who understands me so well. And Parker. Every day, you make me a better version of myself.
Thank you, friends. There are too many of you to name individually, but I don't know what I have done to be so lucky to have you all in my life. And thank you James, my best friend, for your endless patience and support. Marrying you was one of the best decisions I have made in my life.

Dedication

To Parker Jinyoung Moon.
My dearest,
You turned my world upside down,
And my heart cannot be any fuller.

I love you.

Chapter 1: Introduction

I. Peripheral T cell lymphoma

History

T cell lymphomas were first recognized as distinct entities from B cell non-Hodgkin lymphomas (NHLs) in 1974, when Robert Lukes and Robert Collins proposed the Lukes-Collins classification of lymphomas (Lukes and Collins 1974). By 1988, the Kiel classification, a system widely used in Europe and Asia developed by Karl Lennert, was also updated to place lymphomas under separate columns of B cell and T cell types (Feller and Diebold 2004). The specific diagnoses of mature T cell lymphomas became widely accepted with the introduction of the REAL (revised European-American Classification of Lymphoid Neoplasms) classification in 1994 (Harris et al. 1994). The first system of an international consensus, the REAL classification listed over 10 disease entities as “Peripheral T cell and NK-cell neoplasms.”

In 2001, the World Health Organization (WHO) largely adopted the REAL system to develop an internationally authoritative hematologic malignancy classification system and categorized 14 entities of clonal mature T- and NK-cell tumors as one group mostly based on the clinical presentation and histological morphology (Jaffe et al. 2001). The WHO has since updated the system to incorporate the new information uncovered in T cell lymphoma research. The most recent WHO system of 2016 catalogues over 25 discrete diagnoses under the heading of “mature T- and NK-cell neoplasms” (**Table 1.1**), which include both cutaneous T cell lymphoma (CTCL) and peripheral T cell lymphoma (PTCL), reflecting the remarkable heterogeneity of this group of disease that was further elucidated by the molecular advances in the understanding of the tumor pathobiology (Swerdlow et al. 2016).

Table 1.1 – List of mature T and NK cell neoplasm entities based on the 2016 WHO classification

Category	Subtype	Status
Predominantly leukemic diseases	T cell prolymphocytic leukemia	Definite
	T cell large granular lymphocytic leukemia	Definite
	Chronic lymphoproliferative disorder of NK cells	Provisional
	Aggressive NK cell leukemia	Definite
	Systemic EBV+ T cell lymphoma of childhood	Definite
	Hydroa vacciniforme-like lymphoproliferative disorder	Definite
	Adult T cell leukemia/lymphoma	Definite
Predominantly nodal diseases	Peripheral T cell lymphoma, Not otherwise specified	Definite
	Angioimmunoblastic T cell lymphoma	Definite
	Follicular T cell lymphoma	Provisional
	Nodal peripheral T cell lymphoma with TFH phenotype	Provisional
	Anaplastic large-cell lymphoma, ALK+	Definite
	Anaplastic large-cell lymphoma, ALK-	Definite
	Breast implant–associated anaplastic large-cell lymphoma	Provisional
Predominantly extranodal diseases	Extranodal NK-/T cell lymphoma, nasal type	Definite
	Enteropathy-associated T cell lymphoma	Definite
	Monomorphic epitheliotropic intestinal T cell lymphoma	Definite
	Indolent T cell lymphoproliferative disorder of the GI tract	Provisional
	Hepatosplenic T cell lymphoma	Definite
	Subcutaneous panniculitis-like T cell lymphoma	Definite
Predominantly cutaneous diseases	Mycosis fungoides	Definite
	Sézary syndrome	Definite
	Primary cutaneous CD30+ T cell lymphoproliferative disorders - Lymphomatoid papulosis - Primary cutaneous anaplastic large cell lymphoma	Definite
	Primary cutaneous γδ T cell lymphoma	Definite
	Primary cutaneous CD8+ aggressive epidermotropic cytotoxic T cell lymphoma	Provisional
	Primary cutaneous acral CD8+ T cell lymphoma	Provisional
	Primary cutaneous CD4+ small/medium T cell lymphoproliferative disorder	Provisional

Clinical presentation and diagnosis

A diverse array of different T cell neoplasms comprises T cell lymphoma (TCL), potentially related to the heterogeneity of its normal mature T cell counterparts. Even with the 27 distinct entities currently defined by the WHO diagnostic standard (**Table 1.1**), about a third of TCL cases still do not meet the existing criteria for any classification and receive a diagnosis of exclusion, PTCL, not otherwise specified (PTCL, NOS).

WHO diagnostic criterion for each entity involve clinical, phenotypic, and morphological feature of the disease. TCL can be broadly grouped into two categories based on the clinical presentation: cutaneous T cell lymphoma (CTCL) with predominantly cutaneous presentation and peripheral T cell lymphoma (PTCL), which encompasses leukemic (disseminated), nodal, and extranodal diseases (**Table 1.1**) (Campo et al. 2008). Leukemic diseases, like T-prolymphocytic leukemia (T-PLL) and adult T cell leukemia-lymphoma (ATL or ATLL), are characterized by circulating malignant T lymphoid cells that lead to marked lymphocytosis, generalized lymphadenopathy, and hepatosplenomegaly. Nodal PTCLs include some of the better described entities, such as angioimmunoblastic T cell lymphoma (AITL) and anaplastic large cell lymphoma (ALCL). Similar to other aggressive lymphomas, they commonly present with generalized lymphadenopathy and systemic B symptoms and, despite what the name suggests, often involve extranodal disease. On the other hand, extranodal lymphoma frequently is a localized disease without any nodal involvement. They are defined by the localization of the tumor: extranodal NK/T cell lymphoma, nasal type (ENKTCL), subcutaneous panniculitis-like T cell lymphoma (SPTCL), enteropathy associated T cell lymphoma (EATL), and hepatosplenic T cell lymphoma (HSTCL). Lastly, cutaneous T cell lymphomas (CTCLs), the most prominent of which are Sézary syndrome (SS) and mycosis fungoides (MF), present with various manifestations on the skin, which range from plaques to erythema. Lastly, PTCL, NOS, an inherently heterogeneous subgroup, most often presents in the lymph nodes, but can also be extranodal.

Differential diagnosis of PTCL heavily relies on histopathology of the disease. With the exception of Anaplastic Lymphoma Kinase (ALK)-translocated ALCL (ALK+), the only PTCL entity to date defined by a genetic marker, morphologic characteristics represent the hallmark features of each

PTCL subgroup. AITL consists of polymorphous infiltrate involving lymph nodes with a prominent proliferation of high endothelial venules and follicular dendritic cells (Swerdlow et al. 2017). ALCL is composed of large cells with round or pleomorphic, often horseshoe-shaped nuclei with multiple prominent nucleoli. Follicular T cell lymphoma (FTCL) demonstrates a nodular growth pattern in lymph nodes.

Increasing number of studies reveal that each PTCL subtype is a clinically distinct disease that, for efficient treatment, warrants therapeutic strategy uniquely tailored to its underlying pathogenesis. Therefore, diagnostic precision of PTCL has become more important than ever. However, arriving at a confident diagnosis remains difficult. The diagnostic workup varies widely among institutions (I et al. 2017), and pathologists often disagree on the diagnosis of a specific subtype (Vose et al. 2008, Weisenburger et al. 2011a). The overall rarity and heterogeneity of this disease, the complex diagnostic criteria that necessitates exhaustive amounts of testing and expertise, and the lingering ambiguity in boundaries between some entities due to incomplete understanding of the underlying biology all contribute to the challenges of diagnosing and effectively treating these cancers.

Epidemiology

PTCL incidence varies substantially across geographical regions, accounting for 10 to 15% of NHL in Western countries and 20 to 25% in Asia (1997, Anderson et al. 1998, Vose et al. 2008). The PTCL incidence is higher in Asia, Africa, and the Caribbean possibly due to the frequency of endemic Human T-lymphotropic virus 1 (HTLV-1) and Epstein-Barr Virus (EBV) infections, which are associated with ATL and NKTCL respectively (Arber et al. 1993, Jaffe et al. 1996, Au et al. 2009, Laurini et al. 2012, Chihara et al. 2014, Adams et al. 2016). In the United States, the age-adjusted incidence rate for PTCL more than quadrupled from 0.2 to 0.9 cases per 100,000 population from 1992 to 2005 (Abouyabis et al. 2008). The surge in incidence rate is partially explained by the increased awareness of the previously under-diagnosed lymphoma subtypes since the introduction of the WHO classification system. Most PTCL subtypes are more frequent in males, and the incidence increases with age (Abouyabis et al. 2008, Vose et al. 2008, Adams et al. 2016).

The two most common subtypes are PTCL, NOS (25.9%) and AITL (18.5%) (Vose et al. 2008). Reflecting the challenge of subtyping PTCLs under current diagnostic schemes, about 30% of T cell lymphomas in North America and Europe do not meet the criteria for a distinct diagnosis and are classified as PTCL, NOS (Vose et al. 2008, Weisenburger et al. 2011b). The most common discrete PTCL entity, AITL is more frequent in Europe (28.7%) than in North America (16.0%) (Vose et al. 2008, Federico et al. 2013). Both PTCL, NOS and AITL primarily affect the elderly with a median age at diagnosis of 60 years for PTCL, NOS (Weisenburger et al. 2011b) and 65 years for AITL (Federico et al. 2013). While the neoplastic T cells of PTCL, NOS and AITL are not associated with viral infections, studies of their disease biopsies have found that EBV-infected bystander B cells are present in about 50% of the cases (Tan et al. 2006). Other more common PTCL subtypes include ENKTCL (10.4%), ATLL (9.6%), ALK-positive ALCL (6.6%), and ALK-negative ALCL (5.5%) (Vose et al. 2008).

Genetic and molecular landscape of PTCL

Molecular studies of PTCL have demonstrated the potential for a more accurate classification and a more efficient subtype-specific targeted therapy. Early on, gene expression profiling studies have identified distinct signatures enriched in major PTCL entities such as AITL. The gene expression signature of AITL resembles that of follicular T-helper (TFH) cells, a subset of CD4+ T helper cells residing in the germinal centers, establishing TFH cells as the normal counterpart of the AITL tumor (de Leval et al. 2007). Notably, AITL-associated transcriptional signatures were present in about 15% of tumors diagnosed as PTCL, NOS, supporting that molecular characterization may deliver a more accurate PTCL classification than histology (Iqbal et al. 2014).

Advances in genomic sequencing technologies have permitted identification of recurrent genetic alterations in nearly every PTCL subtype albeit stopping short of uncovering entity-defining genetic markers. Across various subtypes, exome sequencing studies have revealed point mutations, indels, and copy number changes in genes involved in epigenetic regulation, T cell receptor (TCR) and co-stimulatory signaling, and JAK/STAT pathway (**Table 1.2**). In addition, a number of recurrent fusion oncogenes have emerged in PTCL, adding to the NPM-ALK gene fusion characteristic of ALK+ ALCL first identified in 1994 (Morris et al. 1994). Considering the important

role that chromosomal rearrangements play in the pathogenesis and clinical management of other hematologic malignancies (Das and Tan 2013, Wang et al. 2017), identification of fusion oncogenes in PTCL may help us better understand the disease and facilitate improved therapy in clinical settings.

The sections below discuss our current insight into the genetic and molecular landscape of some of the more common PTCLs.

Angioimmunoblastic T cell lymphoma

Following the gene expression profiling study that revealed TFH cells as the potential normal counterpart of AITL (de Leval et al. 2007), mutational analyses have uncovered highly recurrent somatic mutations in AITL with roles in TFH transformation. Genes most often altered in AITL include those involved in epigenetic regulation, T cell receptor (TCR) activation, and *RHOA* signaling (**Table 1.2**).

RhoA GTPase, encoded by the *RHOA* gene, is a molecular switch that regulates multiple biological processes, best characterized for its role in cytoskeleton remodeling. Studies in T cells have reported its role in polarization, migration and TCR signaling (del Pozo et al. 1999, Corre et al. 2001, Heasman et al. 2010, Mou et al. 2012). Heterozygous missense mutations of *RHOA* are present in up to 70% of AITL (**Figure 1.1a**), highlighting the central role of *RHOA* in the pathogenesis of AITL (Manso et al. 2014, Palomero et al. 2014, Sakata-Yanagimoto et al. 2014, Yoo et al. 2014, Wang et al. 2015, Ondrejka et al. 2016). *RHOA* G17V allele, which accounts for over 90% of these *RHOA* mutations, functions as an inactive and dominant negative form, likely blocking the activity of wild type *RHOA* (Palomero et al. 2014, Sakata-Yanagimoto et al. 2014, Yoo et al. 2014). Importantly, *RHOA* G17V expression in mouse $CD4^+$ T cells significantly increases differentiation towards the TFH lineage and eventually induces T cell lymphoma that faithfully recapitulate the characteristics of human AITL in cooperation with *TET2* loss (Cortes et al. 2018).

Mutations in epigenetic modulators, such as *TET2*, *DNMT3A* and *IDH2*, are widely present in hematological malignancies. *TET2* inactivating mutations are especially prevalent in AITL (70%) (**Figure 1.1a**) (Palomero et al. 2014, Sakata-Yanagimoto et al. 2014) and are associated with expression of TFH markers, advanced stage disease, and adverse clinical outcome (Lemonnier et

al. 2012). Notably, mice studies have demonstrated that loss of *Tet2* results in increased self-renewal and repopulating ability of hematopoietic stem cells (Ko et al. 2011, Ko and Rao 2011, Koh et al. 2011, Li et al. 2011, Moran-Crusio et al. 2011, Quivoron et al. 2011, Kunimoto et al. 2012, Shide et al. 2012).

IDH2 mutations in PTCL occur exclusively in AITL (20-45%) and involve only the position R172 (**Figure 1.1a**) (Cairns et al. 2012, Wang et al. 2015). R172 mutations in *IDH2* lead to accumulation of the l-enantiomer of 2-hydroxyglutarate, which antagonizes the activity of the *TET* family of enzymes, and reportedly cooperate with the *TET2* inactivation to upregulate the expression of TFH specific genes (Parker and Metallo 2015, Wang et al. 2015).

In addition, recurrent loss of function mutations in *DNMT3A* are present in 10-40% of AITL samples, frequently along with *Tet2* mutations (**Figure 1.1**) (Couronne et al. 2012, Palomero et al. 2014, Sakata-Yanagimoto et al. 2014, Yoo et al. 2014, Wang et al. 2015). In fact, mutations in these epigenetic regulators often co-occur in the same case (**Figure 1.1**), in contrast to myeloid malignancies, in which *IDH2* and *TET2* mutations are mutually exclusive (Wang et al. 2015).

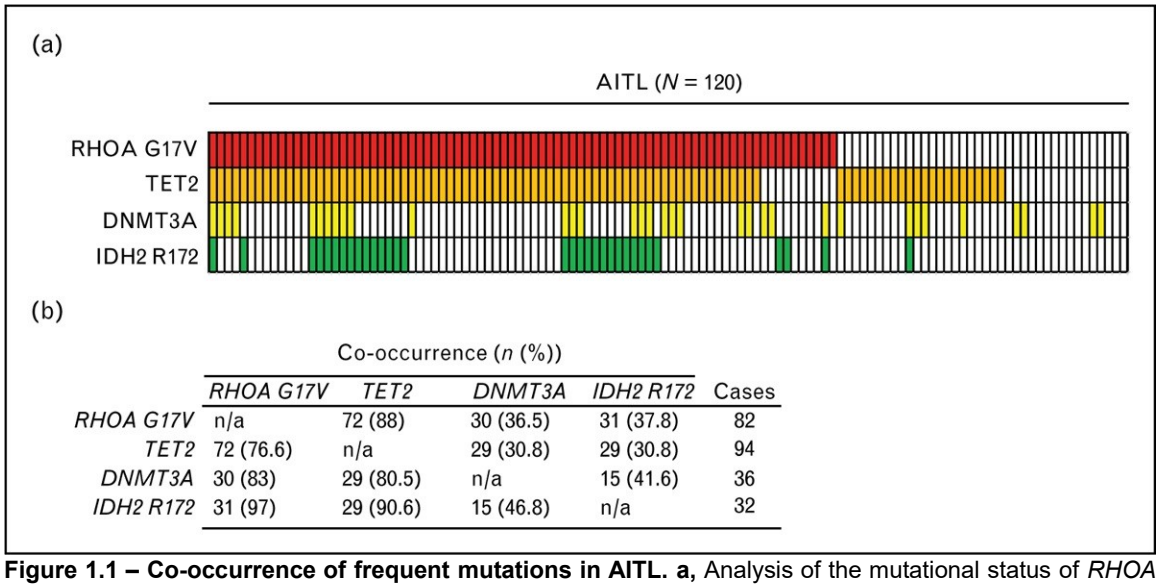

(b)

Co-occurrence (*n* (%))

	RHOA G17V	*TET2*	*DNMT3A*	*IDH2 R172*	Cases
RHOA G17V	n/a	72 (88)	30 (36.5)	31 (37.8)	82
TET2	72 (76.6)	n/a	29 (30.8)	29 (30.8)	94
DNMT3A	30 (83)	29 (80.5)	n/a	15 (41.6)	36
IDH2 R172	31 (97)	29 (90.6)	15 (46.8)	n/a	32

Figure 1.1 – Co-occurrence of frequent mutations in AITL. a, Analysis of the mutational status of *RHOA* G17V, *TET2*, *DNMT3A*, and *IDH2* in a cohort of 120 AITL (information extracted from published data (Palomero et al. 2014, Sakata-Yanagimoto et al. 2014, Yoo et al. 2014, Wang et al. 2015)). Each column represents a patient sample; each row represents mutations in each of the genes of interest. **b,** Quantification of the co-occurrence of mutations in RHOA G17V and epigenetic regulators. In the column on the left are the cases mutated for *RHOA* G17V, *TET2*, *DNMT3A*, and *IDH2* R172; on the upper row the co-occurrence indicated by the number of cases on the left category that also carry the mutation in the genes indicated on the top (n) and the percentage of co-occurrence calculated from the total number of cases [(%) in bold]. Adapted from (Cortés and Palomero 2016).

Detection of these epigenetic regulator mutations in blood cells of normal elderly individuals (Xie et al. 2014) and in non-tumor cells of AML and PTCL patients (Quivoron et al. 2011, Sakata-Yanagimoto et al. 2014) suggest their role as an initial or pre-malignant lesion in hematopoietic progenitors that could eventually lead to malignant transformation in both the T cell and myeloid lineages. Notably, nearly 95% of AITL cases with *RHOA* G17V allele include mutations in at least one of the three aforementioned epigenetic regulators (**Figure 1.1**) (Cortés and Palomero 2016). Based on these findings, a recent study developed a $CD4^+$ T cell mouse lymphoma model that fully recapitulates the features associated with human AITL by expressing *RHOA* G17V in a *Tet2*$^{-/-}$ background (Cortes et al. 2018, Ng et al. 2018). These reports support the two-hit model of AITL lymphomagenesis, in which the second hit *RHOA* mutation drives the full transformation and lineage specification of the pre-malignant progenitor cells harboring the first-hit lesion in epigenetic regulators.

Additionally, gene expression profiling studies have implicated TCR signaling dysregulation as a major factor in AITL pathogenesis (Iqbal et al. 2014), and sequencing of AITL samples have uncovered somatic mutations in genes regulating the TCR activation cascade: *PLCG1*, 14% (Vallois et al. 2016); *CD28*, 10% (Lee et al. 2015, Rohr et al. 2016, Vallois et al. 2016, Vallois et al. 2018); *FYN*, 3% (Palomero et al. 2014, Vallois et al. 2016); *VAV1*, 4% (Vallois et al. 2016, Abate et al. 2017); *CARD11*, 3% (Vallois et al. 2016) (**Figure 1.2**). Additionally, a copy number alteration (l) study has reported frequent gains in a region that harbors *CARD11* (Fujiwara et al. 2008). TCR signaling leads to activation of AP-1, NFAT, and NF-κB transcriptional programs and plays a critical physiologic role in T cell function (**Figure 1.2**). In this context, the somatic mutations in the TCR regulatory elements that are reported in AITL are mostly activating: mutations in PLCγ, an activator of second messenger diacylglycerol (DAG) encoded by *PLCG1*, promote MALT1 cleavage and NFAT activity (Vallois et al. 2016); mutations in CD28, a major co-stimulatory molecule for TCR activation encoded by *CD28*, induce increased NF-κB activity (Lee et al. 2015, Rohr et al. 2016); mutations in the SRC family tyrosine kinase FYN, a crucial proximal element of TCR signaling cascade encoded by *FYN*, disrupt the intramolecular inhibitory interaction of the kinase (Palomero et al. 2014); mutations in hematopoietic-specific guanine nucleotide exchange factor (GEF) VAV1

encoded by *VAV1*, another significant mediator of TCR signaling, often cause in-frame deletions that perturb the autoinhibitory domain of the protein (Abate et al. 2017).

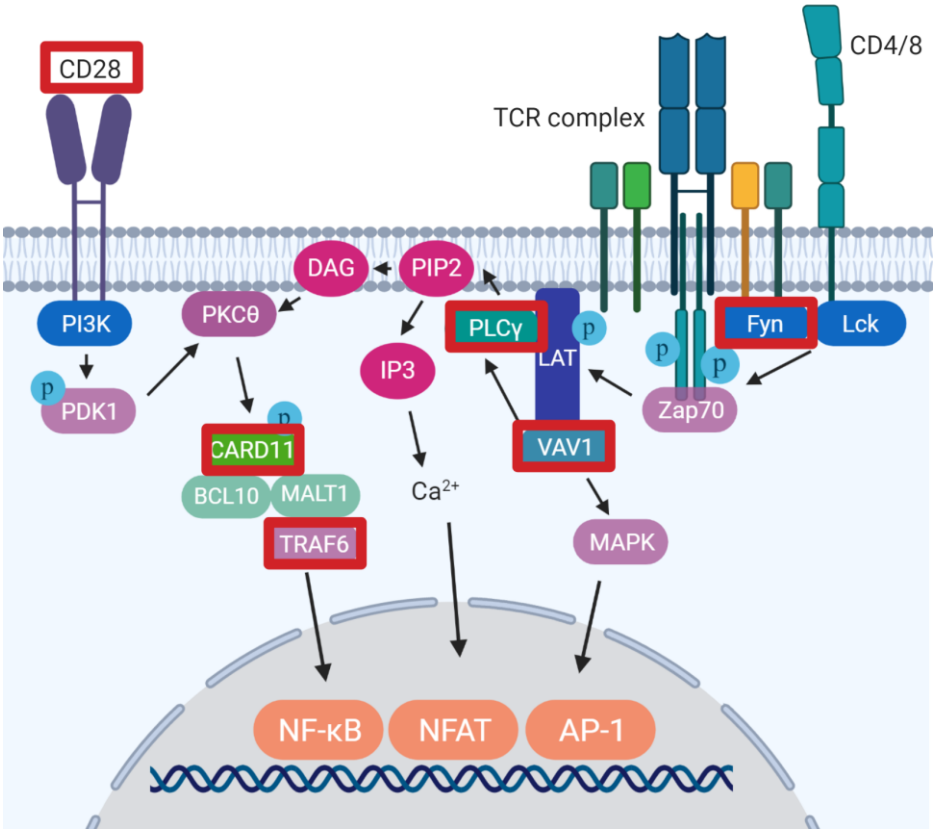

Figure 1.2 – Genes constituting T cell receptor activation pathway are recurrently altered in AITL. Schematic of the T cell receptor (TCR) signaling cascade with a simplified representation of the downstream signaling mediators. Briefly, TCR engagement leads to activation of LCK and FYN kinases which leads to signaling enzymes VAV1 and phospholipase Cγ (PLCγ) docking at Linker of activated T cells (LAT). PLCγ generates Inositol trisphosphate (IP3), which ultimately results in NFAT activation, and diacylglycerol (DAG). DAG-dependent protein kinase C (PKC) θ then translocates to the plasma membrane and phosphorylates CARD11. The phosphorylated CARD11 recruits BCL10 and MALT1 to oligomerize into CBM complex and activate canonical NF-κB in a TRAF6 ubiquitin ligase-dependent manner. CD28 costimulatory molecule upon activation recruits SH2-containing enzymes, including phosphoinositide 3 kinase (PI3K), and induces enhanced signaling, most notably NF-κB activity. For more detailed description of TCR signaling cascade, see page 27. Genes that are recurrently altered in AITL are indicated by red box.

Structural abnormalities identified in AITL involve *CD28* and *VAV1*. Multiple studies have described *CD28* gene fusions, *CTLA4-CD28* and *ICOS-CD28*, while their frequencies in AITL remain uncertain (Gong et al. 2016, Rohr et al. 2016, Yoo et al. 2016a, Yoo et al. 2016b, Vallois et al. 2018). Physiologically, TCR stimulation markedly upregulates *CTLA4* and *ICOS* and downregulates *CD28* (Chen and Flies 2013). As the promoters for *CTLA4* and *ICOS* control the expression of these *CD28* chimeric genes, these fusion events may trigger sustained *CD28*-

costimulatory signaling (Kataoka et al. 2015). While more often found in PTCL, NOS and ALCL, *VAV1* fusion gene is also present in AITL and results in the deletion of the negative regulatory domain of the protein and consequently increased signaling activity (Abate et al. 2017).

Anaplastic large cell lymphoma

ALCL is a general heading for four different entities that differ in clinical presentation and expression of the *ALK* gene rearrangements: ALK-positive ALCL, ALK-negative ALCL, primary cutaneous ALCL, and breast implant-associated ALCL (**Table 1.1**). This section will focus on the more common ALK-positive and ALK-negative ALCLs.

The presence of *ALK* gene fusions define the ALK-positive ALCL, which account for about half of all ALCLs. About 75-85% of *ALK* fusions found in ALCL join nucleophosmin (*NPM1*) and *ALK*. The underlying chromosomal translocation of *NPM1-ALK*, t(2;5)(p23;q35), was the first recurrent genetic abnormality described in PTCL (Rimokh et al. 1989). While *ALK* fusion partners encompass more than 20 genes, all variants of *ALK* chimera demonstrate constitutive ALK tyrosine kinase activity and subsequent downstream activation of oncogenic transcription factor STAT3 (Feldman et al. 2013, Crescenzo et al. 2015, Hapgood and Savage 2015).

ALK-negative ALCL shares a common gene expression signature with ALK-positive ALCL that is distinct from that of PTCL, NOS (Piva et al. 2010, Piccaluga et al. 2013, Iqbal et al. 2014). A recent study has uncovered multiple genomic mechanism in ALK-negative ALCL that can lead to oncogenic STAT3 signaling: mutations in *JAK1* and *STAT3* as well as STAT3-activating gene rearrangements that involve non-*ALK* tyrosine kinase genes, *ROS1* and *TYK2* (Crescenzo et al. 2015). These data suggest that ALCLs, regardless of the ALK status, may be driven by a common oncogenic mechanism, particularly constitutive STAT3 activation.

Other aberrant molecular events identified in ALK-negative ALCL include genetic rearrangements harboring non-tyrosine kinase genes *DUSP22* and *TP63* (Feldman et al. 2011, Vasmatzis et al. 2012), *VAV1* gene fusions (Boddicker et al. 2016), and expression of oncogenic truncated transcripts of *ERBB4* (Scarfo et al. 2016).

Extranodal NK/T cell lymphoma, nasal type

ENKTCL is a lymphoma that most often originates from natural killer (NK) cells, but in some cases, from cytotoxic T cells. The most commonly occurring somatic mutations in ENKTCL involve *JAK3* (35%) and RNA helicase gene *DDX3X* (20%) (Koo et al. 2012, Jiang et al. 2015). Studies have also identified mutations in *STAT5B* and *STAT3*, supporting the role of JAK/STAT signaling in ENKTCL (Kucuk et al. 2015).

Peripheral T Cell lymphoma, not otherwise specified

The molecular characteristics of PTCL, NOS vary widely and overlap significantly with other PTCL subtypes. The most prominent of such is a sizable portion of PTCL, NOS cases that express some TFH immunophenotype and share a gene expression signature (de Leval et al. 2007, Piccaluga et al. 2007) and mutational profile with AITL. The recurrent genetic alterations identified in AITL are also present in PTCL, NOS in varying frequencies: *RHOA* G17V (Palomero et al. 2014, Sakata-Yanagimoto et al. 2014), *TET2* and *DNMT3A* loss (Couronne et al. 2012, Palomero et al. 2014, Sakata-Yanagimoto et al. 2014), somatic mutations in *PLCG1* (Watatani et al. 2019) and *FYN* (Palomero et al. 2014, Watatani et al. 2019), and mutations and fusions involving *VAV1* (Boddicker et al. 2016, Abate et al. 2017, Watatani et al. 2019). In particular, 20-30% of PTCL, NOS harbor both *RHOA* G17V and *TET2* loss (Palomero et al. 2014, Sakata-Yanagimoto et al. 2014, Watatani et al. 2019), the cooperation of which is shown to induce AITL in mice (Cortes et al. 2018, Ng et al. 2018), and may represent AITL cases that the current diagnostic criteria are unable to capture. Reflecting these observations, the most recent diagnostic standard places some cases previously designated as PTCL, NOS under the new provisional categories of follicular T cell lymphoma (FTCL) and nodal peripheral T cell lymphoma with TFH phenotype (**Table 1.1**).

FTCL is a rare subset of such cases that histologically demonstrate a follicular growth pattern. Interestingly, about 20% of FTCL cases contain a recurrent t(5;9)(q33;q22) translocation that results in *ITK-SYK* fusion, an activator of constitutive TCR signaling (Streubel et al. 2006, Huang et al. 2009, Dierks et al. 2010, Pechloff et al. 2010).

Ongoing efforts to further classify the remaining non-TFH PTCL, NOS have similarly examined gene expression signatures and mutational profiles. Previous large-scale gene expression profiling

studies have described two major subgroups of PTCL, NOS based on high expression of either *GATA3* or *TBX21* (Iqbal et al. 2014, Wang et al. 2014). A more recent study that comprehensively examined genetic profiles in a large cohort of PTCL, NOS cases reported frequent loss of tumor suppressors *TP53* (28%) and *CDKN2A* (13%), which define a new proposed subset characterized by marked genomic instability and poorer prognosis.

Table 1.2 – Common chromosomal and molecular abnormalities in peripheral T cell lymphoma.

PTCL	Gene	Involved Pathway	Alleles (Frequency)
AITL	*TET2*	Epigenetic regulation	Loss of function (70%)
	DNMT3A	Epigenetic regulation	Loss of function (10-40%)
	IDH2	Epigenetic regulation	R172 (20-45%)
	RHOA	TCR signaling, actin remodeling	G17V (70%) K18N (3%)
	CD28	TCR costimulatory pathway	D124 (6%) T195 (%) *CTLA4-CD28* (uncertain) *ICOS-CD28* (5%)
	PLCG1	TCR signaling	SNV (14%)
	VAV1	TCR signaling	SNV, in-frame deletion, gene fusion (4%)
	FYN	TCR signaling	SNV (3%)
ALK+ ALCL	*ALK*	JAK/STAT	Gene fusion (100%, by definition): *NPM1-ALK* (>80%) *TPM3-ALK* (3%)
ALK- ALCL	*JAK1*	JAK/STAT	Activating mutations (15%)
	STAT3	JAK/STAT	Activating mutations (10%)
	Tyrosine kinase (*ROS1*, *TYK2*)	JAK/STAT	Gene fusion (22%)
	VAV1	TCR signaling	Gene fusion (16%)
	DUSP22		Rearrangements (30%)
	TP63		Gene fusions (8%)
PTCL, NOS	*TET2*	Epigenetic regulation	Loss of function (45%)
	DNMT3A	Epigenetic regulation	Loss of function (30%)
	RHOA	TCR signaling, actin remodeling	G17V (20-30%)
	FYN	TCR signaling	SNV (3%)
	VAV1	TCR signaling	SNV, in-frame deletion, gene fusion (11%)
	ITK	TCR signaling	*ITK-SYK* in 20% of FTCL *ITK-FER* rare
	TP53	Tumor suppressor	Loss of function (28%)
	CDKN2A	Tumor suppressor	Loss of function (13%)

SNV, single nucleotide variant; TCR, T cell receptor.

Treatment options and outcome

As in B cell lymphomas, CHOP (cyclophosphamide, doxorubicin, vincristine, and prednisone) and CHOP-like combination chemotherapy programs are the standard first-line treatment regimen in PTCLs (**Figure 1.3**). CHOP-based treatments have largely been unsuccessful in PTCL, possibly because this conventional lymphoma therapy originates from clinical trials that included predominantly B cell NHL, a biologically distinct but much more common disease. In non-ALCL PTCLs, CHOP-based therapy achieves complete response (CR) rate of 50% and 5-year overall survival of 37% (Abouyabis et al. 2011). Even in anaplastic large cell lymphomas, which may be the only PTCL subgroup in which conventional CHOP-like regimens are effective, about 40% of patients with ALK-positive disease and over 60% of patients with ALK-negative disease fail to survive after 5 years (Savage et al. 2008). Some younger, healthier patients with chemo-sensitive disease receive autologous stem cell transplantation (ASCT) in first remission (**Figure 1.3**) and report superior outcomes in some studies (Reimer et al. 2009, d'Amore et al. 2012). However, the benefit may be due to patient selection, and most patients are ineligible due to refractory disease or comorbidities.

Given the dismal prognosis under standard treatment options (**Figure 1.4**), there is a pressing need for new therapeutic strategies based on improved understanding of PTCL biology. Ongoing efforts to address the prevalent refractoriness of the disease include incorporating novel agents into CHOP regimen, developing a new doublet treatment platform by combining agents that have shown efficacy in relapsed and refractory PTCL, and further discovering potential drug targets based on identification of mutations and relevant pathways. As a result of these endeavors, the US Food and Drug Administration (FDA) has approved four novel agents in patients with relapsed or refractory PTCL since 2009 (**Table 1.3**). Encouragingly, a recent clinical trial integrating one of the novel drugs that targets CD30 into the traditional regimen has made major advance in the frontline therapy against CD30+ PTCLs (Horwitz et al. 2019). Considering that efforts to empirically modify CHOP with more dose-intense combination chemotherapy have failed to improve outcomes (Escalon et al. 2005, Simon et al. 2010), the success of this trial confirms the potential of the

targeted, rationally designed therapy based on the tumor biology. The sections below briefly discuss the recent and ongoing ventures to improve outcomes in PTCL.

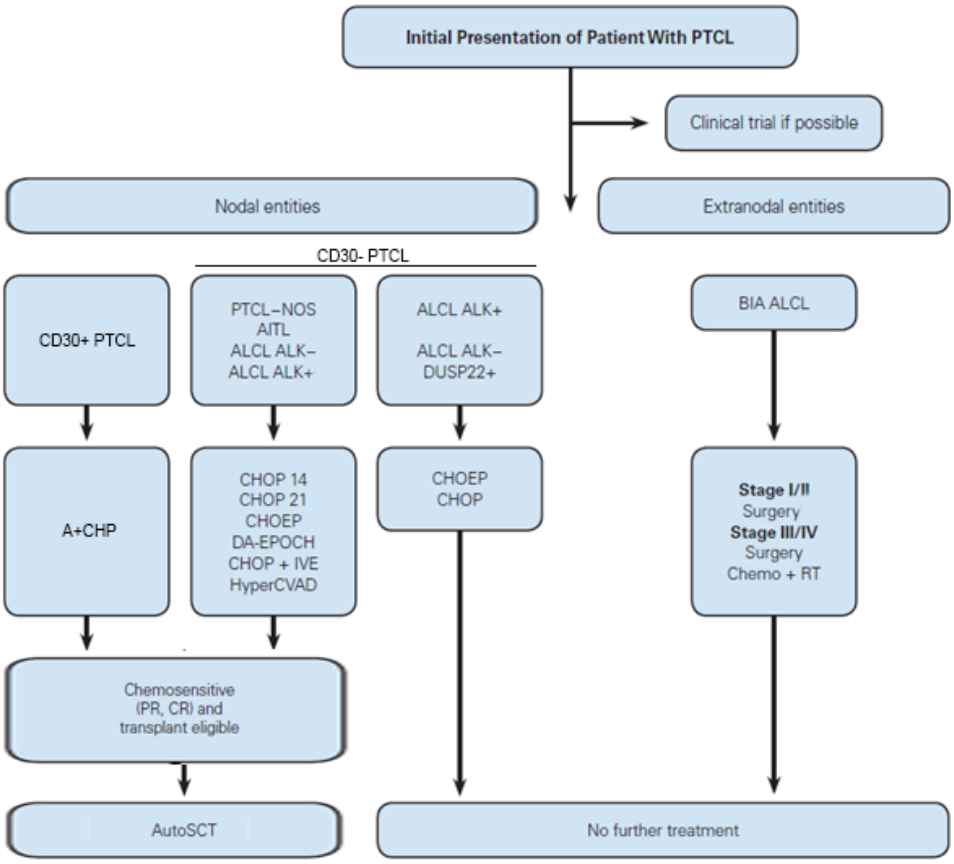

Figure 1.3 – Treatment algorithm for initial presentation of peripheral T- cell lymphoma. AITL, angioimmunoblastic T cell lymphoma; ALCL, anaplastic large cell lymphoma; ALK, anaplastic lymphoma kinase; autoSCT, autologous stem cell transplant; BIA, breast implante-associated; CHOEP, cyclophosphamide + doxorubicin + vincristine + etoposide + prednisone; CHOP, cyclophosphamide + doxorubicin + vincristine + prednisone; IVE, ifosfamide + epirubicin + etoposide; CR, complete response; DA-EPOCH, dose-adjusted etoposide + prednisone + vincristine + cyclophosphamide + doxorubicin; hyperCVAD, cyclophosphamide + vincristine + doxorubicin + dexamethasone – alternating with methotrexate + cytarabine; PTCL-NOS, peripheral T cell lymphoma, not otherwise specified; PR, partial response; RT, radiation therapy. Adapted from (Zing et al. 2018) and updated to reflect changes in 2019.

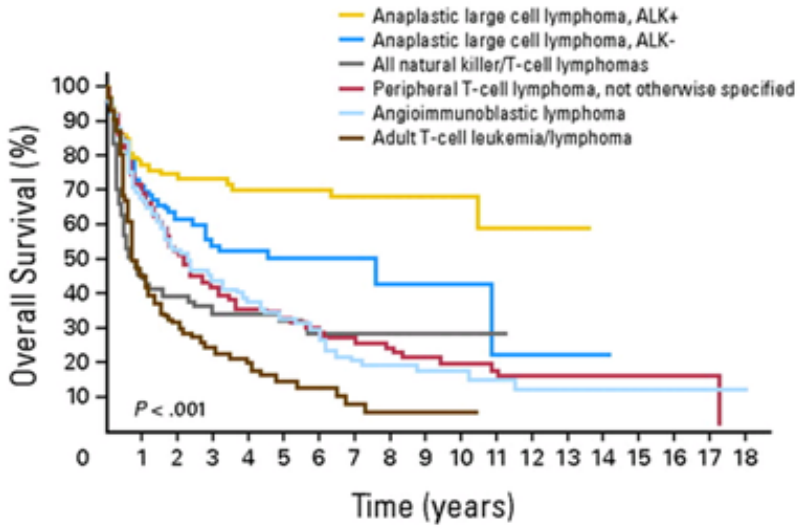

Figure 1.4 – Overall survival of patients with the common subtypes of peripheral T cell lymphoma. Peripheral T cell lymphoma, not otherwise specified, 32%; Angioimmunoblastic T cell lymphoma, 32%; Adult T cell leukemia/lymphoma, 14%; Anaplastic large cell lymphoma, ALK+, 70%; Anaplastic large cell lymphoma, ALK-, 49%. Adapted from (Vose et al. 2008)

FDA-approved agents in relapsed and refractory peripheral T cell lymphomas

Starting with the antifolate pralatrexate approval in 2009, the FDA has approved four new agents for relapsed and refractory PTCL based on the phase II trials that showed statistically significant efficacy (**Table 1.3**). In 2011, the FDA approved the histone deacetylase (HDAC) inhibitor romidepsin for its efficacy shown in 130 patients whose disease had failed to respond to at least one prior systemic therapy with PTCL (Coiffier et al. 2014). Treatment with romidesin achieved an objective response rate of 25%, including 15% with CR, and the responses lasted a median of greater than two years. Brentuximab vedotin, another novel agent approved for PTCL in 2011 by the FDA, is a CD30-targeted immunoconjugate that demonstrated a high response rate of 85% in a phase II study of 58 patients with CD30+ ALCL who relapsed after prior therapy (Pro et al. 2012). Brentuximab vedotin was approved for relapsed, refractory systemic ALCL, but not for patients with other subtypes of PTCL. Most recently in 2014, FDA approved belinostat, a novel pan-HDAC inhibitor based on a phase II trial of 129 patients with relapsed and refractory PTCL that demonstrated meaningful efficacy and a favorable toxicity profile (O'Connor et al. 2015).

Table 1.3 – Novel agents approved for relapsed/refractory peripheral T cell lymphomas

Approved Agent	Indications	Mechanism of Action	Outcomes (ORR, CR, DOR)
Belinostat	PTCL	HDAC inhibitor	26%, 11%, 13.6 mo (O'Connor et al. 2015)
Brentuximab vedotin	ALCL	α-CD30 linked to auristatin (antitubulin agent)	86%, 57%, 13.2 mo (Pro et al. 2012)
Pralatrexate	PTCL	DHFR/thymidylate synthase inhibitor	29%, 11%, 10.1 mo (O'Connor et al. 2011)
Romidepsin	PTCL	HDAC inhibitor	25%, 15%, 28 mo (Coiffier et al. 2014)
			38%, 18%, 8.9 mo (Piekarz et al. 2011)

PTCL, peripheral T cell lymphoma; ALCL, anaplastic large cell lymphoma; ORR, objective response rate; CR, complete response; DOR, duration of response; mo, months.

Incorporating novel agents into the conventional CHOP regimen

Approval of these novel agents has led to attempts to improve upon the CHOP backbone of the frontline PTCL therapy (**Table 1.4**). Several large randomized studies have been recently completed, are ongoing, or have been planned. Most significantly, the recent announcement of results from the phase III ECHELON-2 trial of A+CHP (brentuximab vedotin, cyclophosphamide, doxorubicin, prednisone) versus conventional CHOP chemotherapy assessing 452 patients with untreated CD30+ PTCL demonstrated A+CHP's advantage in progression-free survival (PFS) and an overall survival (OS), resulting in a first-line FDA approval of this regimen (Horwitz et al. 2019). The success of brentuximab vedotin in CD30+ PTCL shows the promise of properly targeted therapies.

Other attempts to use novel agents in combination with CHOP have met with limited success. Phase III trials of chemotherapy combining CHOP with alemtuzumab, a humanized antibody against mature lymphocyte marker CD52, failed to show significant difference in PFS and OS compared to CHOP (Altmann et al. 2018). A phase Ib/II trial combined romidepsin with CHOP (Ro-CHOP) for frontline treatment of 37 patients with PTCLs and demonstrated a 30-month PFS of 41% with OS 70.7%, albeit with more toxicity (Dupuis et al. 2015). Currently, a phase III trial comparing Ro-CHOP with CHOP alone has enrolled 421 patients with primary endpoint analysis due in 2019 (NCT01796002).

Table 1.4 – Key ongoing and recently completed phase III trials

Clinical study	Setting	Therapies being studied	Results
ACT-1 (NCT00646854)	Newly diagnosed, frontline	Alemtuzumab + CHOP vs CHOP	No significant difference in PFS and OS. Increased toxicity in Alemtuzumab.
ECHELON-2 (NCT01777152)	Newly diagnosed, frontline	A+CHP vs CHOP	Median PFS: 48.2 mo in A+CHP vs 20.8 mo in CHOP (Horwitz et al. 2019)
Ro-CHOP (NCT01796002)	Newly diagnosed, frontline	Ro-CHOP vs CHOP	Primary endpoint analysis due in 2019
Azacitidine (NCT03593018)	Relapsed /refractory AITL	Hypomethylating agent Azacitidine vs bendamustine vs romidepsin vs gemcitabine	Recruiting
Lumiere (NCT01482962)	Relapsed /refractory	Aurora A kinase inhibitor Alisertib vs pralatrexate vs romidepsin vs gemcitabine	Alisertib not statistically significantly superior to the comparator arm (O'Connor et al. 2019b)

CHOP, cyclophosphamide + doxorubicin + vincristine + prednisone; PFS, progression-free survival; OS, overall survival; A+CHP, brentuximab vedotin + cyclophosphamide + doxorubicin + prednisone; mo, months; Ro-CHOP, romidepsin + CHOP.

Targeted therapy in peripheral T cell lymphomas

The identification and functional characterization of *ALK* gene fusions, the prevalent, subtype-defining genetic marker of ALK-positive ALCL, has enabled a therapy based on an understood mechanism and defined target. In non-small cell lung cancers, a small molecule tyrosine kinase inhibitor crizotinib successfully targets tumors bearing *ALK* gene rearrangements (Shaw et al. 2013). A small study testing crizotinib in 11 patients with refractory ALK-positive lymphoma demonstrated an objective response rate (ORR) of 91%, OS of 72.7%, and PFS of 63.7% at 2 years (Gambacorti Passerini et al. 2014). In addition, 3 patients experienced a CR for greater than 30 months under continuous crizotinib administration. Given the durable efficacy of the drug, crizotinib is now offered in clinic to patients with ALK-positive ALCL that do not respond to standard therapy or brentuximab vedotin (**Figure 1.5**).

The prevalent *TET2* mutations in AITL and PTCL, NOS are another promising therapeutic target. With the report of benefits of hypomethylating agents in *TET2*-mutated myeloid malignancies (Bejar et al. 2014), recent and ongoing studies have examined the efficacy of those drugs in AITL. A retrospective case series of 12 AITL patients treated with a hypomethylating agent azacytidine reported a 75% ORR including 50% CRs (Lemonnier et al. 2018), prompting initiation of a phase

III trial comparing azacytidine with the investigator's choice of romidepsin, bendamustine, or gemcitabine (NCT03593018). In addition, an ongoing phase Ib/II trial of romidepsin and azacytidine combination (NCT01998035) recently reported an ORR of 73% in TCL with 55% CRs (Falchi et al. 2019, O'Connor et al. 2019a).

In addition, several early phase single-agent clinical trials have demonstrated clinical efficacy of targeting the TCR signaling. A case series of 12 patients with AITL who were treated with cyclosporin A, a calcineurin inhibitor that abrogates TCR signaling effector pathways such as NFAT, demonstrated response in 8 patients including 3 with CR (Advani et al. 2007). In a phase I study, a treatment with phosphoinositide 3 kinase (PI3K) inhibitor duvelisib in 16 patients with refractory or relapsed PTCL achieved a 50% ORR including 3 CRs (Horwitz et al. 2018a). In addition, an ongoing phase Ib/II study combining either romidepsin or bortezomib with duvelisib (NCT02783625) reported an encouraging ORR of 55% (12/22 patients) and CR rate of 27% (6/22) in refractory or relapsed PTCL (Horwitz et al. 2018b). A planned phase II study will test efficacy of duvelisib in 120 patients with refractory or relapsed PTCL (NCT03372057).

Lastly, based on the preclinical activity of JAK/STAT inhibitors, two ongoing phase II trials are testing the oral JAK inhibitor ruxolitinib. One study in relapsed or refractory B cell NHL and PTCL (NCT01431209) has enrolled 71 patients, and the other study exclusively in relapsed or refractory T cell lymphoma (NCT02974647) is enrolling a planned 52 patients.

Ongoing and recently completed single-agent clinical trials in PTCL are summarized in **Table 1.5**.

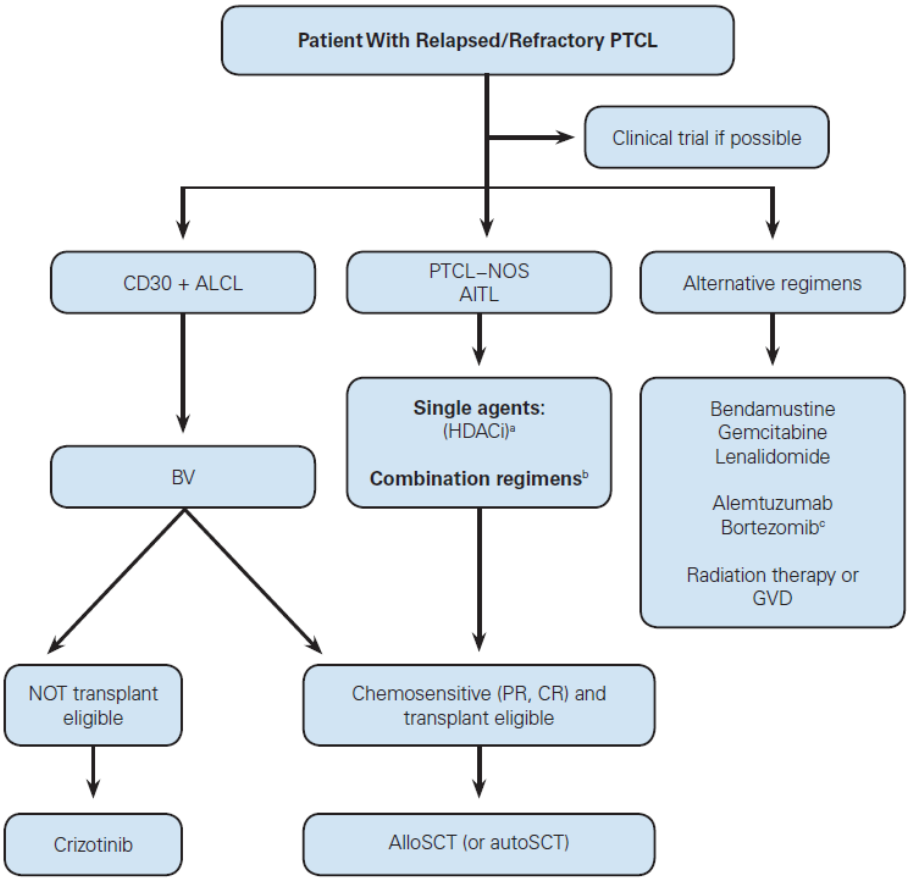

Figure 1.5 – Treatment algorithm for relapsed/refractory peripheral T- cell lymphoma. AITL, angioimmunoblastic T cell lymphoma; ALCL, anaplastic large cell lymphoma; AlloSCT, allogenic stem cell transplantation; autoSCT, autologous stem cell transplantation; BV, brentuximab vedotin; CR, complete response; GVD, gemcitabine + vinorelbine + pegylated liposomal doxorubicin; HDACi, histone deacetylase inhibitor; PTCL, peripheral T cell lymphoma. Adapted from (Zing et al. 2018).

Table 1.5 – Single-agent therapies under investigation for relapsed/refractory peripheral T cell lymphomas

Single-Agent	Mechanism of Action	Phase	Clinical Trial ID
Endostar	Angiogenesis inhibitor	II	NCT02520219
E7777	Diphtheria Toxin Fragment-Interleukin-2 Fusion protein	II	NCT02676778
Selinexor	Selective inhibitor of nuclear export	II	NCT02314247
Tipifarnib	Farnesyltransferase inhibitor	II	NCT02464228
Darinaparsin	Organic arsenic compound	II	NCT02653976
Ixazomib	Proteasome inhibitor	II	NCT02158975
Forodesine	PNP inhibitor	I/II	NCT01776411
Ruxolitinib	JAK inhibitor	II	NCT01431209
		II	NCT02974647
Temsirolimus	mTOR inhibitor	I	NCT01614197
Duvelisib	PI3K inhibitor	II	NCT03372057
Carfilzomib	Proteasome inhibitor	I	NCT01336920
Panobinostat	Pan-deacetylase inhibitor	II	NCT01261247
Clofarabine	DNA synthesis inhibitor	I/II	NCT00644189
MK2006	AKT inhibitor	II	NCT01258998
Sorafenib	Multikinase inhibitor	II	NCT00131937
Alefacept	Immunosuppressive dimeric fusion protein	I	NCT00438802
Pembrolizumab	PD-1 antibody	II	NCT02535247
Fenretinide	Synthetic retinoid derivative	II	NCT02495415
MEDI-570	Anti-ICOS monoclonal antibody	I	NCT02520791
EDO-S101	Alkylating HDAC inhibitor	I	NCT02576496
ALRN-6924	MDM2/MDMX antagonist	I/II	NCT02264613
MLN9708	Proteasome inhibitor	II	NCT02158975

II. NF-κB signaling in lymphoma

Overview of NF-κB signaling pathway

Nuclear factor (NF)-κB is a family of inducible transcription factors critical for a variety of cellular responses. In the steady state, the members of the family form various homodimers and heterodimers that are kept inactive in the cytoplasm by the C-terminal precursor domain or the binding of inhibitory IκB proteins. Physiologic activation of NF-κB occurs in response to stimulation of a wide range of surface receptors and via two common signaling pathways, namely the canonical or the alternative pathway. Both pathways are based on inducible degradation of the C-terminal precursor domain or the IκB proteins following IκB-kinase (IKK) complex-mediated phosphorylation. Subsequent to the removal of IκB from the NF-κB dimers, the NF-κB transcription factors translocate to the nucleus and bind to the DNA κB sites to induce activation of target genes. Biochemical control of NF-κB via IκB, rather than transcriptional regulation, provides a rapid molecular switch that enables instant launch of pre-formed transcription complexes in response to urgent stimuli such as pathogens. In the developmental paradigm, the biochemical induction of transcriptional program also resolves the infinite regression paradox of how expression of the first tissue specific transcription factor occurs, if a tissue-specific transcription factor itself requires a tissue-specific transcription factor (Zhang et al. 2017b).

Under physiologic conditions, NF-κB activation is a transient and highly regulated process and plays a particularly crucial role in development, function, and survival of immune cells. Sections below highlight key molecules and steps of the pathway.

Components of the NF-κB System

NF-κB is a family of related proteins that, as a homo- and hetero-dimer, bind to the enhancers or promoters of hundreds of genes via the κB site, a nearly palindromic DNA sequence with a consensus of 5'-GGGRNWYYCC-3' (http://www.bu.edu/nf-kb/gene-resources/target-genes/) (Sen and Baltimore 1986, Lenardo et al. 1987). The NF-κB family consists of five proteins that share N-terminal Rel homology domain (RHD) followed by nuclear localization sequence (NLS): p105 (precursor of p50), p100 (precursor of p52), Rel A (p65), Rel B, and c-Rel (**Figure 1.6**). Functions

of RHD include sequence-specific DNA binding, dimerization, and inhibitory protein binding, all three of which are essential for the proper regulation and operation of the pathway. To date, 13 of the 15 potential NF-κB dimers have been described. The combinatorial diversity of the dimers, which results in molecules of different affinities to the variants of the κB site and to the co-transcriptional factors, may contribute to the distinct but overlapping gene regulatory patterns observed in NF-κB (Smale 2012).

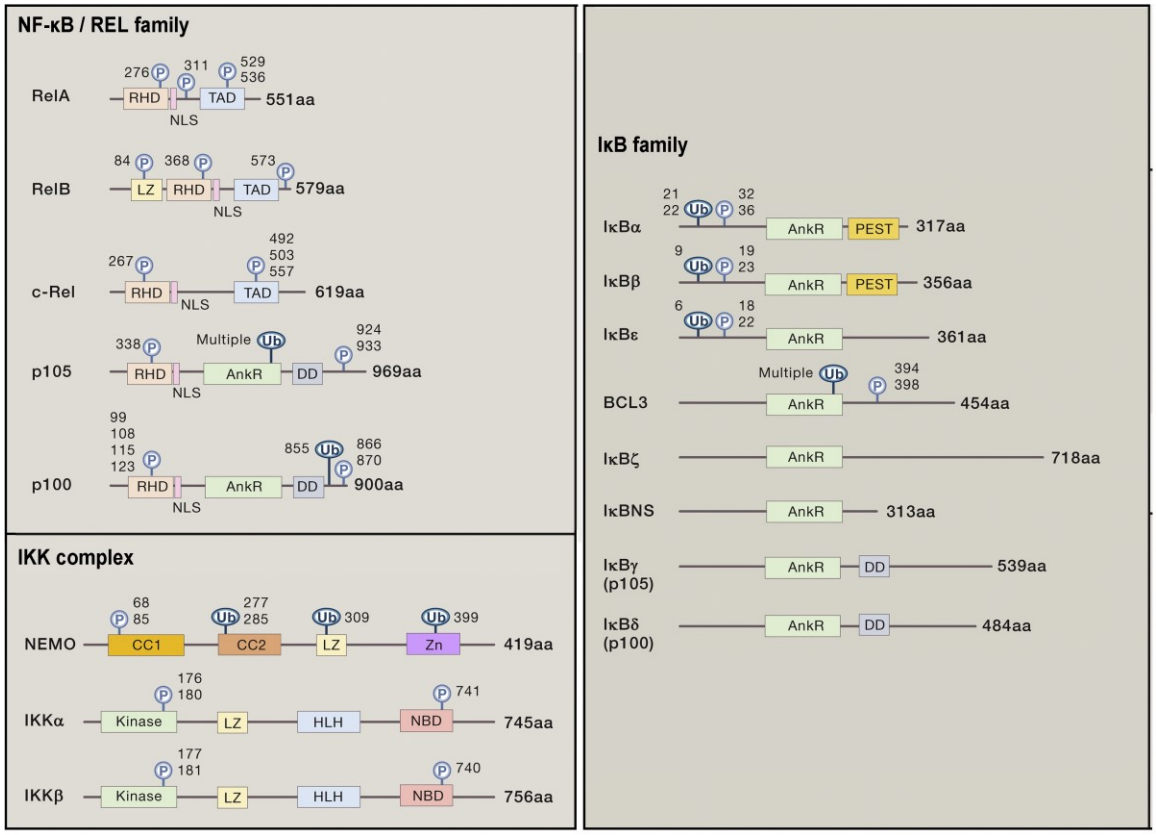

Figure 1.6 – Components of the NF-κB System. Members of the NF-κB, IκB, and IKK proteins family. The number of amino acids in each human protein is indicated on the right. Post-translational modifications that influence IKK activity or transcriptional activation are indicated with P and Ub for phosphorylation and acetylation. RHD, Rel homology domain; TAD, transactivation domain; LZ, leucine zipper domain; HLH, helix-loop-helix domain; Zn, zinc finger domain; CC1/2, coiled-coil domains; NBD, NEMO-binding domain; AnkR, ankyrin repeats; DD, death domain; PEST, region rich in the amino acids proline, glutamic acid, serine, and threonine. Adapted from (Zhang et al. 2017b).

The five NF-κB subunits are synthesized either as mature proteins with C-terminal transactivation domains (TADs) in the case of Rel A, Rel B, and c-Rel or as precursors with C-terminal ankyrin repeats (AnkR) that are post-translationally cleaved in the case of p105 (NFKB1) and p100

(NFKB2). AnkR is a hallmark domain of a dedicated set of inhibitory proteins and domains comprising the “Inhibitor of κB” (IκB) family (**Figure 1.6**). The members of the family–IκBα, IκBβ, IκBε, BCL-3, IκBz, IκBNS, and the C-terminal portions of the precursor proteins p105 (IκBγ) and p100 (IκBδ)–sequester the NF-κB proteins in the cytoplasm in the unstimulated steady state by masking their NLS.

NF-κB dimers are relieved from the inhibitory factors by IKK phosphorylation-mediated degradation of the IκB proteins or by limited proteolysis that eliminates the C-terminal portion of p100 and p105 to make p52 and p50 respectively. The proteolysis occurs constitutively in p105 but only after phosphorylation events in p100 (Hayden and Ghosh 2008). The signaling events that lead to removal of inhibitory factors can occur by the canonical pathway or the alternative pathway (**Figure 1.7**). The two pathways rely on a different set of IKKs, the kinases that phosphorylate IκB proteins (**Figure 1.6**). In the canonical pathway, IKKα, IKKβ, and NEMO form a classical three-factor IKK complex, in which IKKβ phosphorylates the IκB proteins. On the other hand, the alternative pathway utilizes a dimer of IKKα to phosphorylate p100. P100, which is mainly complexed with RelB, blocks NF-κB activation via its IκBδ moiety harboring the AnkR domain (Hacker and Karin 2006).

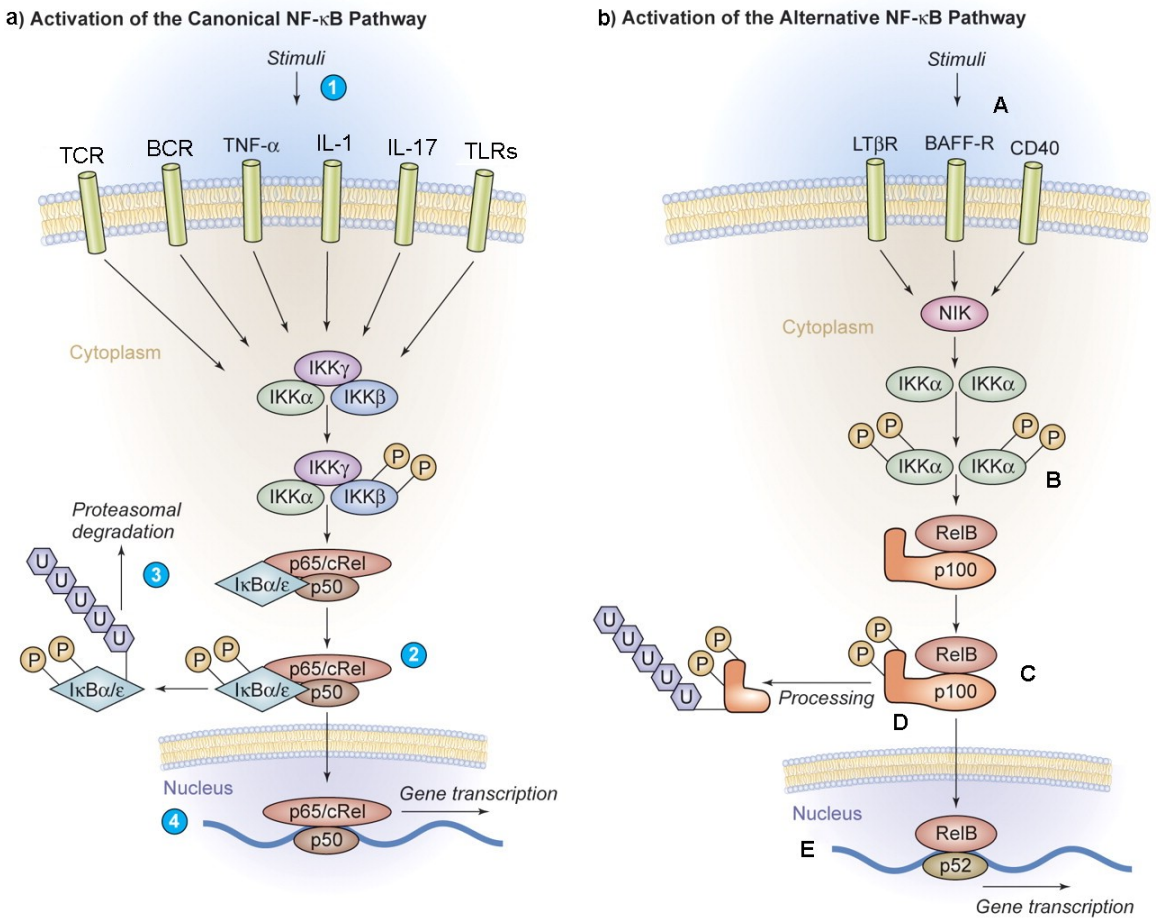

Figure 1.7 – Canonical and alternative pathway of NF-κB activation. a, Activation of the canonical NF-κB pathway. The stimuli that activate the canonical pathway include the antigen receptors TCR/BCR, proinflammatory cytokines (IL-1, IL-17, and TNF-α), and pathogen-associated molecular patterns that bind to TLRs (1). IκB proteins become phosphorylated at two serine residues by the activated IKK complex and subsequently polyubiquitinated by K48-linkage (2), which triggers proteasomal degradation (3). IκB demolition reveals NLS of the NF-κB dimers, which then translocate into the nucleus and activate target genes (4). **B,** Activation of the alternative NF-κB pathway. The members of TNF receptor superfamily, including CD40, the lymphotoxin β receptor, and the BAFF receptor trigger the alternative pathway (A). This pathway culminates in the NIK-mediated activation of IKKα dimer (B), which can directly phosphorylate p100 (C), inducing proteasomal partial proteolysis of p100 to remove the inhibitory ankyrin repeats and to generate p52 (D). The p52 protein preferentially dimerizes with RelB to translocate into the nucleus I. Adapted from (Jost and Ruland 2007).

The canonical pathway

In the canonical NF-κB pathway, also known as the classical pathway, various signaling cascades that involve different adaptor molecules ultimately converge on the classical IKK complex, a cytosolic IKK holoenzyme containing a non-catalytic regulatory subunit NEMO ("NF-κB essential modifier," also called IKKγ) and two kinase subunits IKKα and IKKβ. The upstream signaling

apparatuses transmit the stimuli to the IKK complex by oligomerizing into a polyubiquitinated signalosome, to which NEMO anchors the two kinase subunits by interacting with the ubiquitin chains. Following the activation of the IKK complex, the catalytic IKKβ subunit phosphorylates IκBα on Ser 32 and Ser 36, or IκBβ on Ser 19 and Ser 23. The phosphorylated IκB proteins then undergo proteasomal degradation triggered by the SCFβ−TrCP E3 ubiquitin ligase-mediated, K48-linked polyubiquitination and release the canonical NF-κB transcription factor, most famously the p50-p65 heterodimer (Hayden and Ghosh 2012) (**Figure 1.7a)**.

One of the most notable examples of the canonical NF-κB activation is antigen receptor signaling in T cells triggered by the ligation of the TCR and the costimulatory molecule CD28. Following the receptor engagement, FYN and LCK kinases phosphorylate immunoreceptor tyrosine-based activation motif (ITAM) on CD3ζ, which recruits and activates ZAP70 kinase. ZAP70 promotes signal diversification by phosphorylating Linker for activation of T cells (LAT), a signaling hub that forms numerous interactions with other signaling molecules including phospholipase Cγ (PLCγ). Activated PLCγ hydrolyzes plasma membrane phospholipid phosphatidylinositol 4,5-bisphosphate (PIP2) into two second messengers, diacylglycerol (DAG) and inositol 1,4,5-trisphosphate (IP3). In parallel, CD28 ligation results in phosphorylation of PIP2 by PI3K into phosphatidylinositol 3,4,5-trisphosphate (PIP3), which recruits PDK1 to become auto-phosphorylated. PKCθ, which binds to both DAG and phosphorylated PDK1, then translocates to the plasma membrane and phosphorylates CARD11. Phosphorylated CARD11 undergoes a structural change that allows the formation of the CARD11-BCL10-MALT1 (CBM) signaling complex, a shared intermediary of TCR and BCR signaling pathway that leads to NF-κB activation (Smith-Garvin et al. 2009) (**Figure 1.2**). The assembled CBM complex serves as a central scaffold that recruits ubiquitination and phosphorylation mediators in close proximity to generate signaling events. In conjunction with the E2 ubiquitin-conjugating enzymes ubiquitin-conjugating enzyme 13 (UBC13) and ubiquitin-conjugating enzyme variant 1A (UEV1A), the E3 ubiquitin ligases–tumor necrosis factor (TNF) receptor-associated factor 2 (TRAF2) and TRAF6, cellular inhibitor of apoptosis protein 1 (cIAP1) and cIAP2, and the linear ubiquitin chain assembly complex (LUBAC)–catalyze K63-linked and M1-linked ubiquitination of multiple proteins, including BCL10 and MALT1 themselves. Several of these

E3 ligases may have at least partially redundant functions or operate only in specific settings, as some studies found TRAF6 and LUBAC to be dispensable under certain conditions. The ubiquitination events enable the signaling platform to engage the TGFβ-associated kinase 1 (TAK1) complex, which includes ubiquitin-binding proteins TAK1-binding protein 2 (TAB2) and TAB3, and the classical IKK complex, a regulatory subunit NEMO of which associates with ubiquitin and becomes further ubiquitinated by TRAF6 and LUBAC. The recruited IKK complex becomes activated via TAK1-mediated and trans-auto-phosphorylation and subsequently catalyzes IκBα phosphorylation, which triggers K48-linked polyubiquitination followed by proteasomal degradation. Relieved from the inhibitory protein, NF-κB transcription factors then accumulate in the nucleus and activate target genes (Lork et al. 2019, Ruland and Hartjes 2019).

Newly expressed genes in response to NF-κB activation promote lymphocyte proliferation and specific immune functions such as generation of cytokines in T cells. Aberrant activation of NF-κB can foster immunodeficiency, autoimmune diseases, or lymphoid malignancies. Therefore, to tightly modulate the signaling, several deubiquitinases negatively regulate the pathway by removing ubiquitin chains from the signaling platform. TNF-α inducible protein 3 (TNFAIP3, also known as A20) and CYLD (cylindromatosis) eliminate the K63-linked ubiquitin chains, and more recently described OTULIN cleaves the M1-linked linear ubiquitin chains. NF-κB activation transcriptionally targets some of these deubiquitinases, as well as the IκB proteins, and establishes a negative feedback loop (Sun 2008, Keusekotten et al. 2013).

In addition to the antigen receptor in lymphocytes, the surface receptors that activate the canonical NF-κB pathway include Toll-like receptor (TLR), cytokine receptors, and tumor necrosis factor receptor (TNFR).

The alternative pathway

In the alternative pathway, or the non-canonical pathway, a dimer of IKKα controls the degradation of the inhibitory peptide masking the NF-κB transcription factor, independent of IKKβ, IKKγ, or the classical IKK complex. The most well-described NF-κB dimer of the alternative pathway is p52-RelB, which in resting state exists in the precursor form p100-RelB. IKKα phosphorylates p100 on serines 866 and 870 and induces proteasomal processing to p52, following selective proteolysis of

the C-terminal AnkR-containing precursor inhibitory domain, sometimes called IκBδ. The mature p52-RelB dimer then localizes to the nucleus and activates the NF-κB transcriptional program (Hayden and Ghosh 2008) (**Figure 1.7b**).

Activation of IKKα depends on the turnover of its activating kinase NF-κB-inducing kinase (NIK). Constitutively active, NIK is negatively regulated by TRAF3-mediated polyubiquitination that induces proteasomal degradation. The alternative pathway inducers, via various mechanisms, removes TRAF3 and thereby stabilizes NIK so it can phosphorylate IKKα. Whereas the canonical pathway generates rapid and transient response through oligomerization process, the alternative pathway operates under the control of protein destruction and re-synthesis and therefore in a slower and more sustained kinetics (Hayden and Ghosh 2008).

The receptors that activate the alternative pathway, such as Limphotoxin β receptor (LTβR), Receptor activator of nuclear factor κB (RANK), B cell-activating factor receptor (BAFFR), and CD40, mostly belong to the TNFR superfamily. Upon ligation of the receptor, CD40, for example, recruits TRAF2, which targets TRAF3 to proteasomes or complexes with it to displace NIK by allosteric competition (Hayden and Ghosh 2012). These receptors all share the common downstream NF-κB dimer p52-RelB but engender distinct transcriptional response. LTβR promotes the development of peripheral lymph nodes and Peyer's patches, RANK regulates bone formation and dendritic cell functions, BAFF drives peripheral B cell differentiation and survival, and CD40 controls B cell activation, maturation, germinal center formation, somatic mutation, and class switching. How a single dimer can produce such diverse outcomes is unknown (Zhang et al. 2017b).

Physiologic role of NF-κB signaling in normal lymphoid tissue

Studies have unequivocally demonstrated the pivotal physiologic role of NF-κB in the immune system. Mouse knockouts and human genetic disorders of the key NF-κB components predominantly result in immunological defects (Gerondakis et al. 2006, Steiner et al. 2018), inducers of NF-κB activation are frequently cytokines, antigens, and pathogens (Hayden and Ghosh 2012), and the transcriptional targets of the pathway include hundreds of immunity-related genes (http://www.bu.edu/nf-kb/gene-resources/targetgenes/).

Congruently, NF-κB plays an essential role in every facet of lymphocyte biology, including but not limited to development, activation, proliferation, and survival (Vallabhapurapu and Karin 2009, Gerondakis et al. 2014). The NF-κB target genes relevant for lymphocyte biology include positive cell-cycle regulators, antiapoptotic factors, and receptor ligands such as cytokines and chemokines. The cell-cycle regulators such as cyclin D1, cyclin D2, c-myc, and c-myb drive lymphocyte division (Duyao et al. 1992, Toth et al. 1995, Hinz et al. 1999, Romashkova and Makarov 1999) with the help of proliferation and survival signals provided by cytokine targets including IL-2, IL-6, and CD40L in both autocrine and paracrine fashion. NF-κB also directly induces survival via expression of caspase inhibitors of the cIAP family, the BCL2 family members A1 and BCL-XL, and cellular FLICE inhibitor protein (c-FLIP) (Thome and Tschopp 2001, Karin and Lin 2002).

The diverse expression patterns of these target genes result in a variety of functional outcomes in different stages of lymphocytes. In T cells, constitutive NF-κB activity for survival occurs at all stages of thymocyte differentiation and particularly in the double negative phase during the pre-TCR assembly (Gerondakis et al. 2014). NF-κB also participates in T cell proliferation and survival following TCR activation via myc-induced growth, IL-2 signaling, and death receptor pathways (Kontgen et al. 1995, Grumont et al. 2004, Jones et al. 2005) and contributes to the development and functional divergence of different helper T cell subsets (Oh and Ghosh 2013). B cell maturation requires both canonical and non-canonical NF-κB pathways from early stages of development. NF-κB activation promotes the transition from large to small pre-B cells (Jimi et al. 2005), controls the production of λ-chain B cells (Derudder et al. 2009), triggers anti-apoptotic signals in response to BCR cross-linking and BAFFR signaling (Castro et al. 2009), and enables antibody production and class-switching of mature B cells (Manis et al. 2002).

Pathogenic activation of NF-κB in lymphoid neoplasms

As NF-κB promotes lymphocyte proliferation and survival, its aberrant oncogenic activation has been described in various B and T cell lymphoid malignancies. Sections below discuss a few of the prominent examples.

Diffuse large B cell lymphoma

Diffuse large B cell lymphoma represents the most prevalent type of NHL, comprising about 40% of the cases, and consist of three discrete subtypes: germinal center B cell-like (GCB) DLBCL, activated B cell-like (ABC) DLBCL, and primary mediastinal B cell lymphoma (PMBL), which arise from different stages of normal B cell differentiation and utilize distinct oncogenic pathways (Staudt and Dave 2005).

Constitutive activation of the NF-κB pathway is a hallmark of ABC DLBCL. Gene expression profiling studies revealed enrichment of NF-κB target genes in ABC DLBCL tumor biopsy samples and cell line models (Davis et al. 2001), and genomic profiling identified genetic aberrations activating NF-κB in more than two thirds of the patients (Ngo et al. 2011, Pasqualucci et al. 2011). Consistently, NF-κB inhibition using a non-degradable form of IκBα or a small molecule IKKβ inhibitor resulted in apoptosis in ABC DLBCL cell lines (Davis et al. 2001, Lam et al. 2005).

NF-κB-related genes aberrations detected in ABC DLBCL include activating mutations in the regulators of the BCR – *CARD11* (9%) (Lenz et al. 2008) and *CD79* (21%) (Davis et al. 2010) – and TLR – *MYD88* (30%) (Ngo et al. 2011) – as well as inactivating mutations in the negatively regulating deubiquitinase *TNFAIP3* (30%) (Compagno et al. 2009, Kato et al. 2009). Recently, a report of oncogenic BCR signaling supercomplex (MyD88-TLR9-BCR) described a NF-κB-activating multiprotein signalosome in ABC DLBCL that clusters BCR, CD79a/b, MyD88, and downstream signaling effectors such as IKKs on the endolysosome membrane to facilitate synergistic signaling and crosstalk (Phelan et al. 2018). The clinical success of ibrutinib, a Bruton's tyrosine kinase (BTK) inhibitor that blocks BCR signaling, evidences the oncogenic mechanism of chronic BCR activation in these tumors (Wilson et al. 2015).

NF-κB signaling in ABC DLBCL results in the expression of IRF4 (Lam et al. 2005), which drives plasmacytic differentiation in both normal lymphocytes and in malignant cells (Klein et al. 2006, Sciammas et al. 2006, Shaffer et al. 2008). Interestingly, the tumor cells escape the cell cycle arrest typical in normal plasma cells by halting the differentiation at the plasmablastic stage (Calado et al. 2010), thanks to the frequent genetic lesions that inactivate Blimp-1, another plasma cell

differentiation factor that cooperates with IRF4 in normal B cells (Tam et al. 2006, Schmidlin et al. 2008, Mandelbaum et al. 2010).

Additionally, high expression of IL-6 in response to NF-κB signaling in ABC DLBCL generates an autocrine signaling loop via activation of JAK-STAT pathway. IL-6 binds to its own receptors and triggers JAK-STAT activation and STAT3 phosphorylation, causing interaction between 31hosphor-STAT3 and NF-κB heterodimers to enhance transactivation of NF-κB target genes (Yang et al. 2007, Lam et al. 2008).

In contrast, GCB DLBCL demonstrate little NF-κB activation (Compagno et al. 2009), and PMBL, while the details are still unclear, show NF-κB activity similar to Hodgkin lymphoma (Rosenwald et al. 2003, Savage et al. 2003, Schmitz et al. 2009).

Hodgkin lymphoma

The defining feature of Hodgkin lymphoma is the presence of malignant Hodgkin and Reed/Sternberg (HRS) cells surrounded by a sea of inflammatory cells from a variety of hematopoietic lineages. In approximately a half of Hodgkin lymphoma cases, the HRS cells harbor EBV, which encodes a potent NF-κB activator latent membrane protein 1 (LMP1). Constitutive NF-κB activity is also present in the other half of EBV-negative Hodgkin lymphoma, evidenced by high levels of nuclear p50-p65 heterodimers (Bargou et al. 1996) and IκBα super repressor-induced toxicity (Bargou et al. 1997). Mutational profiling of Hodgkin lymphoma later revealed inactivating mutations in negative regulators of the canonical NF-κB pathway, including IκBα-encoding *NFKBIA* (20%) (Cabannes et al. 1999, Emmerich et al. 1999, Jungnickel et al. 2000, Lake et al. 2009), IκBε-encoding *NFKBIE* (Emmerich et al. 2003), and *TNFAIP3* (44%) (Schmitz et al. 2009). In addition, some reports have documented evidence in support of a role for the inflammatory milieu surrounding the malignant cells in contributing to the NF-κB activation in the malignant cells via paracrine signaling (Schwab et al. 1982, Gruss et al. 1994, Carbone et al. 1995, Pinto et al. 1996, Molin et al. 2002).

MALT lymphoma

Mucosa-associated lymphoid tissue (MALT) lymphoma, a form of marginal zone lymphoma, occurs most commonly in the stomach but also in a variety of anatomical sites near mucosal surfaces. MALT lymphoma frequently arises in the setting of extrinsic BCR activation attributable to autoimmune reactions induced by infectious agents such as *Helicobacter pylori*, *Chlamydia psittaci*, *Campylobacter jejuni*, *Borellia burgdorferi*, and hepatitis C virus (Ferreri and Zucca 2007). Remarkably, eradication of *H. pylori* by antibiotic treatment causes sustained complete remissions in many low-grade gastric MALT lymphoma patients (Wotherspoon et al. 1993).

However, a substantial portion of cases fail to regress after eradication of the underlying extrinsic cause, suggesting an acquisition of antigen independent growth. Several chromosomal translocations that trigger intrinsic oncogenic NF-κB activity have been described in MALT lymphoma. About 25% of gastric MALT lymphoma and 40% of lung MALT lymphoma contain a t(11:18) translocation that results in a fusion protein cIAP2-MALT1 (Akagi et al. 1999, Dierlamm et al. 1999, Morgan et al. 1999, Streubel et al. 2004). Less commonly, a t(14;18) translocation (7% in ocular adnexa and 6% in lung) and a t(1;14) translocation (9% in lung and 4% in stomach) induce overexpression of MALT1 and BCL10 protein respectively by juxtaposing the genes encoding them with the immunoglobulin heavy chain (IgH) locus (Willis et al. 1999, Zhang et al. 1999, Sanchez-Izquierdo et al. 2003). Splenic hyperplasia and increased and constitutive NF-κB activity in mice harboring these genetic rearrangements (Baens et al. 2006, Li et al. 2009) coincide with the essential roles of MALT1 and BCL10 in BCR-triggered NF-κB activation (Ruland and Hartjes 2019). The cIAP2-MALT1 fusion protein aberrantly activates both the canonical pathway and the alternative pathway. Mechanistically, it constitutively activates canonical NF-κB pathway via heterotypic interaction between the BIR1 domain of the cIAP2 and the C-terminal region of MALT1 that results in auto-oligomerization (Zhou et al. 2005, Lucas et al. 2007). Reminiscent of the NF-κB-activating artificial MALT1 dimers (Lucas et al. 2001, Sun et al. 2004, Zhou et al. 2004), the oligomerized fusion proteins may serve as a multivalent platform for the recruitment of the ubiquitin ligases like TRAF6 (Zhou et al. 2005, Noels et al. 2007) and ubiquitin-binding signaling factors such as IKK complex (Gyrd-Hansen et al. 2008), ultimately facilitating the NF-κB signaling. In addition,

cIAP2-MALT1 oligomerization can activate the paracaspase function of the fusion protein's MALT1 moiety, cleaving TNFAIP3 and CYLD and eliminating the negative regulators of the pathway (Coornaert et al. 2008, Staal et al. 2011). A positive feedback loop may exist between cIAP2-MALT1 and NF-κB activation, as the expression of the fusion protein is under the control of the cIAP2 promoter, an NF-κB target (Hosokawa et al. 2005).

The alternative pathway activation by cIAP2-MALT1 fusion arise from its interaction with NIK. The cIAP2 moiety recruits NIK and places it in close proximity of MALT1 protease domain, which cleaves NIK at Arg 325. The resulting C-terminal NIK fragment resists TRAF3-dependent proteasomal degradation but maintains the kinase activity to constitutively activate the signaling (Rosebeck et al. 2011).

Multiple myeloma

Multiple Myeloma (MM) is an aggressive malignancy derived from plasmacytic cells dwelling in the bone marrow and represents the second most prevalent hematological malignancy. Gene expression profiling studies from as early as 2007 have demonstrated the role of deregulated NF-κB activity in MM. A distinct patient cluster characterized by NF-κB enrichment responded substantially better to bortezomib, a proteasome inhibitor that blocks IκB degradation, as compared to other patient groups (Chng et al. 2007). Later studies revealed molecularly heterogeneous mechanisms of NF-κB activation in MM.

Reports of NF-κB-activating mutations in MM emerged as early as in 2007, mapping close to 20% of genetic mutations onto various regulators and effectors of NF-κB signaling (Annunziata et al. 2007, Keats et al. 2007). Subsequent sequencing studies substantiated the prevalence of NF-κB-activating mutations in a diverse set of genes, ranging from those in the canonical pathway such as *TLR4*, *IKBKB* (encoding IKKβ), *CARD11*, *CYLD*, and *TNFAIP3*, to those in the alternative pathway including *MAP3K14* (encoding NIK) and *TRAF3* (Chapman et al. 2011, Lohr et al. 2014, Troppan et al. 2015, Walker et al. 2015). Signals from the tumor microenvironment, including physical cell-cell communications and autocrine and paracrine soluble factors like IL-1β, IL-6, and TNF-α, augments the NF-κB signaling in both tumor and non-tumor cells (Hideshima et al. 2007, Fairfield et al. 2016). Importantly, the therapeutic efficacy of immunomodulatory drugs such as

thalidomide and lenalidomide in MM has been at least in part attributed to their ability to inhibit the aforementioned pro-inflammatory cytokines (Quach et al. 2010). Additional NF-κB-activating tumor microenvironment factors documented in MM pathogenesis include BAFF (Moreaux et al. 2004, Hengeveld and Kersten 2015), and a proliferation-inducing ligand (APRIL) (Tai et al. 2016), RANK ligand (RANKL) (Schmiedel et al. 2013).

Many have explored the tumor growth and drug resistance effects of NF-κB activation in MM, mediated by both the direct anti-apoptotic targets and the indirect signal inducer targets that further perpetuates the pro-survival signaling (Hideshima et al. 2007, Fairfield et al. 2016, Touzeau et al. 2018). Consistently, therapeutic intervention for MM involves proteasome inhibitors that block IκB degradation and ultimately NF-κB signaling and immunomodulatory drugs that attenuates NF-κB autocrine and paracrine loops by acting on pro-inflammatory cytokines (Chim et al. 2018).

Peripheral T cell lymphoma

The NF-κB signaling in PTCL may be best characterized in adult T cell leukemia-lymphoma (ATL), a lymphoma caused by human T cell leukemia virus type 1 (HTLV-1) infection that occurs more frequently in HTLV-1–endemic areas such as southwestern Japan, the Caribbean Islands, Central and South America, intertropical Africa, and the Middle East (Iwanaga et al. 2012, Ishitsuka and Tamura 2014). Constitutive NF-κB activation in ATL (Mori et al. 1999) stems from various molecular mechanisms. *In vitro* and *in vivo* studies have demonstrated that the HTLV-1 Tax 34hosphor-oncoprotein drives tumor development via NF-κB activation (Zhang et al. 2017a). Cell intrinsic mechanisms of NF-κB activation include NIK overexpression mediated by miR-31 silencing (Saitoh et al. 2008, Yamagishi et al. 2012) and mutations in genes involved in the lymphocyte antigen receptor-NF-κB axis such as *PLCG1* (36%), *PRKCB* (33%; encoding PKCβ, a B cell counterpart of PKCθ), *CARD11* (24%) and *VAV1* (18%) (Kataoka et al. 2015).

Other subtypes of PTCL have also shown evidence of NF-κB activation. Initial gene expression profiling and immunohistochemical (IHC) studies done in small scale or in cell line model to assess NF-κB activation status in PTCL have reported mixed results (Martinez-Delgado et al. 2004, Martinez-Delgado et al. 2005, Ballester et al. 2006, Piccaluga et al. 2007, Odqvist et al. 2013), but the more recent genetic, biochemical, and animal model studies demonstrate a more coherent

relationship between NF-κB activity and PTCL pathogenesis, especially in AITL and PTCL, NOS. A large-scale gene expression profiling study examining 144 lymphomas with broad representation of PTCL subtypes successfully delineated the biological subgroups, re-classified many PTCL, NOS cases based on the clustering, and reported a shared common signature of NF-κB enrichment in the AITL and PTCL, NOS cases that belong to the AITL subgroup (Iqbal et al. 2010). In addition, genomic sequencing studies, as discussed in the previous sections of the chapter ("Genetic and Molecular Landscape of PTCL"), have revealed diverse recurrent genomic abnormalities that lead to aberrant TCR and co-stimulatory signaling and in particular downstream NF-κB effector pathway in PTCL (**Figure 1.2** and **Table 1.2**). Moreover, activated TCR or NF-κB signaling is described in all existing genetically manipulated murine models of AITL and PTCL, NOS (Pechloff et al. 2010, Wang et al. 2011, Beachy et al. 2012, Cortes et al. 2018, Mondragon et al. 2019, Kim and Cortés unpublished). In particular, PTCL development in T cell-conditional *Nfkbia* knockout mouse, whose lack of IκBα results in the constitutive NF-κB signaling, emphatically illustrates the capacity of NF-κB activity to transform T cells (Mondragon et al. 2019). Despite these recent advances, however, the genetic and biochemical mechanism by which NF-κB is aberrantly activated as well as the oncogenicity of the NF-κB-activating genetic lesions in human PTCL remain unclear.

Therapeutic targeting of NF-κB

The crucial role of aberrant NF-κB activation in the pathogenesis of lymphoid malignancies presents a compelling rationale in support of therapeutic targeting of NF-κB in these diseases. Small molecule inhibitor that modulates NF-κB activity have achieved some success in clinics, including BTK inhibitor ibrutinib in ABC DLBCL (Wilson et al. 2015) and proteasome inhibitors bortezomib (Richardson et al. 2006), carfilzomib (Groen et al. 2019), and ixazomib (Richardson et al. 2018) in MM. Ibrutinib blocks BCR signaling and consequently BCR-mediated NF-κB activation (Young et al. 2015). Proteasome inhibitors prevent degradation of the canonical NF-κB inhibitor IκBα among many other proteins (Manasanch and Orlowski 2017). These pharmacologic inhibitors, however, do not selectively target the core components of the pathway and thus limited in their use.

Many have aggressively pursued IKK inhibition as one of the key druggable points in the NF-κB pathway (Karin et al. 2004). However, multiple drugs that appeared to have succeeded in preclinical models have failed in clinical trials due to either safety concerns or lack of efficacy resulting from dose-limiting toxicity of the global NF-κB blockade

(Prescott and Cook 2018).

Some of the more promising NF-κB drug targets currently in development include other components of the IKK complex IKKα or NEMO, IκBα Degradation and NF-κB subunits (Begalli et al. 2017, Bennett et al. 2018).

III. Fyn Src family kinase

Src family kinases (SFKs) are a group of non-receptor tyrosine kinases that include Src, Yes, Fyn, Fgr, Lck, Hck, Blk, Lyn, and Frk. In the 1970s, Mike Bishop and Harold Varmus isolated the gene encoding the first member of the family to be identified, *SRC*, and described its role in cancer development, defining what we now know as proto-oncogenes (Martin 2001). Multiple studies subsequently implicated SFKs in the development and maintenance of several cancers, including hematological malignancies (Zhang and Yu 2012, Ku et al. 2015).

Among the nine Src family members, T cells throughout their lifespan primarily express Lck and Fyn. The two kinases serve specific and overlapping functional roles in T cell development and activation. This section will briefly discuss the structure and function of the Fyn kinase in the context of T cells.

Domain structure of Fyn kinase

Structural domains of Fyn are typical of SFKs: N-terminal Src-homology 4 (SH4) domain that contains attachment sites for saturated fatty acid addition, a “unique” domain particular to each member of the family, an SH3 and SH2 domain protein interaction domains, a tyrosine kinase domain SH1, and a C-terminal negative regulatory domain (**Figure 1.8a**). Post-translationally, the myristoylation of glycine 2 and the palmitoylation of cysteines 3 and 6 following the removal of the start methionine in SH4 domain anchor the kinase to the plasma membrane (Rawat and Nagaraj 2010). Some studies in T cells have also indicated that Fyn interacts with the CD3 chain of the TCR complex, and in particular with ITAMs, via the SH4 domain (Timson Gauen et al. 1992, Timson Gauen et al. 1996, zur Hausen et al. 1997). The unique domain is the most divergent among the SFKs and likely to contribute substantially to the functional specificity of Lck and Fyn in T cells. The better characterized Lck unique domain, for example, contains a di-cysteine motif that mediates the kinase’s association with the CD4 and CD8 co-receptors (Turner et al. 1990, Kim et al. 2003). The SH3 and SH2 domains facilitate intra- and inter-molecular protein interactions and may confer adapter functions to the kinase in addition to its role as a tyrosine kinase (Zamoyska et al. 2003). Notably, even the SH1 kinase domain of Lck, the region that shows the most sequence homology

with Fyn (**Figure 1.8a**), does not fully share its function with the Fyn kinase domain (Lin et al. 2000). Not surprisingly given such difference, Fyn and Lck have overlapping but different sets of interacting partners (**Table 1.6**).

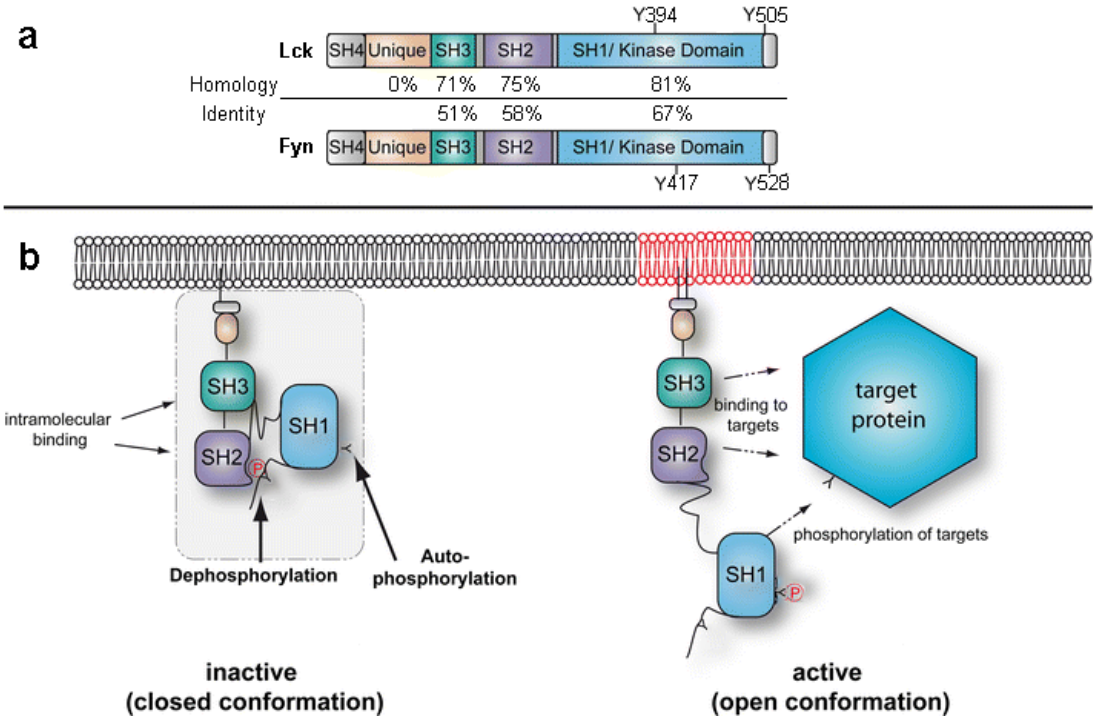

Figure 1.8 – Fyn and Lck, Src family kinases. A, Domain structure of of Fyn (bottom) and Lck (top) kinases. Sequence homology and identity between the two related kinases are also indicated. **b,** Self-inhibitory mechanism of the Src family kinases. In the inactive or basal state, the kinase is in a closed conformation due to intramolecular binding of the SH2 domain with the phosphorylated tyrosine residue of the C-terminal regulatory region. Additionally, the SH3 domain interacts with a polyproline type II linker helix between the SH2 and SH1 domains to further lock the inactive conformation. Upon dephosphorylation of the C-terminal tyrosine or binding of external ligands to SH2 or SH3 domains, the conformation changes to an open form that is regarded as the active state. Intermolecular autophosphorylation of tyrosine in the SH1 kinase domain stabilizes the active state. Adapted from (Zamoyska et al. 2003) and (Kramer-Albers and White 2011).

Table 1.6 – Selected list of published Fyn and Lck interacting partners. Adapted from (Zamoyska et al. 2003).

Protein	Binds to	Published in
CD3	Fyn	(Samelson et al. 1990, Timson Gauen et al. 1992, Osman et al. 1996, Timson Gauen et al. 1996)
Pyk2	Fyn	(Qian et al. 1997)
SAP/SLAM	Fyn	(Marie-Cardine et al. 1998)
Shc	Fyn	(Wary et al. 1998)
Gab-2	Fyn	(Parravicini et al. 2002)
WASp	Fyn	(Badour et al. 2004)
Zap-70	Fyn, Lck	(Duplay et al. 1994, Fusaki et al. 1996)
PI3K	Fyn, Lck	(Thompson et al. 1992, Susa et al. 1996)
c-Cbl	Fyn, Lck	(Tsygankov et al. 1996, Hawash et al. 2002)
Sam68	Fyn, Lck	(Fusaki et al. 1997)
CD2	Fyn, Lck	(Beyers et al. 1992)
IL-2R	Fyn, Lck	(Hatakeyama et al. 1991, Kobayashi et al. 1993)
Fas	Fyn, Lck	(Atkinson et al. 1996, Schlottmann et al. 1996)
CD4/8	Lck	(Turner et al. 1990, Kim et al. 2003)
CD45	Lck	(Schraven et al. 1991, Ng et al. 1996)
MAPK	Lck	(August and Dupont 1996)
RasGAP	Lck	(Amrein et al. 1992)
Raf-1	Lck	(Pathan et al. 1996)
Lad	Lck	(Choi et al. 1999)

Regulation of Fyn activation

As in other SFKs, autoinhibitory mechanism regulates the activity of the Fyn kinase. In the inactive state, the phosphorylated Tyr 528 at the C-terminus negative regulatory region forms an intramolecular bond with the SH2 domain of the kinase, keeping the kinase in an inactive closed conformation. In addition to the Tyr 528 phosphorylation, mediated by C-terminal Src kinase (Csk), the SH3 domain of Fyn interacts with the polyproline type II linker helix between the SH2 and SH1 domains to further lock the inactive conformation. Upon dephosphorylation of Tyr 528 by phosphatase CD45, the C-terminal of the kinase releases the SH2 domain to unmask the catalytic region of the protein and activate the kinase. Additionally, the kinase trans-phosphorylate each other at Tyr 417 to stabilize the active state (**Figure 1.8b**) (Salmond et al. 2009).

The role of Fyn in T cell development and function

Mechanistically, Fyn along with Lck plays a crucial role in initiating the TCR signaling by phosphorylating and activating the cytoplasmic tail of the CD3 subunit in the receptor complex. For a more detailed overview of the proximal signaling following TCR activation, see section "NF-κB signaling in lymphoma – Overview of NF-κB signaling pathway – The Canonical Pathway." In addition, mouse model studies have demonstrated the functional significance of Fyn in T cells.

One of the major steps of the thymocyte development occurs following the TCR β chain rearrangement to select for only the cells that express functional β chains. In this process, called the β selection, cells cannot survive without signaling triggered via pre-TCR, a signaling complex formed by the β chain and pre-TCRα.

The complete lack of cells that pass the β selection in the double knockout *Lck*$^{-/-}$ *Fyn*$^{-/-}$ mice indicates the crucial role of these SFKs in T cell development (Groves et al. 1996, van Oers et al. 1996). In single knockout mouse models, *Fyn*$^{-/-}$ mice are normal in numbers and proportions of thymocytes (Appleby et al. 1992, Stein et al. 1992), in contrast to Lck deficient mice, which show about 90% reduction in the number of thymocytes that survive the β selection (Molina et al. 1992). Similarly, Lck-deficient mouse T cells have a 10-fold decreased proliferative response after CD3 stimulation (Molina et al. 1992), whereas Fyn-deficient mouse T cells show only mild impairment apart from the dramatic reduction in IL-2 production (Appleby et al. 1992, Stein et al. 1992). These mouse models suggest that while both Lck and Fyn play important roles in T cell development and activation, Fyn function appears to overlap significantly with the role of Lck.

IV. NF-κB activating signal transducer, TRAF3IP2

TRAF3IP2 encodes the NF-κB activating signal transducer TRAF3IP2, also known as Act1 or CIKS, which belongs to the similar expression of fibroblast growth factor/ interleukin-17 receptor (SEFIR) domain protein family. SEFIR is a homotypic protein interaction domain that is distantly related to the toll/interleukin-1 receptor (TIR) homology domain of toll-like receptors (TLRs), interleukin-1 receptor (IL-1R), and their adaptor proteins such as Myd88 (Novatchkova et al. 2003). The only member of the SEFIR family identified besides the interleukin-17 (IL-17) receptors, TRAF3IP2 binds to the SEFIR domain of IL-17Rs and serves an essential role in all known IL-17-dependent signaling pathways, most prominently NF-κB activation (Gu et al. 2013). Of note, structure studies have shown that TRAF3IP2 can also homo-oligomerize via the SEFIR domain (Mauro et al. 2003, Zhang et al. 2013).

IL-17 promotes inflammatory response either by transcriptional activation of the proinflammatory genes or by stabilization of target mRNA transcripts. As hematopoietic cells largely lack expression of IL-17 receptor C (IL-17RC), an essential subunit of the predominant form of the IL-17R complex, the response to IL-17 primarily arise from non-hematopoietic cells (Ho et al. 2010, Amatya et al. 2017).

IL-17R signaling is analogous to IL-1R/TLR pathways in that the proximal signal transduction occurs via homotypic protein-binding domain interaction between the receptor and the adaptor protein. Upon receptor ligation, TRAF3IP2 via its C-terminal SEFIR domain (**Figure 1.9**) binds to the IL-17R complex. In addition to its role as an adaptor that links the receptor signal and the effector tumor necrosis factor receptor (TNFR)-associated factor (TRAF) proteins, TRAF3IP2 also serves as a K63 E3 ubiquitin ligase via the U-box domain (Liu et al. 2009) (**Figure 1.9**). TRAF3IP2 recruits another K63 E3 ligase TRAF6 via the N-terminal TRAF-binding motif (Ryzhakov et al. 2011, Sonder et al. 2011) and together initiates a poly-ubiquitinated scaffold that brings TAK1 and IKK complex to ultimately activate the canonical NF-κB signaling (**Figure 1.10**) (see section “NF-κB signaling in lymphoma – Overview of NF-κB signaling pathway – The Canonical Pathway” for details on the role of protein oligomerization, ubiquitination, and IKK recruitment in the canonical NF-κB activation). In addition to NF-κB activation, TRAF3IP2 also participates in mitogen-activated

protein kinase (MAPK) pathways and TRAF2 and TRAF5-mediated stabilization of target gene mRNAs (Amatya et al. 2017) (**Figure 1.10**). NF-κB activation, however, is the most prominent event downstream of TRAF3IP2, as evidenced by the overrepresentation of NF-κB promoter elements in IL-17 target genes (Shen et al. 2006).

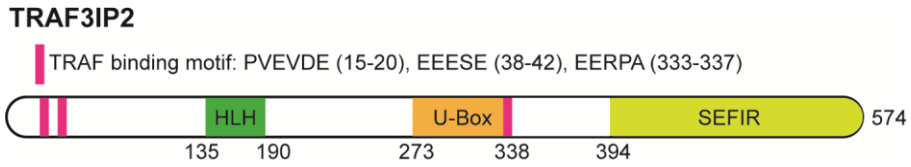

Figure 1.9 – Domain structure of TRAF3IP2. HLH, Helix-loop-helix domain; SEFIR, similar expression of fibroblast growth factor/ interleukin-17R (SEFIR) domain. The amino acid sequence and the location of the three TRAF binding motif are indicated.

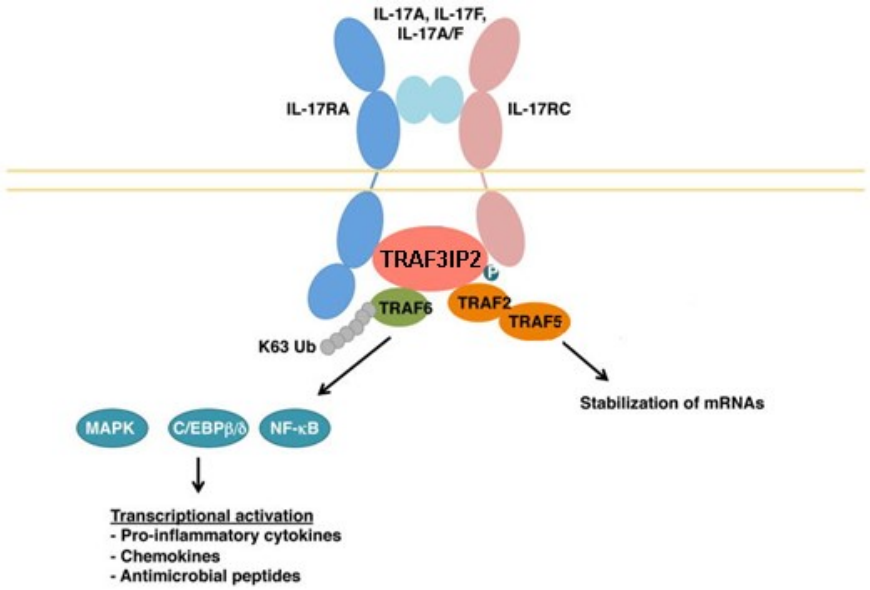

Figure 1.10 – Activation of IL-17 Signal Transduction. Receptor ligation enables homotypic interactions between the SEFIR domains in the receptor and in TRAF3IP2. TRAF3IP2-induced K63-linked ubiquitination of TRAF6 activates the MAPK, C/EBPβ and NF-κB pathways, triggering transcriptional activation of downstream target genes, including pro-inflammatory cytokines, chemokines and antimicrobial peptides. Additionally, TRAF3IP2, when phosphorylated at amino acid 311, recruits TRAF2 and TRAF5 to stabilize mRNA transcripts of certain target genes. Adapted from (Monin and Gaffen 2018).

Unexpectedly, in B cells that lack the classical IL-17 receptor, TRAF3IP2 serves as a negative regulator of BAFF and CD40 signaling (Qian et al. 2004). While the mechanism is not entirely clear, protein interaction studies seem to indicate that TRAF3IP2 suppresses the signaling by recruiting

TRAF3 (Qian et al. 2004). Given the role of TRAF3 in NIK activity (see section “NF-κB signaling in lymphoma – Overview of NF-κB signaling pathway – The Alternative Pathway”), TRAF3IP2 may negatively mediate the alternative NF-κB signaling and positively regulate the canonical pathway depending on the context.

Given the significant role that TRAF3IP2 plays in NF-κB activation and inflammation, TRAF3IP2 is implicated in various inflammatory diseases, including psoriasis (Hobbs et al. 2017), candidiasis (Okada et al. 2016), and ischemic injury (Erikson et al. 2017).

V. Specific Aims

Peripheral T cell lymphomas (PTCL) are highly aggressive lymphoid tumors derived from post-thymic mature T cells. Angioimmunoblastic T cell lymphoma (AITL) and PTCL, not otherwise specified (PTCL, NOS) account for about half of the cases and show poor outcomes under current therapeutic options. Despite major advances in the understanding of PTCL tumor biology over the past few years, AITL and PTCL, NOS still lack clear actionable targets. Therefore, discovering new oncogenic drivers and defining their mechanism of action are major research imperatives in AITL and PTCL, NOS.

Previous exome sequencing studies have revealed a diverse set of point mutations, indels, and copy number changes in AITL and PTCL, NOS, but reports of gene fusions have been scarce. Considering the important role that chromosomal rearrangements play in the pathogenesis and clinical management of other hematologic malignancies, my central hypothesis is that gene fusions induce oncogenesis in AITL and PTCL, NOS by aberrantly activating a specific pathway that is central to the pathogenesis of the disease. In that context, identification and characterization of fusion oncogene in AITL and PTCL, NOS will enable us to better understand the disease and facilitate the development of effective therapeutics. Thus, the central goal of this thesis was to identify and functionally characterize fusion genetic drivers of T cell transformation in AITL and PTCL, NOS. Towards this goal, I proposed the following aims:

Aim 1: To identify recurrent fusion genes in AITL and PTCL, NOS.

Aim 2: To functionally characterize the role of novel fusion genes in T cell transformation *in vitro* and *in vivo*.

Aim 3: To therapeutically target the downstream effector pathogenic mechanism of PTCL fusion oncogenes.

Chapter 2: Identification of a *FYN-TRAF3IP2* gene fusion in PTCL

With the goal of identifying new therapeutic targets in PTCL, we investigated the presence of new recurrent gene fusion events in RNAseq data from a cohort of 101 PTCL samples consisting of AITL (n=60) and PTCL, NOS (n=41) cases (Abate et al. 2017). These analyses identified the presence of chimeric reads spanning exon 8 of *FYN* and exon 3 of *TRAF3IP2* in two AITL cases supporting expression of a new recurrent *FYN-TRAF3IP2* fusion joining the *FYN* non-receptor tyrosine kinase gene (Palacios and Weiss 2004) and *TRAF3IP2*, which encodes a cytoplasmic adapter signaling protein downstream of the interleukin 17 receptor (IL17R) (Li et al. 2000, Chang et al. 2006, Qian et al. 2007) (**Figure 2.1a** and **Table 2.1**).

Table 2.1 – Chimeric FYN-TRAF3IP2 RNAseq reads.

Sample	Diagnosis	*FYN* breakpoint	*TRAF3IP2* breakpoint	Reads	Split reads
TP47	AITL	111,702,885	111,592,094	37	29
TP58	AITL	111,702,885	111,592,094	11	9

Reverse-transcription PCR (RT-PCR) amplification and dideoxynucleotide sequencing validated the expression of the *FYN-TRAF3IP2* fusion mRNAs in each of these index samples (**Figure 2.1b**). In addition, extended analysis by RT-PCR and sequencing of an independent panel of PTCL RNA samples with broad representation of PTCL subtypes (**Table 2.2**) revealed the presence of *FYN-TRAF3IP2* fusion transcripts in 8/28 cases (28%), which included 4/9 (44%) AITLs, 3/6 (50%) PTCL, NOS cases and one extranodal NK/T cell lymphoma, nasal type sample (**Figure 2.1c** and **2.2**).

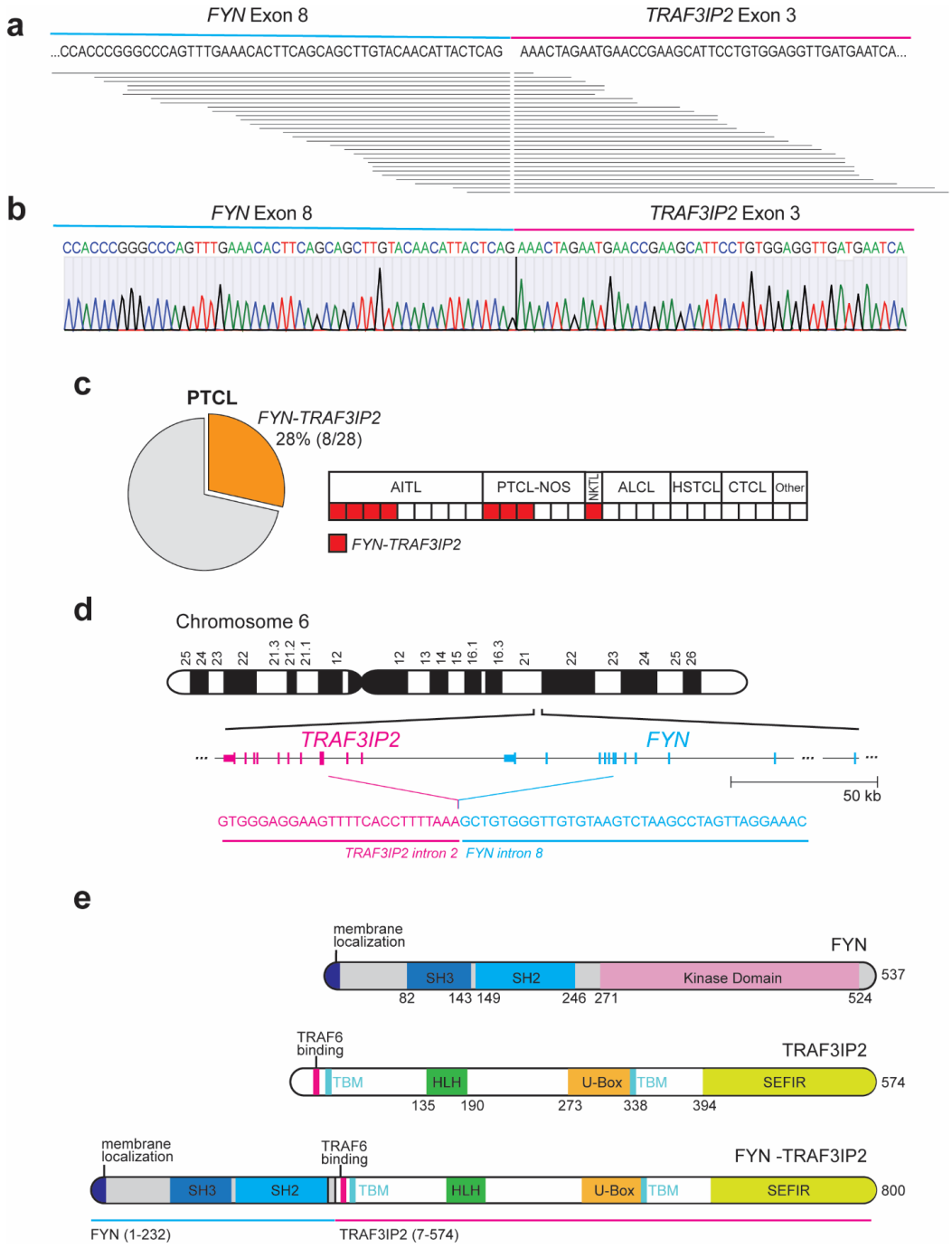

Figure 2.1 – Identification of the FYN-TRAF3IP2 gene fusion in PTCL. A, Schematic representation of the *FYN-TRAF3IP2* fusion transcripts identified in RNAseq. Each horizontal line represents a chimeric *FYN-TRAF3IP2* RNAseq read. **B,** Representative dideoxynucleotide sequencing result of the *FYN-TRAF3IP2* cDNA from a PTCL index sample. **C,** Frequency and distribution across PTCL groups of samples harboring the *FYN-TRAF3IP2* fusion transcript (total, n=28; AITL, n=9; PTCL, NOS, n=6; Extranodal NKTCL, nasal type, n=1; ALCL, n=2; HSTCL, n=3; CTCL, n=3; ATL, n=1; SPTCL, n=1). **D,** Schematic representation of the chromosomal rearrangement event resulting in expression of the *FYN-TRAF3IP2* fusion RNA and breakpoint sequence identified by whole genome sequencing. **E,** Schematic representation of the structures of the FYN kinase, TRAF3IP2 protein, and FYN-TRAF3IP2 fusion protein. SH3, Src homology 3 domain; SH2, Src homology 2 domain; TBM, TRAF-binding motif; HLH, Helix-loop-helix domain; SEFIR, SEF/IL-17R signaling domain.

Table 2.2 – List of patient samples analyzed by reverse transcription and PCR amplification.

Sample #	Tumor % Estimate	Tissue Site	Reduced Diagnosis	Fusion
1	40%	Lymph Node, Left Axillar	AITL	
2	30%	Lymph Node, Left Posterior Cervical	AITL	
4	30%	Lymph Node, Right Neck	PTCL, NOS TFH	yes
5	50%	Spleen	HSTCL	
6	40%	Lymph Node, Right Level 4	AITL, recurrent	yes
7	15%	Spleen	PTCL, NOS	yes
8	70%	Lymph Node, Neck Level 2	ATL	
9	40%	Lymph Node, Right Axillary	PTCL, NOS, recurrent	
10	50%	Lymph Node, Neck Left Deep Cervical	PTCL, NOS Lennert-like	
11	25%	Mediastinum and Lymph Node, Supraclavicular	ALK+ ALCL	
12	25%	Lymph Node, Right Inguinal	AITL	
13	30%	Abdomen, Abdominal Wall	SPTCL	
14	20%	Lymph Node, Right Groin	AITL	
15	25%	Lymph Node, Left Axillary	AITL	
16	40%	Lymph Node, Left Groin	PTCL, NOS TFH, recurrent	yes
17	70%	Lymph Node, Left Axilla	CTCL	
18	20%	Lymph Node, Left Supraclavicular	ALK+ ALCL	
19	25%	Spleen	HSTCL	
22	30%	Lymph Node, Left Axillary	CTCL	
23	70%	Testis, Right	ENKTCL, nasal type	yes
24	20%	Lymph Node, Left Axillar	AITL	yes
25	50%	Spleen	HSTCL	
28	50%	Lymph Node, left inguinal	ALK- ALCL	
30	40%	Lymph Node, left iliac	PTCL, NOS TFH	
32	5%	Lymph Node, right groin	CTCL	
33	20%	Lymph Node, left axillary	AITL	yes
34	15%	Lymph Node, left neck	AITL	yes
35	15%	Lymph nodes, anterior mediastinal and right paratracheal	ALK- ALCL	

AITL, angioimmunoblastic T cell lymphoma; ALCL, anaplastic large cell lymphoma; ALK, anaplastic lymphoma kinase; ATL, adult T cell lymphoma; CTCL, cutaneous T cell lymphoma; ENKTCL, extranodal NK/T cell lymphoma; HSTCL, hepatosplenic T cell lymphoma; PTCL, NOS, peripheral T cell lymphoma, not otherwise specified; SPTCL, subcutaneous panniculitis-like T cell lymphoma; TFH, follicular helper T cell.

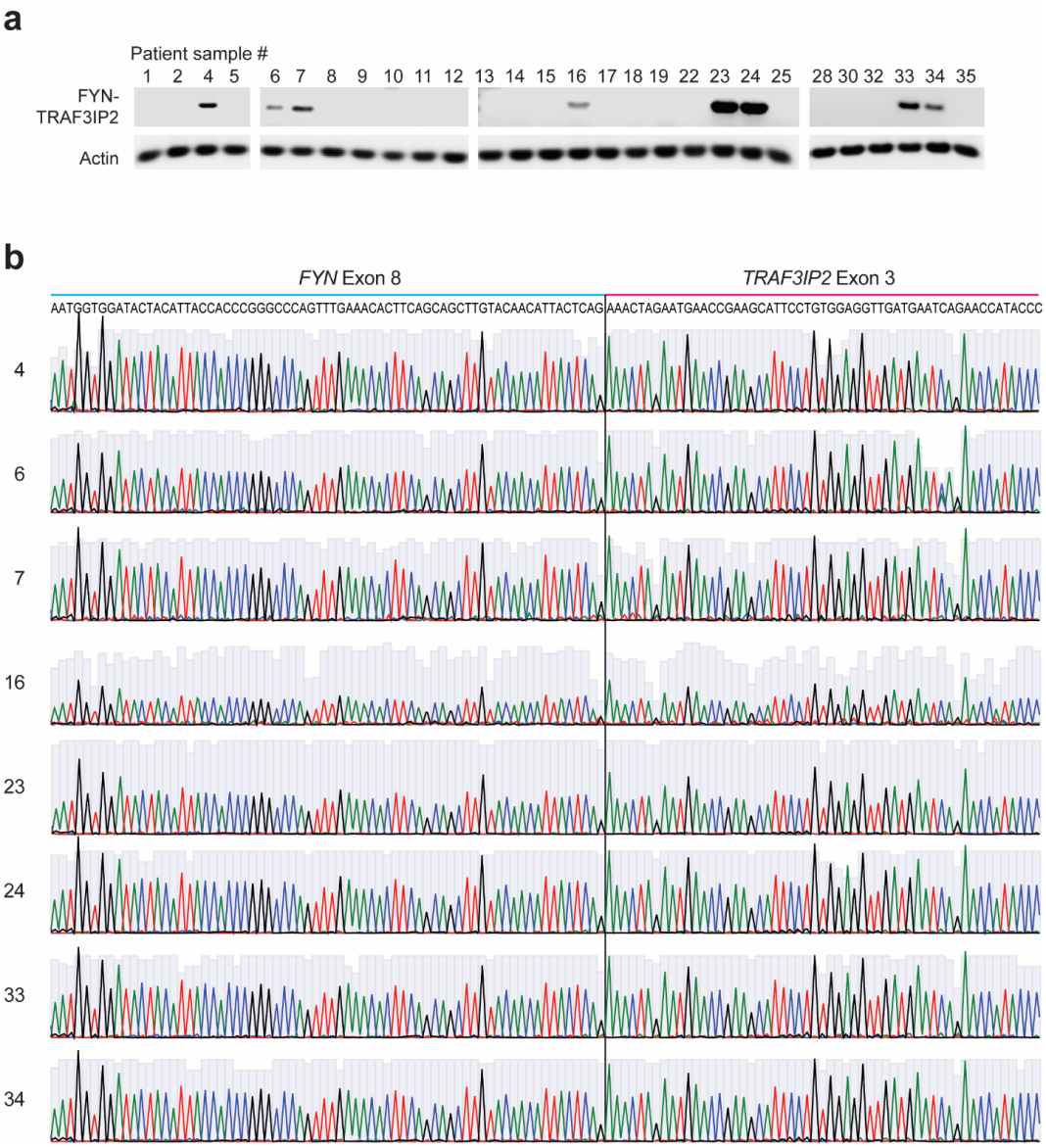

Figure 2.2 – *FYN-TRAF3IP2* detection by RT-PCR and dideoxynucleotide sequencing. A, Reverse-transcription PCR (RT-PCR) amplification results of an independent panel of 28 PTCL RNA samples spanning the region of *FYN-TRAF3IP2* fusion breakpoint. **B,** DNA sequencing chromatograms of the RT-PCR amplicons generated in **a**.

Structurally, *FYN* and *TRAF3IP2* are adjacently located loci in head to tail orientation with the *TRAF3IP2* gene positioned 53.4 kb centromeric from *FYN* in the long arm of chromosome 6 (**Figure 2.1d**). To investigate the mechanism underlying the expression of *FYN-TRAF3IP2* fusion mRNAs in PTCL, we performed deep (100x) whole genome sequencing of a *FYN-TRAF3IP2*-expressing AITL sample with available genomic DNA. Analysis of structural abnormalities identified a

chromosome 6 rearrangement joining *FYN* intron 8 (Chr6:111,702,370) and *TRAF3IP2* intron 2 (Chr6:111,592,704) (**Figure 2.1d** and **Table 2.3**). This genetic alteration spanning 109,666 base pairs generates a gene fusion predicted to express a *FYN-TRAF3IP2* chimeric RNA with *FYN* exons 1-8 splicing into exon 3 of *TRAF3IP2*, in concordance with the results of RNAseq analyses in this sample.

Table 2.3 – Genomic breakpoint of *FYN*-TRAF3IP2 fusion analyzed by whole genome sequencing.

Sample	Diagnosis	*FYN* breakpoint	*TRAF3IP2* breakpoint	Reads	Split reads
TP58	AITL	111,702,370	111,592,704	2	2

Table 2.4 – Mutational profile of *FYN-TRAF3IP2* harboring sample analyzed by whole genome sequencing.

Sample	Chr	Position	Ref	Var	Gene	AA	Transcript ID	Variant Frequency
TP58	3	49412973	C	A	*RHOA*	G17V	NM_001664	13
TP58	4	105236364	G	T	*TET2*	E808*	NM_001127208	14
TP58	7	2928644	T	G	*CARD11*	N570H	NM_032415	9
TP58	7	2928646	C	A	*CARD11*	G569V	NM_032415	5
TP58	20	41162516	T	G	*PLCG1*	F193V	NM_182811	8
TP58	20	41163397#	G	A	*PLCG1*	R270H	NM_182811	54
TP58	20	41163423#	A	G	*PLCG1*	S279G	NM_182811	54
TP58	20	41168825#	T	C	*PLCG1*	I813T	NM_182811	100

Chr, chromosome number; Ref, reference; Var, variant; AA, amino acid change.
* stop gain. # germline single nucleotide polymorphism.

Chapter 3: Functional characterization of *FYN-TRAF3IP2*

The chimeric protein encoded by *FYN-TRAF3IP2* contains the N-terminal membrane localization motif and the SH3 and SH2 domains (aa1-232) of FYN, but not its SH1 kinase domain, in fusion with all known motifs and domains of TRAF3IP2 (aa7-574) including its helix-loop-helix domain, a TRAF6-ubiquitinating U-Box domain, three putative TRAF-binding motifs and its IL-17R-associating SEFIR domain (**Figure 2.1e**). Mechanistically, this protein configuration suggests that FYN-TRAF3IP2 could result in aberrant TRAF3IP2-mediated signaling rather than inducing oncogenic FYN kinase activity.

The TRAF3IP2 adaptor protein plays an important role in mediating NF-κB signaling downstream of the IL17 receptor(Li et al. 2000, Chang et al. 2006, Qian et al. 2007). However, IL17R is not functionally expressed in T cells (**Figure 3.1a**) (Kuestner et al. 2007, Gaffen 2009, Ishigame et al. 2009). Consistently, IL17 treatment failed to elicit increased NF-κB signaling in GFP NF-κB reporter Jurkat T cells infected with empty vector, wild type TRAF3IP2 and FYN-TRAF3IP2 expressing lentiviruses (**Figure 3.1b**).

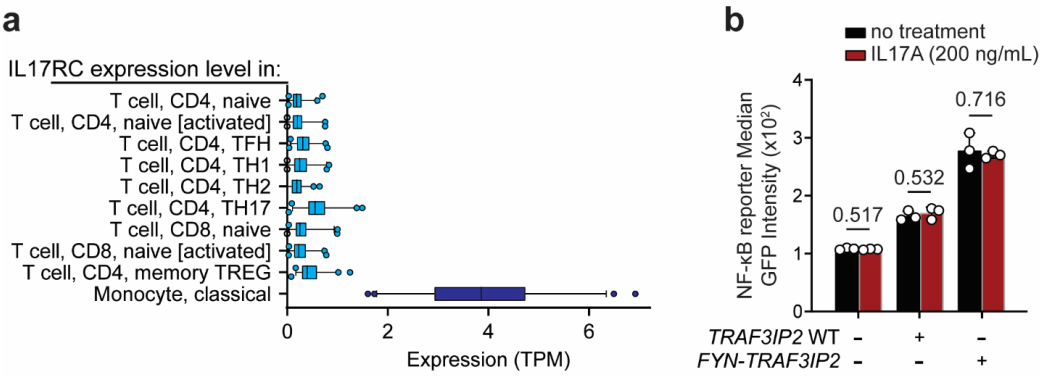

Figure 3.1 – T cells do not functionally express IL17 receptors. A, RNA expression level of *IL17RC*, essential for a functional IL17 receptor (Ho et al. 2010), in T cells and monocytes represented from DICE (Database of Immune Cell Expression, Expression quantitative trait loci and Epigenomics). **B,** NF-κB-GFP reporter activity in transduced Jurkat cells after stimulation with 200 ng/mL IL17A. Results are reported as mean of triplicate values (bar) ± standard deviation (error bar) with individual values (white circles). P values were calculated using two-tailed Student's t-test.

In this context, and given the prominent role of TCR signaling as driver of PTCL proliferation and survival (Wilcox 2016), we proposed an aberrant adaptor role for *FYN-TRAF3IP2* linking TCR

activation to NF-κB signaling. In agreement with this hypothesis, TCR stimulation of *FYN-TRAF3IP2*-expressing Jurkat cells with an anti-CD3 antibody led to significantly increased NF-κB reporter activity compared with controls (**Figure 3.2b**). Similarly, treatment with phorbol 12-myristate 13-acetate (PMA), which mimics the effects of diacylglycerol, a second messenger inducing protein kinase C (PKC) activation downstream of TCR signaling, induced markedly increased NF-κB reporter responses in *FYN-TRAF3IP2*-expressing Jurkat cells compared with wild type TRAF3IP2 expressing and empty vector infected controls (**Figure 3.2c**). In all, these results support a role for *FYN-TRAF3IP2* as a driver of NF-κB activation downstream of TCR-induced PKC signaling in PTCL.

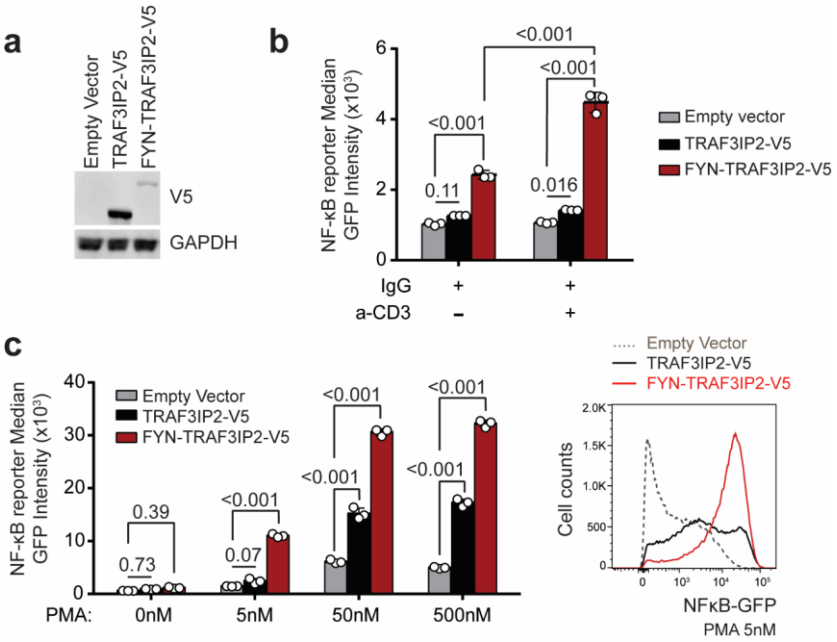

Figure 3.2 – FYN-TRAF3IP2 drives NF-κB activation in response to TCR-induced PKC signaling. a, Immunoblot analysis of Jurkat NF-κB-GFP reporter cells lentivirally transduced with empty vector or with viruses driving expression of wild type *TRAF3IP2-V5* or the *FYN-TRAF3IP2-V5* fusion. IB, immunoblot. **B,** NF-κB-GFP reporter activity in Jurkat cells as in **a** after stimulation with anti-CD3 (a-CD3) antibody. **C**, NF-κB-GFP reporter activity in Jurkat cells as in **a** after treatment with increasing doses of PMA. Bar graphs indicate the mean of triplicate values. Error bars indicate ± standard deviation. Individual values are shown as white circles. P values were calculated using two-tailed Student's t-test.

Recruitment of adaptor and signaling factors to multiprotein complexes in the plasma membrane plays an important role in TCR signal transduction (Chakraborty and Weiss 2014). The *FYN* N-terminal sequence GCVQCKDK is myristoylated (at the Gly site) and palmitoylated (at the two Cys

sites) and targets localization of the FYN protein to the plasma membrane (Wolven et al. 1997, Sato et al. 2009) (**Figure 3.3a**). The presence of this motif in FYN-TRAF3IP2 supports a potential role for aberrant membrane recruitment of this fusion protein in NF-κB activation. Subcellular fractionation analyses of cells expressing TRAF3IP2 or the FYN-TRAF3IP2 fusion recovered FYN-TRAF3IP2 in the membrane fraction, while wild type TRAF3IP2 was primarily located in the cytosol (**Figure 3.3b**). Moreover, mutation (ASVQSKDK) of the FYN-TRAF3IP2 FYN membrane localization motif (Wolven et al. 1997) (**Figure 3.3a**) resulted in delocalization of this fusion protein to the cytosolic compartment (**Figure 3.3b**). Consistently, immunofluorescence analysis of C-terminal 3xFlag-tagged proteins showed plasma membrane localization of FYN-TRAF3IP2 and a diffuse cytosolic localization pattern for wild type TRAF3IP2 and ASVQSKDK FYN-TRAF3IP2 (**Figure 3.3c**). Moreover, and in support of a mechanistic functional role of plasma membrane localization in FYN-TRAF3IP2-mediated signaling, introduction of the ASVQSKDK membrane localization motif mutation in FYN-TRAF3IP2 abrogated the capacity of this fusion protein to activate NF-κB in reporter assays (**Figure 3.3d**).

Activation of NF-κB downstream of PKCθ after TCR activation involves the assembly of a multiprotein complex containing CARD11, BCL10 and MALT1 (CBM signalosome) (Meininger and Krappmann 2016), which upon activation, recruits and activates TRAF6. This, in turn, triggers multiple K63-linked (TRAF6 and BCL10-mediated) and M1-linear (linear ubiquitin chain assembly complex (LUBAC)-mediated) ubiquitination events, which collectively mediate phosphorylation and activation of the IKK complex (Meininger and Krappmann 2016) leading to degradation of the IκBα NF-κB inhibitory factor, leading to NF-κB nuclear localization and consequently, to activation of NF-κB target gene expression (Meininger and Krappmann 2016) (**Figure 3.6**).

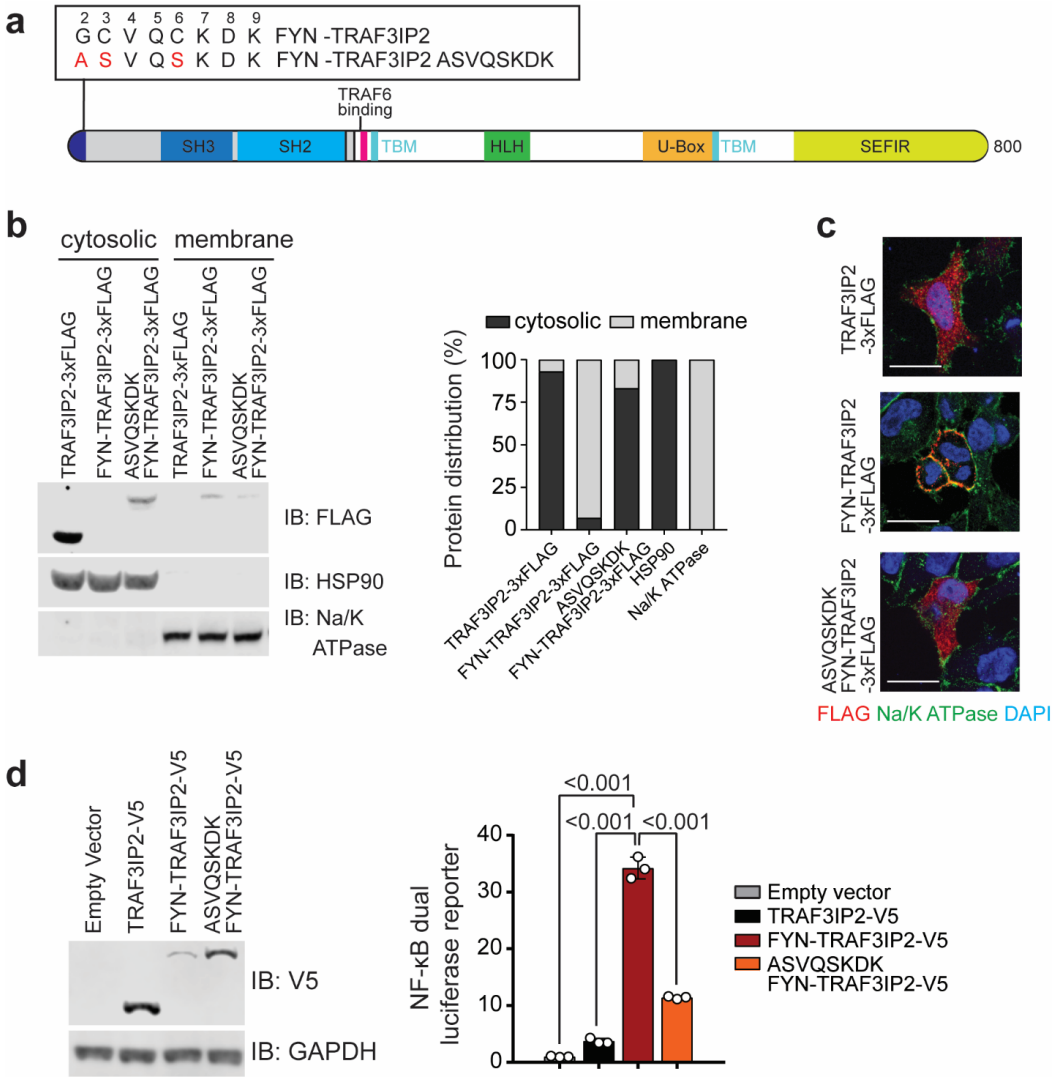

Figure 3.3 – Membrane localization of FYN-TRAF3IP2. A, Schematic representation of the FYN-TRAF3IP2 fusion protein indicating the wild type and mutant membrane localization motif sequences. **B**, Immunoblot analysis (left) and quantification (right) of cytosolic and membrane-associated FLAG-tagged proteins after subcellular fractionation in Jurkat cells expressing wild type TRAF3IP-3xFLAG, FYN-TRAF3IP2-3xFLAG, or membrane localization mutant ASVQSKDK FYN-TRAF3IP2-3xFLAG. **C,** Immunofluorescence analysis of cellular localization of FLAG-tagged proteins in HeLa cells expressing wild type TRAF3IP2-3xFLAG, FYN-TRAF3IP2-3xFLAG, and membrane localization mutant ASVQSKDK FYN-TRAF3IP2-3xFLAG. FLAG-tagged proteins are shown in red, the Na/K ATPase membrane marker in green, and DAPI-stained nuclei in blue. Scale bar = 20 μm. **D,** NF-κB dual luciferase reporter activity (right) and immunoblot analysis (left) of 293T cells transduced with empty vector or lentivirus driving expression of wild type TRAF3IP2-V5, FYN-TRAF3IP2-V5, or mutant ASVQSKDK FYN-TRAF3IP2-V5. Bar graphs indicate the mean of triplicate values. Error bars indicate ± standard deviation. Individual values are shown as white circles. P values were calculated using two-tailed Student's t-test. IB, immunoblot.

To test if FYN-TRAF3IP2 could activate NF-κB via the CBM complex, we analyzed the ability of PKC activation induced by PMA treatment to trigger expression of a NF-κB-GFP reporter in wild type and *CARD11* knockout Jurkat cells (Wang et al. 2002) (**Figure 3.4**) expressing FYN-

TRAF3IP2. In these experiments, empty vector control and wild type TRAF3IP2-expressing *CARD11* deficient cells showed a marked impairment in NF-κB signaling triggered by PMA treatment, which was effectively rescued by lentiviral expression of CARD11-HA (**Figure 3.5a**,**b**). In contrast, *CARD11* knockout Jurkat cells expressing FYN-TRAF3IP2 readily activated the NF-κB-GFP reporter in response to PMA treatment (**Figure 3.5a**,**b**). This result demonstrates a CBM-independent role for FYN-TRAF3IP2 as mediator of TCR-induced NF-κB activation in PTCL.

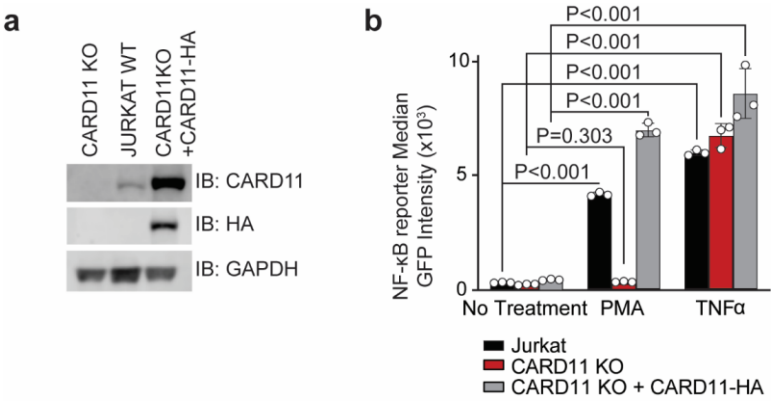

Figure 3.4 – Knock out and reconstitution of *CARD11* in Jurkat cells. Immunoblot analysis **a** and NF-κB-GFP reporter activity after stimulation with 25 nM of PMA or 20 ng/mL TNFα **b** of JPM50.6 *CARD11* knockout and JPM50.6 cells reconstituted by *CARD11-HA* expression. Results are reported as mean of triplicate values (bar) ± standard deviation (error bar) with individual values (white circles). P values were calculated using two-tailed Student's t-test.

Interestingly, both IL17R signaling and TCR-CBM signalosome NF-κB activation engage TRAF6, a ubiquitin ligase prominently involved in NF-κB signaling upstream of IKKβ activation (Walsh et al. 2015). Moreover, TRAF6 can directly interact with TRAF3IP2, via association with TRAF-binding motifs present in the FYN-TRAF3IP2 fusion protein (Liu et al. 2009, Ryzhakov et al. 2011, Sonder et al. 2011), suggesting a potential role for TRAF6 in FYN-TRAF3IP2-mediated NF-κB activation. Consistent with this possibility, immunoprecipitation and western blot analyses demonstrated that, similar to wild type TRAF3IP2, the FYN-TRAF3IP2 protein can prominently interact with TRAF6 (**Figure 3.5d**). Moreover, introduction of a disruptive focal mutation (PVAVAA) (Ryzhakov et al. 2011) in the TRAF3IP2 TRAF6-binding motif of FYN-TRAF3IP2 (**Figure 3.5c**) impaired the ability of this fusion protein to interact with TRAF6 (**Figure 3.5d**) and its capacity to respond to PMA in Jurkat NF-κB-GFP reporter assays (**Figure 3.5e**).

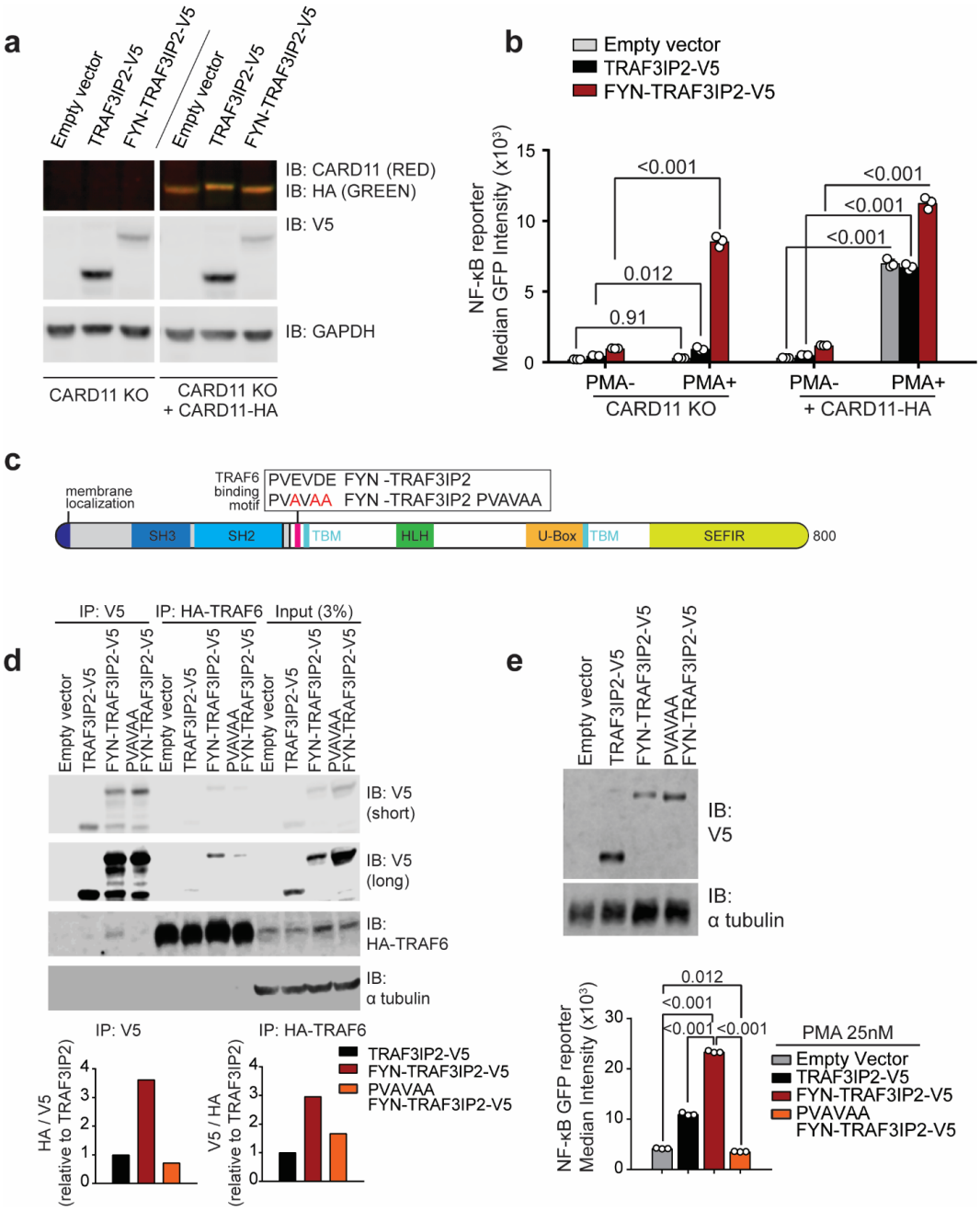

Figure 3.5 – FYN-TRAF3IP2 engages TRAF6 to activate CARD11-independent NF-κB signaling. a, Immunoblot analysis of *CARD11* knockout Jurkat cells and CARD11-HA reconstituted *CARD11* knockout cells infected with empty vector or lentiviruses driving expression of TRAF3IP2-V5 or the FYN-TRAF3IP2-V5 fusion. **b,** NF-κB-GFP reporter activity after stimulation with 25 nM PMA in Jurkat cells as in **a**. **c,** Schematic representation of the FYN-TRAF3IP2 fusion protein indicating the wild type and mutant TRAF6-binding motif. **d,** Micrograph (top) and quantification (bottom) of IP western analyzing the interaction between HA-TRAF6 and V5-tagged proteins in 293T cells expressing wild type TRAF3IP2-V5, FYN-TRAF3IP2-V5 or PVAVAA FYN-TRAF3IP2-V5 or in the empty vector control. **e,** Immunoblot analysis of Jurkat cells transduced with empty vector or lentivirus driving expression of wild type TRAF3IP2-V5, fusion FYN-TRAF3IP2-V5, or mutant PVAVAA FYN-TRAF3IP2-V5 (top) and corresponding NF-κB-GFP reporter activity (bottom) after stimulation with 25nM PMA. IP, immunoprecipitation; IB, immunoblot. Bar graphs in **a** and **e** indicate the mean of triplicate values. Error bars indicate ± standard deviation. Individual values are shown as white circles. P values were calculated using two-tailed Student's t-test. Bar graphs in **d** indicate protein interaction levels normalized to TRAF3IP2-V5.

Collectively, these results suggest a mechanism in which localization of FYN-TRAF3IP2 at the membrane rewires the TCR signal transduction pathway resulting in enhanced and dysregulated NF-κB signaling. Analogous to the CBM signaling, NF-κB activation by FYN-TRAF3IP2 also responds to TCR and PKC activation, but redirects this input signal to directly recruit TRAF6 and activate NF-κB circumventing the CBM complex (**Figure 3.6**).

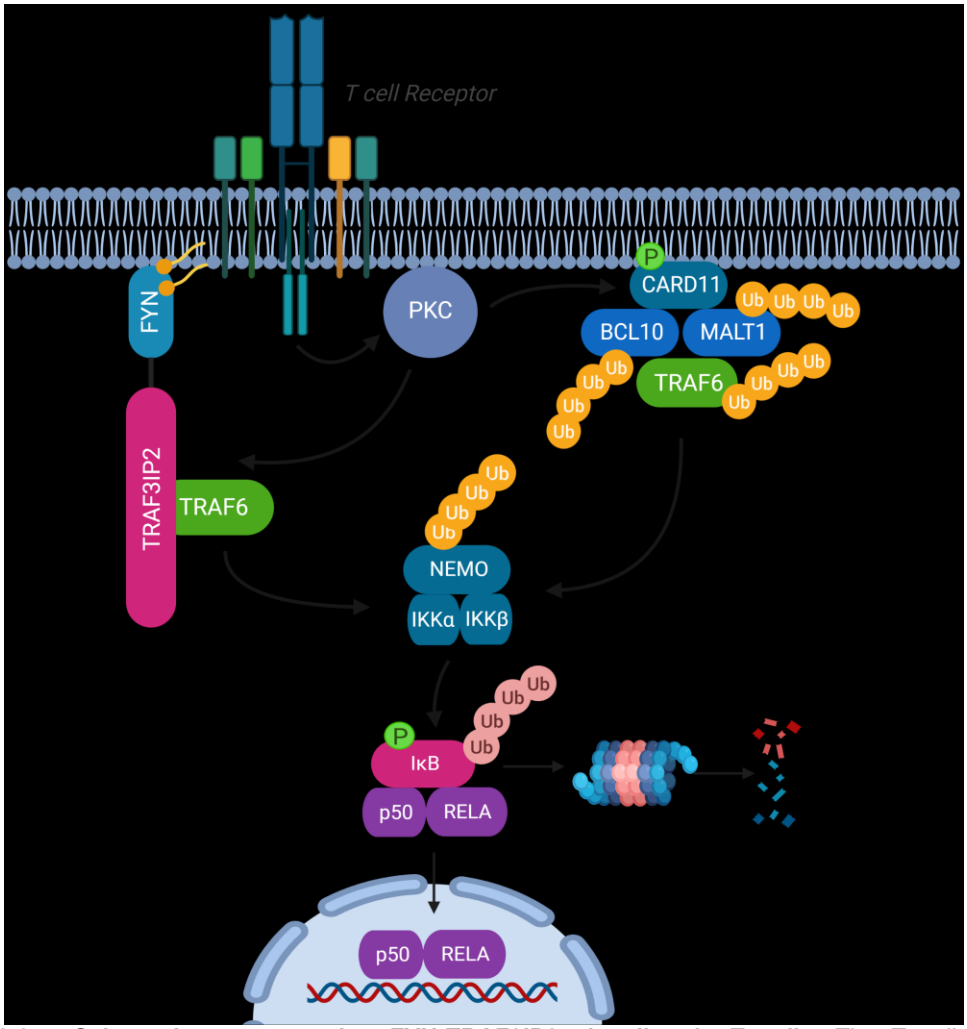

Figure 3.6 – Schematic representation FYN-TRAF3IP2 signaling in T cells. The T cell receptor downstream second messenger diacylglycerol activates and recruits PKC to the plasma membrane. In physiologic T cells, CARD11, upon phosphorylation by PKC, nucleates the CARD11-BCL10-MALT1 (CBM) complex, which involves several factors including TRAF6 to form a polyubiquitinated signaling platform to activate the classical IKK complex. The activated IKK complex subsequently catalyzes IκBα phosphorylation, which triggers K48-linked polyubiquitination of the substrate followed by proteasomal degradation. Relieved from the inhibitory protein, NF-κB transcription factors then accumulate in the nucleus and activate target genes. Analogous to the physiologic signaling, NF-κB activation by FYN-TRAF3IP2 also responds to TCR and PKC activation. Localization of FYN-TRAF3IP2 at the membrane rewires the TCR signal transduction pathway by redirecting the input TCR signals to circumvent the CBM complex and directly recruit TRAF6, resulting in enhanced and dysregulated NF-κB signaling.

Chapter 4: Oncogenic role of *FYN-TRAF3IP2* in PTCL

Loss-of-function *TET2* mutations are highly recurrent genetic lesions in PTCL (Couronne et al. 2012, Lemonnier et al. 2012, Palomero et al. 2014, Sakata-Yanagimoto et al. 2014), can be found in association with *FYN-TRAF3IP2* (**Table 2.4**), and accelerate the development of PTCL in mice (Cortes et al. 2018). To investigate the oncogenic activity of FYN-TRAF3IP2 we analyzed the lymphomagenic effects of expressing this gene fusion alone and in cooperation with loss of the *Tet2* tumor suppressor gene *in vivo*. In these experiments, we first infected hematopoietic progenitors from CD4-specific tamoxifen-inducible Cre *Tet2* conditional knockout mice (CD4 Cre-ERT2, $Tet2^{fl/fl}$) with bicistronic retroviruses expressing wild type *TRAF3IP2* and *GFP*, *FYN-TRAF3IP2* and *GFP*, or *GFP* alone and injected these intravenously into isogenic recipients (**Figure 4.1**) Transplanted mice were then treated with vehicle only, to test the oncogenic effects of *TRAF3IP2*, *FYN-TRAF3IP2* or *GFP* expression; or with tamoxifen, to evaluate the effects of *TRAF3IP2*, *FYN-TRAF3IP2* or *GFP* expression in concert with genetic loss of *Tet2* in CD4 T cells. In this setting, all animals transplanted with *GFP*-expressing progenitors remained lymphoma free at the end of follow up and one animal transplanted with wild type *TRAF3IP2 GFP* expressing cells developed a CD8+ T cell lymphoma (**Figure 4.2a**,**b**). In contrast, and most notably, 4/10 (40%) vehicle treated mice transplanted with *FYN-TRAF3IP2*-expressing cells developed clonal CD4-restricted mature T cell lymphomas with a latency of 28 weeks in support of a driver oncogenic role for *FYN-TRAF3IP2* in PTCL (**Figure 4.2a**). In addition, mice transplanted with *FYN-TRAF3IP2*-expressing progenitors and treated with tamoxifen to delete *Tet2* in the CD4 T cell compartment showed accelerated mortality with a latency of 22 weeks, supporting a cooperative role between *Tet2* loss and *FYN-TRAF3IP2* in lymphoma development. By 44 weeks post-transplant, 7/10 of mice in this group were euthanized with signs of disease (**Figure 4.2c**). Of these, 5/7 were diagnosed with CD4-positive T cell lymphoma based on histopathological and flow cytometry analyses, for an overall lymphoma penetrance of 50% (5/10) at the end of follow up.

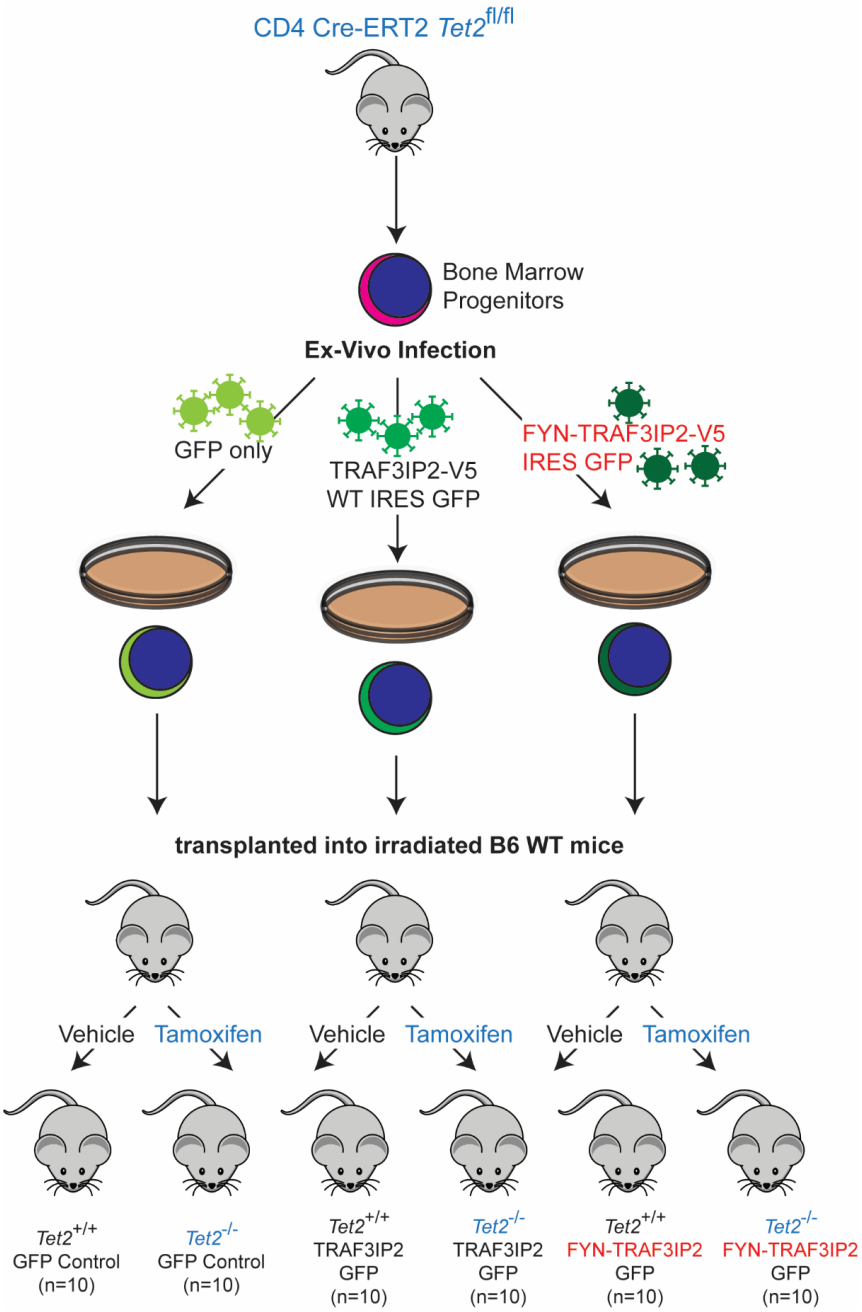

Figure 4.1 – Schematic representation of bone marrow transplant experiment analyzing the lymphomagenic activity of *FYN-TRAF3IP2*. We transduced hematopoietic progenitors from CD4 Cre-ERT2 *Tet2*$^{fl/fl}$ mice with bicistronic retroviruses driving the expression of *GFP*, *FYN-TRAF3IP2-V5* and *GFP* or wild type *TRAF3IP2-V5* and *GFP*. We intravenously transplanted the infected cells into lethally irradiated C57BL/6 recipient mice and treated them 8 weeks post-transplant with vehicle only or with tamoxifen to preserve or delete *Tet2* in CD4$^+$ T cells, respectively. These cohorts of mice were then immunized with sheep red blood cells every 4-5 weeks to induce peripheral T cell activation.

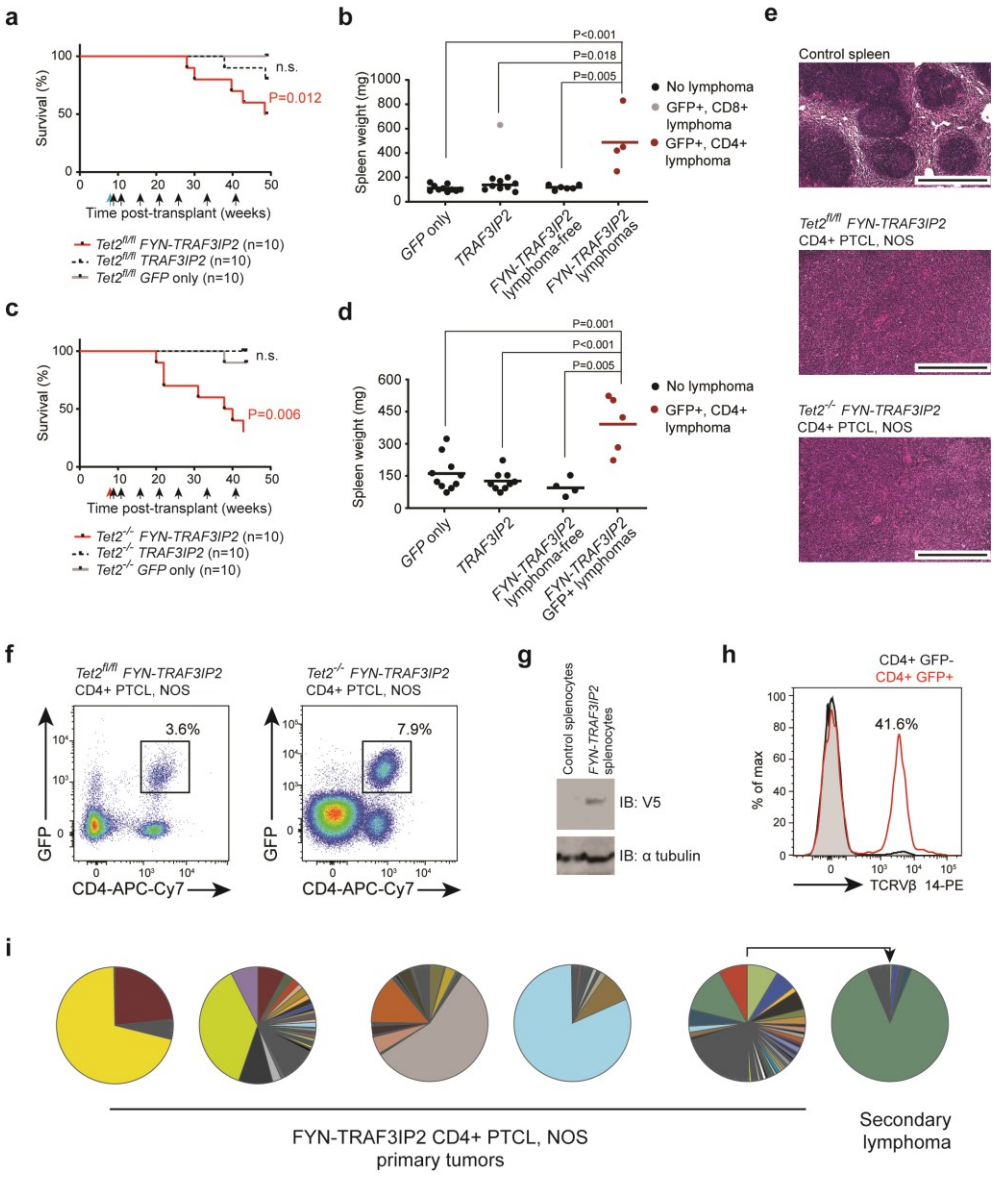

Figure 4.2 – Expression of FYN-TRAF3IP2 in mouse hematopoietic progenitors induces PTCL, NOS. **a,** Kaplan-Meier survival curves of mice transplanted with bone marrow progenitor cells from CD4 Cre-ERT2 *Tet2*$^{fl/fl}$ mice retrovirally transduced to express *GFP* only, wild type *TRAF3IP2* and GFP, or fusion *FYN-TRAF3IP2* and GFP treated with vehicle (blue arrow) 8 weeks post-transplant. **b,** Splenic weight of animals at the endpoint after transplantation as in **a**. Red circles, GFP+ CD4+ lymphoma; black circles, no lymphoma; gray circle, GFP+ CD8+ lymphoma; horizontal line, mean value. P values were calculated using two-tailed Student's t-test. **c,** Kaplan-Meier survival curves of mice transplanted with bone marrow progenitor cells from CD4 Cre-ERT2 *Tet2*$^{fl/fl}$ mice retrovirally transduced to express *GFP* only, wild type *TRAF3IP2* and GFP, or fusion *FYN-TRAF3IP2* and GFP treated with tamoxifen (red arrow) 8 weeks post-transplant. **d,** Splenic weight of animals at the endpoint after transplantation as in **c**. Red circles, GFP+ CD4+ lymphoma; black circles, no lymphoma; horizontal line, mean value. P values were calculated using two-tailed Student's t-test. **e,** Histological micrographs of hematoxylin-eosin stained spleen sections of immunized control mice and *FYN-TRAF3IP2*-induced CD4+ PTCL, NOS. Scale bar = 400 μm. **f,** Representative FACS plot showing GFP$^+$ CD4$^+$ lymphoma cells in lymphoma-infiltrated spleens from *FYN-TRAF3IP2* diseased mice. **g,** Immunoblot analysis of FYN-TRAF3IP2-V5 protein expression in control splenocytes and in the lymphoma-infiltrated spleen of a *FYN-TRAF3IP2* diseased mouse. **h,** Tcr Vβ clonality in *FYN-TRAF3IP2* lymphoma cells (GFP$^+$ CD4$^+$) and normal CD4 T cells (GFP$^-$ CD4$^+$) from a diseased mouse. **i,** *Tcrb* clonal distribution in *FYN-TRAF3IP2*-induced CD4$^+$ primary tumors and in a representative allografted secondary lymphoma. Sectors represent the fraction of reads corresponding to individual *Tcrb* sequences.

Mice harboring *FYN-TRAF3IP2*-induced lymphomas showed splenomegaly and generalized lymphadenopathy (**Figure 4.2b**,**d** and **Figure 4.3a**,**b**). Histopathological examination of enlarged lymph nodes and spleen showed replacement of lymphoid follicles with a diffuse pleomorphic lymphohistiocytic infiltrate composed predominantly of atypical lymphocytes (**Figure 4.2e**). Flow cytometry analysis of splenocytes in lymphoma bearing mice demonstrated the presence of GFP^+ cells derived from *FYN-TRAF3IP2* GFP infected progenitors (**Figure 4.2f**) and immunoblot analysis verified the expression of the FYN-TRAF3IP2 protein (**Figure 4.2g**). In addition, histological and flow cytometry analyses of extranodal sites revealed infiltration of the bone marrow and peripheral tissues including liver, kidneys and lungs by GFP^+ tumor cells indicating disseminated disease (**Figure 4.3c**-**e**). GFP^+ tumor cells in *FYN-TRAF3IP2*-induced lymphoma showed a $CD4^+$ immunophenotype (**Figure 4.2f**). In addition, analyses of TFH markers showed upregulation of ICOS and PD1, but variable and generally limited expression of CXCR5 and BCL6 (**Figure 4.4b**,**c** and **Table 4.1**). Moreover, sequencing and flow cytometry analyses of the TCR repertoire of *FYN-TRAF3IP2* lymphoma cells revealed clonal expansion of T cell populations (**Figure 4.2h**,**i**). Finally, transplantation of splenic cells from diseased mice into secondary recipients led to accelerated development of secondary lymphomas (**Figure 4.5a**), which retained the histological and immunophenotypic features of the primary tumor (**Figure 4.5b**-**e**) with increased T cell clonality (**Figure 4.2** and **Figure 4.5f**).

Table 4.1 – TFH marker expression in mouse *FYN-TRAF3IP2* PTCL, NOS

Sample ID	Genotype	CD4	PD1	CXCR5	ICOS	BCL6
Lymphoma_1	*Tet2$^{-/-}$ FYN-TRAF3IP2*	o	o	x	o	x
Lymphoma_2	*Tet2$^{-/-}$ FYN-TRAF3IP2*	o	o	x	o	x
Lymphoma_3	*Tet2$^{-/-}$ FYN-TRAF3IP2*	o	o	x	o	o
Lymphoma_4	*Tet2$^{-/-}$ FYN-TRAF3IP2*	o	o	o	o	x
Lymphoma_5	*Tet2$^{-/-}$ FYN-TRAF3IP2*	o	o	x	o	x
Lymphoma_6	*Tet2$^{fl/fl}$ FYN-TRAF3IP2*	o	o	x	o	x
Lymphoma_7	*Tet2$^{fl/fl}$ FYN-TRAF3IP2*	o	o	x	o	x
Lymphoma_8	*Tet2$^{fl/fl}$ FYN-TRAF3IP2*	o	o	x	o	x
Lymphoma_9	*Tet2$^{fl/fl}$ FYN-TRAF3IP2*	o	o	x	o	x

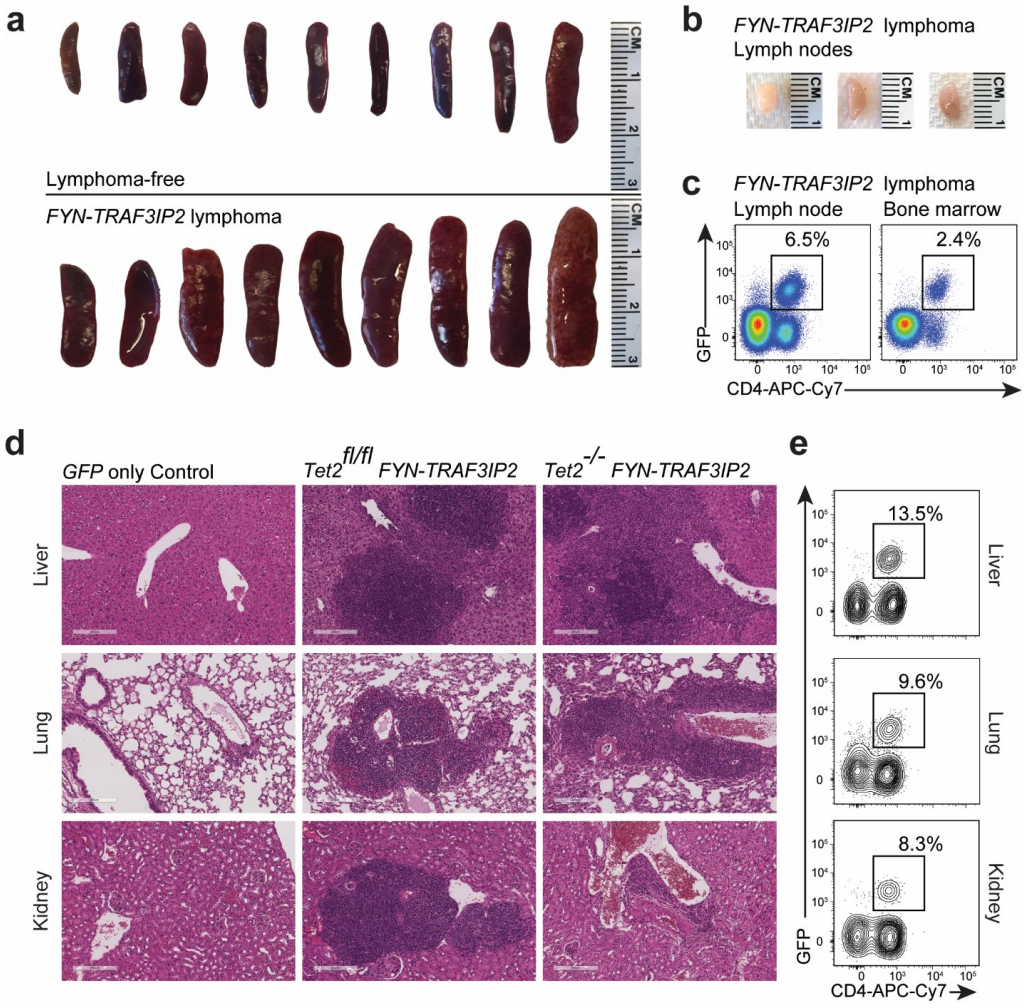

Figure 4.3 – *FYN-TRAF3IP2*-induced lymphomas infiltrate lymphoid organs, bone marrow and solid tissues in mice. a, Spleens from *FYN-TRAF3IP2*-induced lymphoma-bearing mice (bottom) and nine representative mice that were lymphoma-free at the end of follow up (top). **b,** Representative lymph nodes from *FYN-TRAF3IP2*-induced lymphoma-bearing mice. **c,** Representative FACS plots showing GFP^+ $CD4^+$ *FYN-TRAF3IP2* lymphoma cells infiltrating lymph nodes and bone marrow. **d,** Representative histological micrographs of H&E stained liver, lung, and kidney of $Tet2^{fl/fl}$ or $Tet2^{-/-}$ *FYN-TRAF3IP2*-induced lymphoma-bearing animals and the *GFP* only control. **e,** Representative FACS plots of mononuclear cells collected from liver, lung, and kidney of *FYN-TRAF3IP2*-induced lymphoma-bearing animals, showing GFP^+ $CD4^+$ cell infiltration.

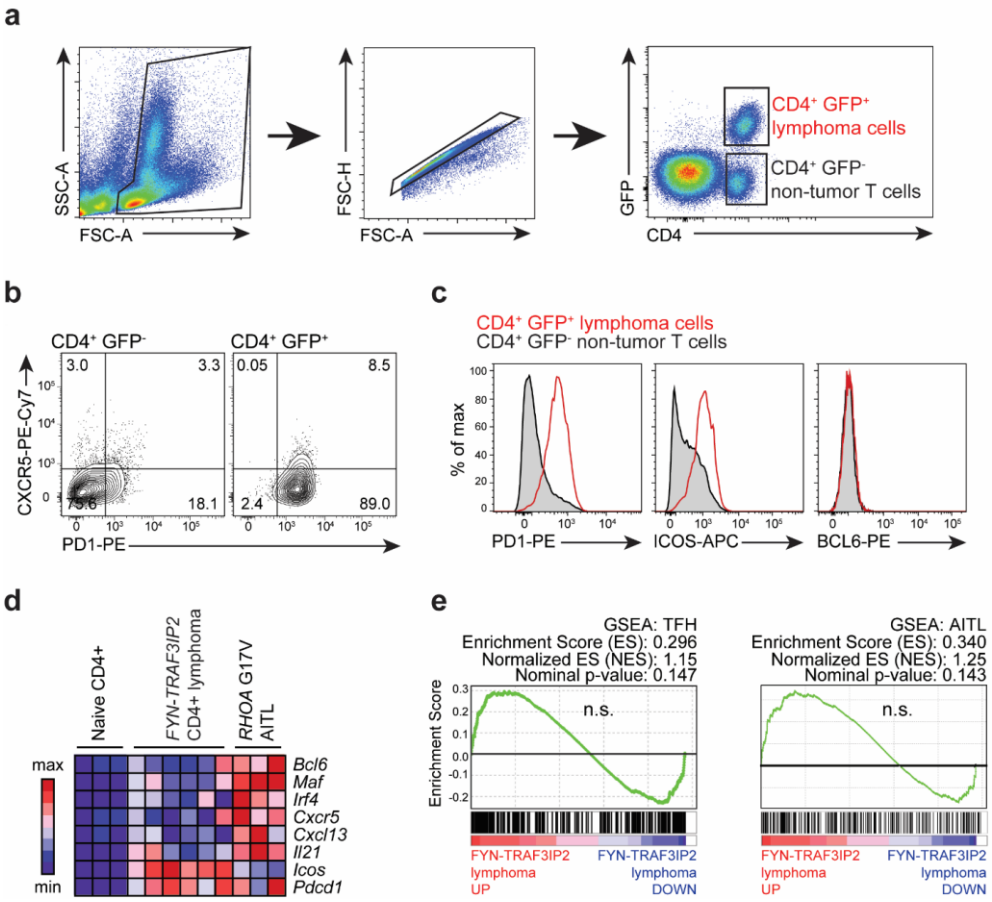

Figure 4.4 – *FYN-TRAF3IP2*-induced mouse lymphoma T cells show limited TFH features. a, Gating strategy for CD4⁺ GFP⁻ non-tumor cell and CD4⁺ GFP⁺ tumor cell population. **b,** Flow cytometry analysis of PD1 and CXCR5 TFH cell marker expression in CD4⁺ GFP⁻ non-tumor cells and CD4⁺ GFP⁺ tumor cells from a representative *FYN*-TRAF3IP2-induced lymphoma-bearing spleen. **c**, Representative flow cytometry analyses of PD1, ICOS and BCL6 TFH cell marker expression in CD4⁺ GFP⁺ spleen tumor cells compared to CD4⁺ GFP⁻ non-tumor cells from the same spleen. **d**, Heatmap representation of TFH-associated marker expression in CD4⁺ naïve wild type T cells, *FYN-TRAF3IP2*-induced CD4⁺ GFP⁺ lymphoma cells and *RHOA* G17V AITL-like mouse tumor cells (Cortes et al. 2018). **e**, GSEA enrichment plots of differentially expressed genes associated with *FYN-TRAF3IP2*-induced mouse lymphoma cells compared to wild type naïve CD4⁺ T cells. AITL geneset: top differentially upregulated genes in AITL compared with PTCL, NOS (fold change 1.5, p <0.002) (de Leval et al. 2007). TFH geneset: top 100 genes associated with TFH cells (Chtanova et al. 2004).

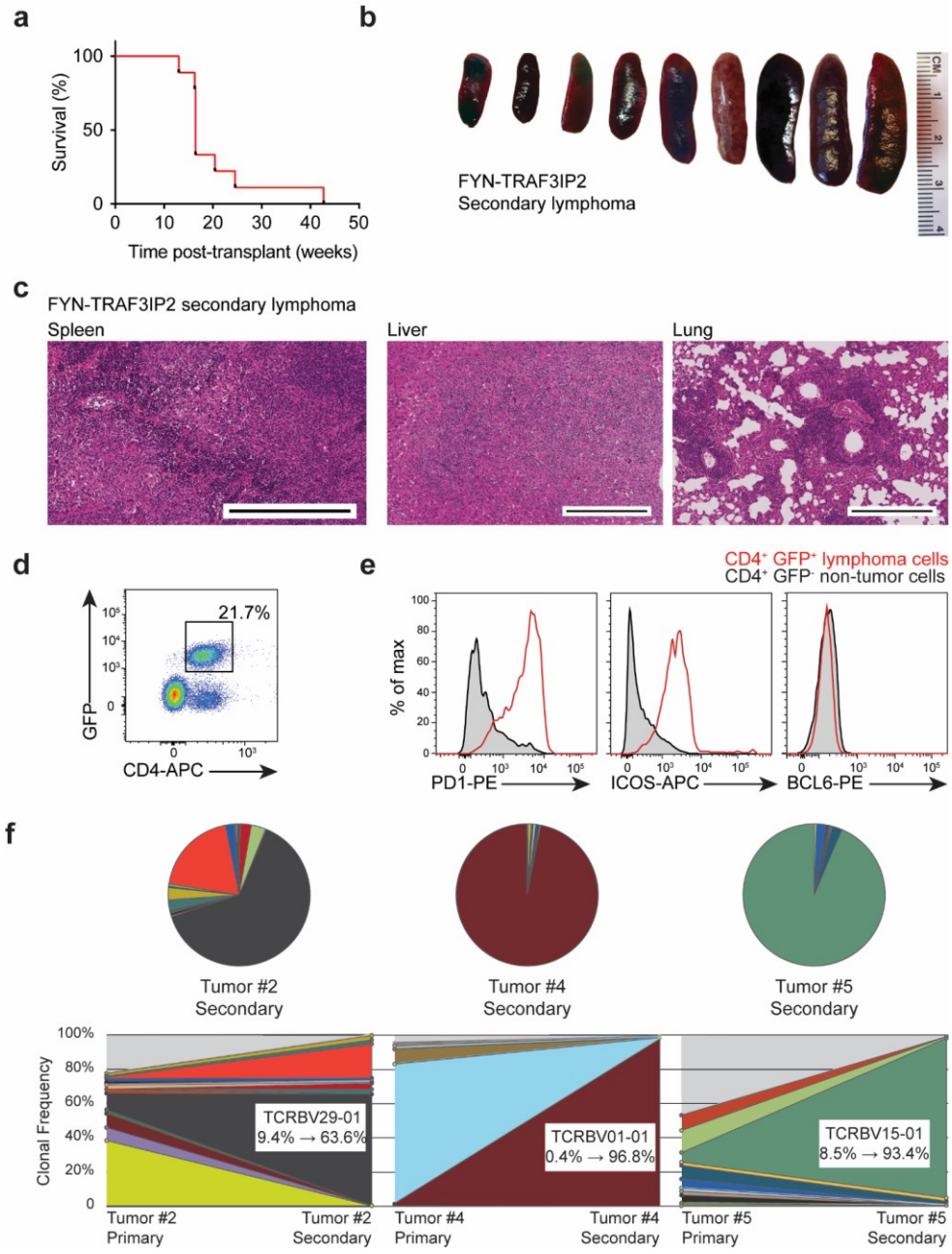

Figure 4.5 – *FYN-TRAF3IP2*-induced mouse PTCL, NOS are transplantable. a, Kaplan-Meier survival curve of mice transplanted with cell suspension containing *FYN-TRAF3IP2* GFP$^+$ lymphoma infiltrate. **b,** Spleens of secondary recipients transplanted with *FYN-TRAF3IP2*-induced lymphoma infiltrate. **c,** Representative histological micrographs of H&E stained spleen, liver, and lung of lymphoma transplanted mice at the endpoint showing lymphoma infiltration. Scale bar = 400 µm. **d,** Representative FACS plot showing GFP$^+$ CD4$^+$ lymphoma infiltrates in spleens from diseased secondary recipients. **e,** Representative flow cytometry analyses of PD1, ICOS and BCL6 TFH cell marker expression in CD4$^+$ GFP$^+$ spleen tumor cells compared to CD4$^+$ GFP$^-$ non-tumor cells from the same spleen. **f,** Pie chart representation of *Tcrb* gene clonal analysis of three secondary *Tet2*$^{-/-}$ *FYN-TRAF3IP2* GFP$^+$ lymphomas (top) and side-by-side representation of *Tcrb* sequence reads from primary and secondary *Tet2*$^{-/-}$ *FYN-TRAF3IP2* GFP$^+$ lymphomas (bottom), indicating the retention and expansion of specific lymphoma clone with unique *Tcrb* rearrangements after transplantation.

Chapter 5: NF-κB activation as driver and therapeutic target in *FYN-TRAF3IP2*-induced PTCL

In agreement with a role of FYN-TRAF3IP2 as driver of NF-κB activation, examination of nuclear RelA/p65 NF-κB subunit in *FYN-TRAF3IP2* $CD4^+$ GFP^+ mouse lymphoma cells showed clear nuclear localization pattern of NF-κB transcription factor by immunofluorescence analysis (**Figure 5.1a**,**b**) and significantly increased levels of active phosphorylated p65 proteins by flow cytometry analysis (**Figure 5.1c**). Transcriptomic profiling of FYN-TRAF3IP2 lymphoma tumor lymphocytes by RNAseq compared with normal $CD4^+$ T cells (**Figure 5.2a**-**c**) revealed marked enrichment of gene sets indicative of NF-κB activation, including NF-κB transcriptional targets and constitutive canonical NF-κB activation in lymphoma (Saba et al. 2016) (**Figure 5.1d**-**f**). Finally, and consistently with immunophenotypic analyses, *FYN-TRAF3IP2* $CD4^+$ GFP^+ lymphoma cells showed upregulation of *Pdcd1* and *Icos*, but not of other TFH/AITL-associated genes including *Bcl6*, *Maf*, *Irf4*, *Cxcl13* and *Cxcr5* (**Figure 4.4d**). Similarly, GSEA analyses revealed no significant enrichment of TFH (Chtanova et al. 2004) and AITL (de Leval et al. 2007)-associated gene signatures in *FYN-TRAF3IP2* $CD4^+$ GFP^+ tumor cells (**Figure 4.4e**). In all, these analyses support an oncogenic role for FYN-TRAF3IP2 in the development of PTCL, NOS tumors in mice.

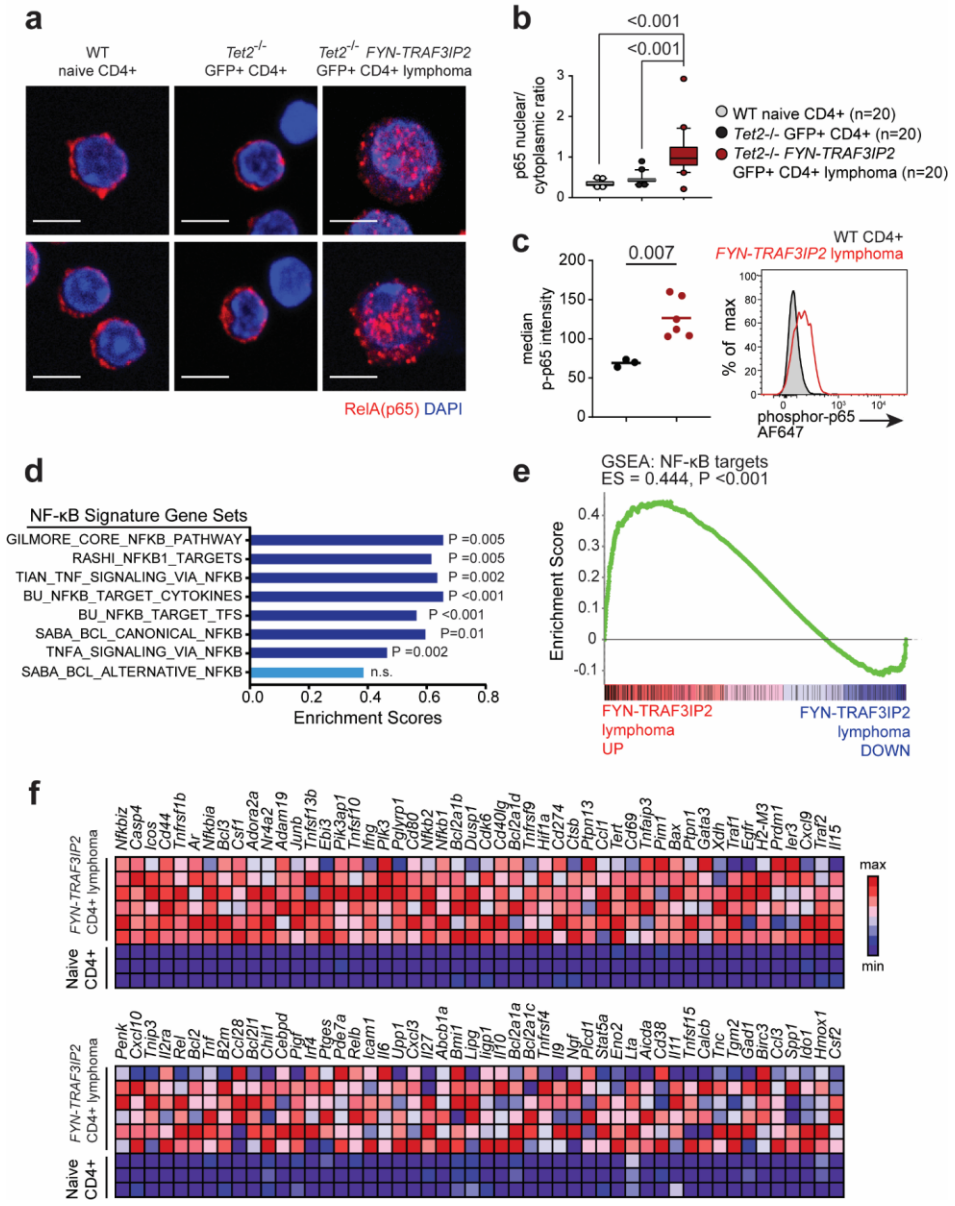

Figure 5.1 – NF-κB activation in *FYN-TRAF3IP2*-induced mouse PTCL, NOS. a, Immunofluorescence analysis of p65 NF-κB intracellular localization in normal CD4$^+$ cells from mice transplanted with GFP$^+$ expressing retroviruses, in GFP$^+$ *Tet2*$^{-/-}$ *FYN-TRAF3IP2* CD4$^+$ lymphoma cells and in isogenic wild type CD4$^+$ naïve T cells. p65 proteins shown in red and DAPI-stained nuclei in blue. Scale bar = 5 μm. **b,** Quantitation (n=20 cells per group) of p65 NF-κB intracellular nuclear/cytoplasmic localization in CD4$^+$ cells as in **a**. N/C ratio, nuclear / cytoplasmic ratio. Boxplot shows lines represent median, boxes represent 25–75% intervals, whiskers represent 10–90% intervals and circles represent data points outside the 10–90% interval. P values were calculated using two-tailed Student's t-test. **c,** Flow cytometry analysis of phospho-p65 NF-κB transcription factor levels in *FYN-TRAF3IP2*-induced CD4$^+$ GFP$^+$ lymphoma cells compared to wild type CD4$^+$ T cell controls. Horizontal lines in the graph indicate the mean, and circles represent values for six independent tumors (two *Tet2*$^{fl/fl}$ *FYN-TRAF3IP2* and four *Tet2*$^{-/-}$ *FYN-TRAF3IP2* lymphomas) and three normal CD4$^+$ T cell control samples. The P value was calculated using two-tailed Student's t-test. AF647, Alexa Fluor 647. **d,** Bar graph representation of enrichment scores for NF-κB gene signatures obtained by Gene Set Enrichment Analysis (GSEA) of differentially expressed genes associated with *FYN-TRAF3IP2*-induced mouse CD4$^+$ PTCL, NOS. BCL, B cell lymphoma. **e,** GSEA plot cprresponding to analysis of the NF-κB target geneset of the BU Gilmore lab database as in **d**. **f,** Heat map representation of differential gene expression for GSEA leading edge genes as in **e**. Scale bar shows color-coded differential expression, with red indicating higher levels of expression and blue indicating lower levels of expression.

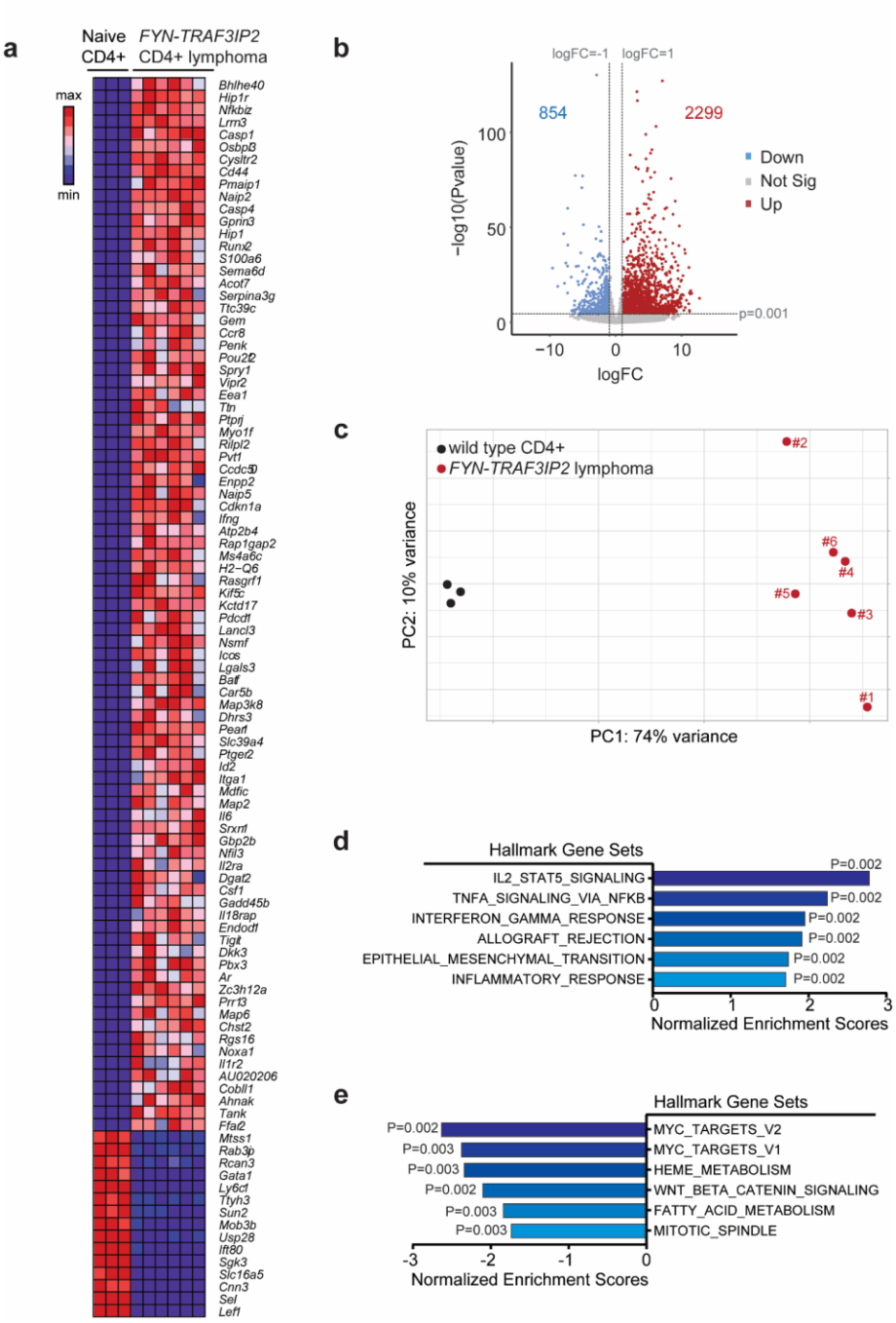

Figure 5.2 – Transcriptomic profiling of *FYN-TRAF3IP2* mouse PTCL, NOS by RNAseq. a-c, RNAseq data of six independent *FYN-TRAF3IP2*-induced mouse CD4$^+$ GFP$^+$ lymphomas and wild type isogenic mouse naïve CD4$^+$ T cells: **a,** heat map of the top 100 differentially expressed genes between *FYN-TRAF3IP2*-induced tumors and wild type CD4$^+$ naïve T cells (mouse genes without known human orthologues excluded; scale bar shows color-coded differential expression, with red indicating higher levels of expression and blue indicating lower levels of expression); **b,** Volcano plot of all differentially expressed genes as in **a** (P value <0.001 and $|\log_2(\text{fold change})|$> 1 deemed significant). Blue, significantly downregulated genes. Red, significantly upregulated genes. The number of significantly downregulated or upregulated genes is indicated; **c,** Principal component analysis plot of RNAseq data as in **a**. **d-e,** GSEA analyses of differentially expressed genes associated with *FYN-TRAF3IP2*-induced mouse lymphomas based on the RNAseq data and the Hallmark signatures (Liberzon et al. 2015) from MSigDB. The top 6 upregulated signatures **d** and top 6 downregulated signatures **e** are represented as bar graphs of normalized enrichment scores and P values.

Activation of NF-κB by FYN-TRAF3IP2 in cell reporter assays and a prominent NF-κB-associated gene signature in *FYN-TRAF3IP2*-induced lymphomas support a driver role and potential therapeutic target for NF-κB signaling in PTCL. To test this hypothesis, we evaluated the therapeutic activity of IKK inhibitors, which block NF-κB signaling downstream of TRAF6 activation (Awasthee et al. 2019). *In vitro* treatment of *FYN-TRAF3IP2* mouse tumor cells with the IKK inhibitors BMS-345541 (Burke et al. 2003) and IKK-16 (Waelchli et al. 2006) induced strong dose-dependent anti-lymphoma effects (**Figure 5.3a**) with G1 cell cycle arrest (**Figure 5.3c**) and increased apoptosis (**Figure 5.3b**). To further test the antitumor activity of IKK inhibition *in vivo* we treated mice bearing luciferized *FYN-TRAF3IP2* mouse tumors with BMS-345541, an allosteric IKK2 inhibitor with verified activity *in vivo* (Burke et al. 2003) and monitored therapeutic response by *in vivo* bioimaging. In these experiments, IKK inhibitor treatment of *FYN-TRAF3IP2* lymphomas resulted in marked anti-tumor effects (**Figure 5.3e**) with prolonged survival (**Figure 5.3f**) and reduced splenic tumor burden at the end of follow up (**Figure 5.3g**,**h**). Mechanistically, treatment of *FYN-TRAF3IP2* tumors with BMS-345541 induced suppression of NF-κB activation *in vivo* as evidenced by loss of RelA/p65 nuclear localization (**Figure 5.3d**), along with decreased lymphoma cell proliferation and increased apoptosis as determined by immunohistochemical analyses of Ki67 and cleaved caspase 3, respectively (**Figure 5.3i**). These results support a driver mechanistic role for NF-κB signaling in *FYN-TRAF3IP2* tumor cell proliferation and survival and as therapeutic target for the treatment of PTCL.

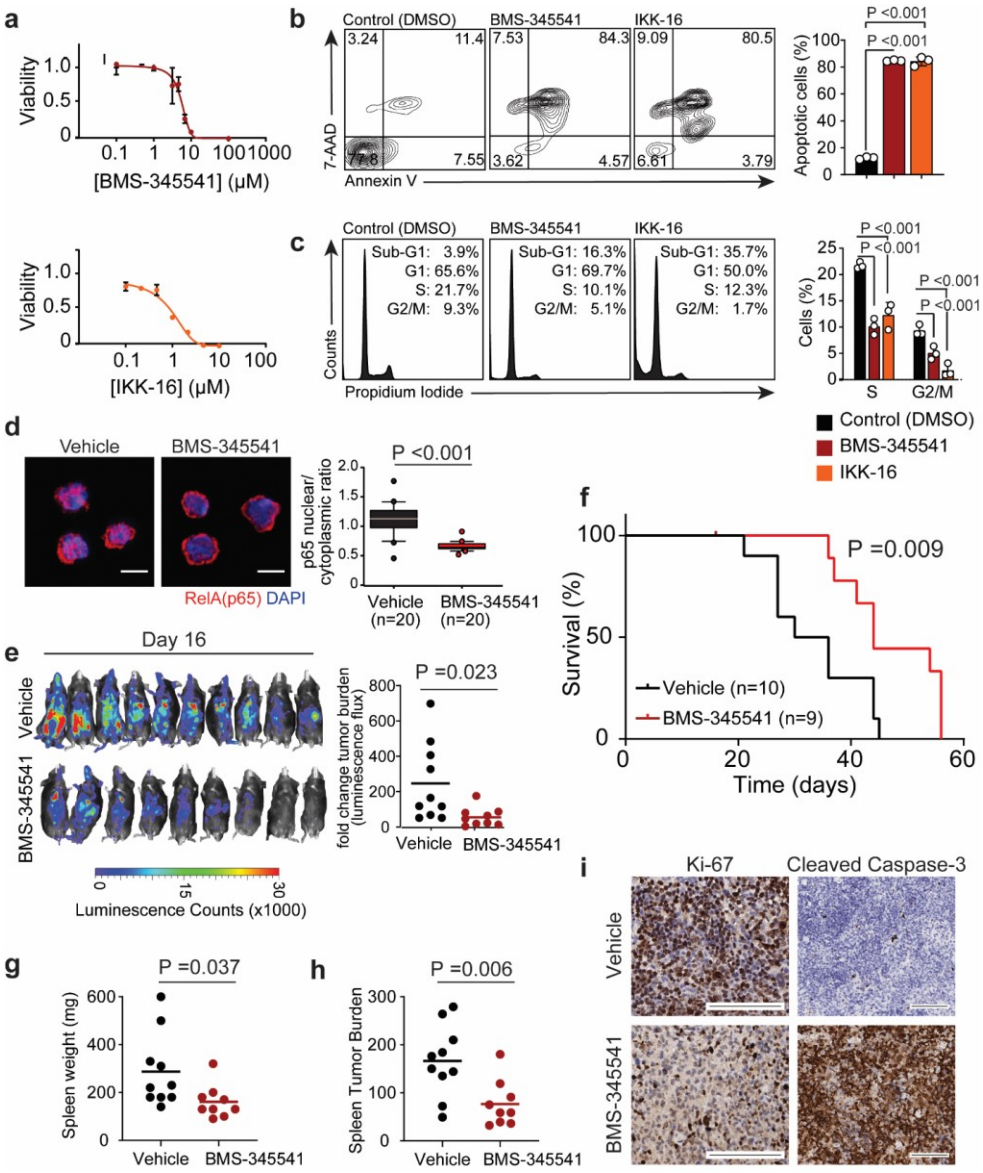

Figure 5.3 – Anti-lymphoma effects of NF-κB inhibition in *FYN-TRAF3IP2*-induced PTCL tumors. a, *In vitro* dose response analysis of *FYN-TRAF3IP2*-induced mouse lymphoma cells to IKK beta inhibitors, BMS-345541 and IKK-16. **b,** Representative FACS plots and quantitation of apoptosis in *FYN-TRAF3IP2*-induced mouse lymphoma cells treated *in vitro* with DMSO and IC50 concentration of BMS-345541 (5 μM) and IKK-16 (2 μM). **c,** Flow cytometry analysis of cell cycle as in **b**. **d,** Immunofluorescence analysis and quantitation (n=20 cells per group) of p65 NF-κB nuclear/cytoplasmic localization in *FYN-TRAF3IP2*-induced mouse lymphoma cells after treatment with vehicle or BMS-345541 *in vivo*. P65 protein is shown in red and DAPI-stained nuclei in blue. Scale bar = 5 μm; N/C ratio, nuclear / cytoplasmic ratio. The boxplot lines indicate the median, boxes represent 25–75% intervals, whiskers represent 10–90% intervals and circles represent data points outside the 10–90% intervals. **e,** Luciferase *in vivo* bioimaging analysis of response of *FYN-TRAF3IP2*-induced mouse lymphomas treated with vehicle or BMS-345541 (n=10 mice in the vehicle group and n=9 mice in the treatment group). Graph indicates fold changes in bioluminescence relative to the basal signal before treatment. **f,** Kaplan-Meier survival curve of the mice treated with BMS-345541 or vehicle as in **e**. **g,** Spleen weight of *FYN-TRAF3IP2*-induced lymphoma-bearing mice treated with vehicle only or BMS-345541 at the endpoint as in **e**, **f**. **h,** Splenic tumor burden as in **g**. **i,** Immunohistochemistry analysis of cell proliferation (Ki67) and apoptosis (cleaved caspase-3) in spleen sections of *FYN-TRAF3IP2*-induced lymphoma-bearing mice after treatment with vehicle only or BMS-345541. Scale bar = 100 μm. Horizontal lines in graphs shown in **e**, **g**, and **h** indicate mean and circles correspond to individual values. P values in **b**, **c**, **d**, **e**, **g** and **h** were calculated using two-tailed Student's t-test. P value in **f** was calculated using the log-rank test.

Conclusions

The clinical and biological heterogeneity of PTCLs has been a major challenge in developing an effective treatment strategy for the disease. While advances in genomic sequencing technologies have facilitated the detection of recurrent genetic alterations in each PTCL subtype, the rarity of the most identified mutations has hindered the development of targeted therapy and improvement in clinical outcomes.

AITL and PTCL, NOS are the two most common subtypes of PTCL, together accounting for almost half of all cases. As discussed in chapter 1, exome sequencing studies in AITL and PTCL, NOS have revealed an overlapping set of point mutations, indels, and copy number changes in genes involved in epigenetic regulation and T-cell receptor (TCR) signaling. However, few oncogenic driver mutations identified so far are prevalent and targetable to promise clinical success, and the survival rates of AITL and PTCL, NOS remain to be about 30% at 5 years.

Identification and characterization of chromosomal rearrangements have contributed significantly to the understanding and clinical management of other neoplasms, perhaps most famously in hematologic malignancies (Das and Tan 2013, Wang et al. 2017). In AITL and PTCL, NOS, however, few have reported recurrent oncogenic gene fusions with the exception of the rare *ITK-SYK* and *VAV1* chimeric oncogenes.

In chapter 2, this study reports a novel fusion oncogene *FYN-TRAF3IP2* that is present in about 40% of AITL and PTCL, NOS. As described in chapter 3, FYN-TRAF3IP2 aberrantly activates NF-κB signaling in response to TCR stimulation or to the treatment with the diacylglycerol analog, and independently of CBM signalosome, a multiprotein complex that translates the proximal TCR signal into NF-κB activation effector pathway. The physiologic role of TRAF3IP2 protein and the necessity of the ubiquitin ligase TRAF6 in the signal transduction strongly indicate the canonical pathway activation in FYN-TRAF3IP2 signaling. While elucidating the exact mechanism requires further study, FYN-TRAF3IP2 most likely initiates NF-κB signaling by forming a poly-ubiquitinated signalosome, to which (1) binding partners of FYN SH3 and SH2 domains, (2) FYN SH4-mediated membrane localization and CD3 interaction, and resultant proximity to other TCR activation

downstream complexes, (3) inherent ubiquitin ligase activity of TRAF3IP2, and (4) trans-auto-binding of TRAF3IP2 moiety by homotypic SEFIR interaction may all contribute. In addition, it may be illuminating to explore the role of diacylglycerol analog in FYN-TRAF3IP2 signaling. Diacylglycerol is a second messenger that binds to and activates protein kinase C (PKC) isozymes and other C1 domain-containing proteins, such as protein kinase D (PKD) isozymes, Ras guanyl nucleotide-releasing proteins (RasGRPs), chimaerins, diacylglycerol kinases (DGKs), and Munc13 proteins (Griner and Kazanietz 2007). Is it PKC, a classic target of diacylglycerol-mediated activation, or another C1 domain-containing enzyme that activates and amplifies FYN-TRAF3IP2 signaling in T cells? Are any of them binding partners and activators of the FYN-TRAF3IP2 protein?

As described in chapter 4, expression of *FYN-TRAF3IP2* in murine hematopoietic progenitors induces NF-κB activated $CD4^+$ mature T-cell lymphoma *in vivo* that recapitulates the characteristics of human PTCL, NOS. The $CD4^+$ immunophenotype of all *FYN-TRAF3IP2*-induced lymphomas suggests T-cell specific nature of the fusion oncogene and coincide with the mechanistic data indicative of the *FYN-TRAF3IP2* function in translating TCR signal to aberrant NF-κB activity.

In fact, chapter 5 describes NF-κB activation in *FYN-TRAF3IP2*-induced mouse PTCL, NOS, evidenced by p65 nuclear localization, increased phospho-p65 levels, and enrichment of NF-κB signature in transcriptomic profiling. Moreover, NF-κB inhibition by IKK inhibitors exerts significant anti-lymphoma effect on *FYN-TRAF3IP2*-induced mouse PTCL, NOS, highlighting the driving role of NF-κB activation in *FYN-TRAF3IP2*-mediated T-cell transformation.

Previous studies have provided evidence of NF-κB activation in AITL and PTCL, NOS as discussed in chapter 1: sequencing studies in AITL and PTCL, NOS have reported mutations in a diverse set of genes involved in NF-κB activation; a large-scale gene expression profiling study across PTCL subtypes in human implicated NF-κB signaling in AITL and some PTCL, NOS; and all published AITL and PTCL, NOS mouse models document NF-κB activation in the tumors.

Taken together, *FYN-TRAF3IP2* induces T cell transformation by aberrantly activating NF-κB, which may be the shared oncogenic mechanism of AITL and a subset of PTCL, NOS.

This interpretation is also consistent with the overrepresentation of AITL and PTCL, NOS in the *FYN-TRAF3IP2* distribution pattern across PTCL subtypes. Of note, while it expresses some TFH

markers that are also NF-κB target genes, *FYN-TRAF3IP2*-induced mouse PTCL, NOS does not seem to have originated from TFH.

Therapeutically, marked improvement in survival and tumor burden in response to IKK inhibitor BMS-345541 in *FYN-TRAFIP2* lymphoma-bearing mice suggests NF-κB inhibition as a strong candidate for targeted clinical intervention in PTCL. As reviewed in chapter 1, constitutive NF-κB activation drives oncogenesis in several other lymphoid neoplasms by promoting survival and proliferation of tumor cells and by supporting the microenvironment via angiogenesis and inflammation. Drawing comparison, transcriptomic profiling of *FYN-TRAF3IP2*-induced mouse PTCL shows strong enrichment in NF-κB target genes involved in anti-apoptosis and inflammation. Relatedly, the strong response to NF-κB inhibition in these mouse tumors may stem from the inhibitor's action against both the tumor cells and the microenvironment components that support lymphoma progression. Given that the microenvironmental components are a major fraction of the disease infiltrate, the supposed dual function of the NF-κB inhibition may be particularly effective in PTCL. Interestingly, recent phase Ib/IIa trial tested the combination of proteaseome inhibitor carfilzomib, immunomodulatory drug lenalidomide, and HDAC inhibitor romidepsin in PTCL and showed promising results in patients with relapsed and refractory AITL (CR in 4/5 patients) (Mehta-Shah et al. 2016). The combination resembles the multiple myeloma treatment strategy which suppresses tumorigenic NF-κB activation by combining proteasome inhibitor and immunomodulatory drug in addition to steroid.

In conclusion, this study highlights the role of NF-κB signaling as a driver of T-cell transformation and as therapeutic target in PTCL.

Materials and Methods

Patient samples

Tumor banks at the Columbia University Medical Center (New York, New York, USA) and Cornell University Medical Center (New York, NY, USA) provided DNA and RNA samples from PTCL biopsies. Samples were obtained with informed consent, and analysis was conducted under the supervision of the Columbia University Medical Center Institutional Review Board.

FYN-TRAF3IP2 gene fusion detection and validation

We analyzed a panel of 101 RNAseq PTCL samples generated by Illumina HiSeq paired-end sequencing as previously described (Abate et al. 2017). To detect gene fusions in the data we used the ChimeraScan algorithm (Iyer et al. 2011), which identifies gene fusion candidates by detecting read pairs discordantly mapping to two different genes. From this analysis, we then successively reduced the candidate list by applying homology-based filters and by detecting reads spanning junction breakpoints (split reads). To further improve our search for driver oncogenic fusions, we applied the Pegasus pipeline (Abate et al. 2014). Briefly, Pegasus reconstructs the entire fusion sequence and annotates lost and preserved protein domains in the gene partners. Next, the algorithm applies a pre-trained classification model to the candidate fusion to derive a probability of it being an oncogenic driver event (termed the Pegasus driver score). In-frame gene fusions with a Pegasus driver score greater than 0.5 were selected for further experimental validation.

To investigate the presence of the *FYN-TRAF3IP2* fusion mRNAs in each of the index samples and in the additional independent panel of 28 samples, we synthesized cDNA from patient total RNA isolated from frozen PTCL biopsies using oligo$(dT)_{20}$ primers and the SuperScript™ IV First-Strand Synthesis System (Invitrogen #18091050) following manufacturer's protocol. We then PCR amplified the region flanking the fusion breakpoint using KAPA HiFi HotStart ReadyMix PCR Kit (Kapa Biosystems #KK2601) and the following primers: *FYN_466-488_FWD* GAAAAGATGCTGAGCGACAGC and *TRAF3IP2_91-70_REV* CCTCTTCCGGGGAATATTCTGG and validated the fusion transcript by dideoxynucleotide sequencing (GENEWIZ, South Plainfield, NJ).

We analyzed the genomic DNA extracted from the patient lymphoma biopsy harboring *FYN-TRAF3IP2* fusion mRNA after deep (100x) whole genome sequencing performed by GENEWIZ on Illumina HiSeq platform following the DNA library preparation using NEBNext® Ultra™ DNA Library Prep Kit. Briefly, acoustic shearing with a Covaris LE220 instrument fragmented the genomic DNA, which was then end repaired, adenylated and ligated with adapters at the 3' ends. Enrichment of the ligated fragments by limited cycle PCR generated the DNA library, which was validated using D1000 ScreenTape on the Agilent 4200 TapeStation (Agilent Technologies, Palo Alto, CA, USA) and was quantified using Qubit 2.0 Fluorometer and by real time PCR (Applied Biosystems, Carlsbad, CA, USA). DNA sequencing was performed on the Illumina HiSeq platform in a 2x 150 paired-end (PE) configuration using the HiSeq Control Software (HCS) on the HiSeq instrument for image analysis and base calling. Raw sequencing data (.bcl files) generated from Illumina HiSeq was converted into fastq files and de-multiplexed using Illumina's bcl2fastq software. One mismatch was allowed for index sequence identification.

We identified structural variants (SV) from the whole genome sequencing data using LUMPY (Layer et al. 2014), which integrates multiple alignment signals, including read depth, splitter and discordant reads.

Cell line and culture

We cultured the Jurkat T cell line (American Type Culture Collection, ATCC), NF-κB/Jurkat/GFP transcriptional reporter cell line (System Biosciences), and CARD11-null Jurkat JPM50.6 cell line (Wang et al. 2002) (kindly provided by Dr. Andrew Snow, Uniformed Services University, Bethesda, MD) in RPMI-1640 containing 10% FBS, 100 U/mL penicillin G, and 100 µg/mL streptomycin. We cultured the HEK293T and HeLa cell lines (ATCC) in DMEM supplemented with 10% FBS, 100 U/mL penicillin G, and 100 µg/mL streptomycin. We cultured the *FYN-TRAF3IP2*-induced murine PTCL cells in RPMI-1640 supplemented with 20% FBS, 100 U/mL penicillin G, 100 µg/mL streptomycin, 100 µM 2-mercaptoethanol and 10ng/mL IL2 (Peprotech #200-02).

We maintained all cell cultures at 37˚C in a humidified atmosphere under 5% CO_2 and regularly tested them for mycoplasma contamination.

Drugs

We purchased IL17A (#200-17) and TNFα (#300-01A) from Peprotech, phorbol 12-myristate 13-acetate (PMA; #P1585) and tamoxifen (#T5648) from Sigma-Aldrich, BMS-345541 (#S8044) and IKK-16 (#S2882) from Selleckchem, and XenoLight D-Luciferin (#122799) from Perkin Elmer. For *in vitro* assays we dissolved IL17 in sterile water and PMA, BMS-345541, and IKK-16 in DMSO. For *in vivo* studies we resuspended 100 mg tamoxifen in 100 µL of ethanol and added corn oil to reach a final concentration of 30 mg/mL. We then rotated the tamoxifen suspension for 1 hour at 55°C and froze in aliquots at −20°C. We administered tamoxifen as a single 100 µL intraperitoneal injection per mouse. For intraperitoneal injections of BMS-345541, we prepared fresh 6 mg/mL aliquots in 2% DMSO, 30% PEG-400 immediately prior to each round of treatment. We used 2% DMSO 30% PEG-400 solution without drug for vehicle injection controls. For *in vivo* bioimaging, we resuspended luciferin in PBS to a final concentration of 15 mg/mL and administered it intraperitoneally 10 minutes before imaging (150 mg/kg).

Plasmid and vectors

We obtained pLX304-blast-V5 construct encoding *TRAF3IP2* and *CARD11* from the Broad Lentiviral Expression Library, pcDNA3 Flag-*TRAF6* (#66929) from Addgene, and FUW-mCherry-Puro-Luc from (Kimbrel et al. 2009). We cloned *TRAF6* into pcDNA3.1 vector (Invitrogen #V79020) with N-terminal HA tag and mutagenized pLX304-*CARD11* plasmid to switch the V5 tag into HA tag at the C-terminal using the QuikChange II XL Site-Directed Mutagenesis kit (Agilent #200522) according to the manufacturer's instructions.

We cloned the gene fusion *FYN-TRAF3IP2*, synthesized by GENEWIZ, and *TRAF3IP2* into pLenti-CMV-Puro vector (Addgene #17452) for human cell line lentiviral infection experiments, pMSCV Puro IRES GFP vector (Addgene #18751) for mouse primary cell retroviral infection experiments, and pcDNA3.1 vector (Invitrogen #V79020) for transient transfection experiments, with N-terminal Kozak sequence GCCACCATG and C-terminal V5 or 3xFLAG tag. We generated the ASVQSKDK and PVAVAA mutants of *FYN-TRAF3IP2* by site directed mutagenesis as described above.

Virus production and infection

To generate infectious viral particles, we transfected HEK293T cells with lentiviral constructs, pCMV ΔR8.91 and pMD.G VSVG or with retroviral constructs and pMCV-copac packaging vector using JetPEI transfection reagent (Polyplus #101-01), according to the manufacturer's protocol.

To transduce Jurkat, NF-κB/Jurkat/GFP, and JPM50.6 cell lines, we collected the lentiviral supernatants 48 hours after transfection and infected the cells by spinoculation. After infection, we selected cells for 1 week in medium containing 1 µg/mL puromycin or 2 weeks in medium containing 1 µg/mL blasticidin. To transduce mouse primary cells, we harvested viral supernatants at 48 hours and 72 hours after transfection and infected the cells by spinoculation on two consecutive days.

NF-κB reporter assays

To analyze NF-κB activity in Jurkat cell line, we measured the median GFP intensity of NF-κB/Jurkat/GFP cells transduced with empty vector or stably expressing wild type *TRAF3IP2*, fusion *FYN-TRAF3IP2*, or mutant constructs by flow cytometry under basal conditions, 12 hours after stimulation with 200 ng/mL IL17, 12 hours after stimulation with antibodies against human CD3, or 6 hours after stimulation with phorbol 12-myristate 13-acetate (PMA) as indicated. To stimulate the cells with a-hCD3 antibodies, we incubated the ice-chilled cells with 0.5 µg/mL anti-hCD3 antibodies (BD Biosciences #555329) on ice for 15 minutes, washed the cells with ice-cold PBS, and resuspended the cell pellet after centrifugation in 37°C warm complete culture media with 10 µg/mL goat anti-mouse Ig (BD biosciences #553998) to 10 x 10^6 cells/mL. After 15 minutes of stimulation in Ig-containing media, we diluted the cell suspension to 1 x 10^6 cells/mL in complete media and cultured the cells for 12 hours before analysis.

We similarly analyzed NF-κB reporter activity in JPM50.6 (*CARD11* knockout, NF-κB-GFP reporter-expressing Jurkat (Wang et al. 2002)) cells by measuring median GFP intensity using flow cytometry under basal conditions or 6 hours after stimulation with 25 nM PMA or 20 ng/mL TNFα.

We acquired flow cytometry data using a FACS Canto cytometer (BD Biosciences) and analyzed it using FlowJo software (TreeStar). The results represented in the figures are representative technical triplicates of at least three independent experiments.

To analyze NF-κB activity by transient transfection followed by dual luciferase reporter assay, we transfected HEK293T cells with 200 ng inducible NF-kB firefly luciferase reporter plasmid (Promega #E8491) and 50 ng constitutively expressed *Renilla* luciferase plasmid (Promega #E2231) together with 1 ng of empty pcDNA3.1 vector or pcDNA3.1 constructs encoding wild type *TRAF3IP2*, fusion *FYN-TRAF3IP2*, or mutant ASVQSKDK *FYN-TRAF3IP2*. We measured luciferase 24 hours after transfection in 96-well format using Dual-Luciferase Reporter Assay Kit (Promega #E1960) and Microplate Reader (Promega #9300-062) according to the manufacturer's protocols.

Cell fractionation

To generate whole cell lysate, we washed cells in PBS, lysed them for 30 minutes in RIPA buffer (50mM Tris, pH 7.5, 150mM NaCl, 1% NP-40, and 0.1% sodium deoxycholate) and centrifuged the samples for 10 minutes at 15,000 x g, 4°C to clear the lysate.

For cytosolic and membrane protein extractions, we used Mem-PER™ Plus Membrane Protein Extraction Kit (Thermo Scientific #89842). Briefly, we extracted cytosolic proteins by resuspending the cell pellet in Cell Permeabilization Buffer and collecting the supernatant after centrifuging at 400 x g, 4°C. To recover the membrane proteins from the pellet, we thoroughly washed the pellet in PBS, resuspended it in plasma membrane lysis buffer (50 mM Tris pH7.5. 150 mM NaCl, 1% NP40), incubated the sample at 4°C with shaking overnight, and collected the supernatant after centrifuging at 16,000 x g for 15 minutes at 4°C.

We supplemented all extraction and wash buffers with by cOmplete™ protease inhibitor cocktail (Sigma Aldrich #4693159001) and PhosSTOP™ phosphatase inhibitor cocktail (Sigma Aldrich #4906837001) and kept them ice-cold before use.

Immunoblot analysis

We separated the protein extract by SDS-PAGE and transferred to nitrocellulose membranes using standard procedures. We detected the immunoblots using following primary antibodies against: V5 (dilution 1:2,000) (Cell Signaling Technology #13202), GAPDH (dilution 1:10,000) (Cell Signaling Technology #5174), FLAG (dilution 1:1,000) (Sigma Aldrich #F1804), HSP90 (dilution 1:1,000) (Cell Signaling Technology #4874), Na/K ATPase (dilution 1:1,000) (Cell Signaling Technology

#3010), CARD11 (dilution 1:1,000) (Cell Signaling Technology #4440), HA (dilution 1:1,000) (Roche #11867423001), α-Tubulin (dilution 1:5,000) (Sigma Aldrich #T9026). We visualized the immunoblots using IRDye Secondary Antibodies (LI-COR biosciences) and Odyssey Infrared Imaging System (LI-COR Biosciences). We performed quantification analysis of the immunoblots using Image Studio software (LI-COR biosciences).

Immunofluorescence

To analyze the cellular localization of the TRAF3IP2 proteins, we cultured HeLa cells on the Poly-D-Lysine-coated 12 mm glass coverslips (Corning™ #354086) and transfected them with pcDNA3.1 construct encoding *TRAF3IP2*, *FYN-TRAF3IP2*, or *FYN-TRAF3IP2* ASVQSKDK tagged with 3xFLAG at the C-terminal. 48 hours after the transfection, we fixed the cells on the coverslip with 4% paraformaldehyde in PBS (Electron Microscopy Sciences #15700) for 20 min at room temperature and permeabilized and blocked them in saponin blocking buffer (3% BSA, 0.1% saponin in PBS) for 2 hours at room temperature. To detect the proteins, we incubated the coverslips overnight at 4°C in primary antibodies against FLAG (dilution 1:500) (Sigma Aldrich #F1804) and Na/K ATPase (dilution 1:500) (Abcam #ab76020) diluted in saponin blocking buffer. After washing the coverslip in 0.1% saponin in PBS, we stained the samples at room temperature for 1 hour in dark using fluorescently-labeled secondary antibodies: Alexa Fluor 488 against rabbit (dilution 1:500) (Invitrogen #A21206) and Alexa Fluor 568 against mouse (dilution 1:500) (Abcam #ab175700). We then washed the coverslips in PBS and mounted them in Prolong Diamond mounting media with DAPI (Invitrogen #P36966).

For mouse cells, we sorted the CD4+ or CD4+ GFP+ population accordingly and resuspended the cell pellet in 3% paraformaldehyde, 2% sucrose in PBS to fix. We attached the fixed cells on the coverslips by layering the cell suspension over the Poly-D-Lysine-coated coverslips and centrifuging at room temperature for 10 minutes at 1200 rpm. We then washed the coverslips in PBS and permeabilized the cells in 0.25% TritonX-100 in PBS at room temperature for 10 minutes. After washing and blocking the coverslips in PBST (0.1% Tween-20 in PBS) and 4% BSA in PBST respectively, we labeled the p65 proteins overnight at 4°C using primary antibody (Cell Signaling Technology #8242) diluted 1:200 in 4% BSA-PBST. The following morning, we washed the

coverslips in PBST and stained the protein for 1 hour at room temperature in the dark using Alexa Fluor 647-conjugated antibody against rabbit (dilution 1:500) (Cell Signaling Technology #4414). After washing, we counterstained the cells with DAPI before mounting the coverslip in Prolong Glass mounting media (Invitrogen #P36982). Cells were imaged and scored the next morning. We acquired images on Nikon Ti Eclipse inverted confocal microscope using NIS-Elements software. We prepared the images for display and quantitated the fluorescent signals using NIH ImageJ/FIJI software. To quantify p65 intensity in cytosol and nucleus, we measured the integrated density over the nuclear and cytosolic area and subtracted each by background signal (calculated by multiplying mean gray value of background times area of region of interest).

Immunoprecipitation

We transfected HEK293T cells with pcDNA3.1-*HA-TRAF6* and empty vector or pcDNA3.1 constructs encoding wild type *TRAF3IP2-V5*, fusion *FYN-TRAF3IP2-V5*, or mutant PVAVAAA-*FYN-TRAF3IP2-V5*, using JetPEI transfection reagent (Polyplus #101-01) according to the manufacturer's protocol. After 24 hours, we collected the cells by scraping, washed in cold 1x PBS, and lysed for 30 minutes in Immunoprecipitation Lysis buffer (50 mM Tris pH7.5. 150 mM NaCl, 1% NP40 supplemented with protease and phosphatase inhibitors). After clearing the lysate by 15 minute 15,000 x g centrifugation at 4˚C, we incubated the protein extract overnight at 4°C with either EZview Red Anti-HA Affinity gel (Sigma Aldrich #E6779) or Anti-V5 Agarose Affinity Gel (Sigma Aldrich #A7345). We then washed the beads in the Immunoprecipitation Lysis buffer and eluted the immunoprecipitates from the beads by boiling in Laemmli sample buffer before analyzing them by SDS-PAGE and immunoblotting.

Mice

We maintained all animals in filter-topped cages on autoclaved food and water in specific pathogen-free facilities at the Irving Cancer Research Center at Columbia University Medical Center campus. All animal procedures were approved by the Institutional Animal Care and Use Committee (IACUC) at Columbia University Medical Center (Protocol # AAAU8468). The *Tet2*$^{fl/fl}$ mouse line was generously provided by Dr. Ross Levine at MSKCC (New York, NY) (Moran-Crusio et al. 2011).

CD4CreER^{T2} line (Tg(Cd4-cre/ERT2)11Gnri) mice, which expresses a tamoxifen-inducible form of the *Cre* recombinase under the control of the mouse *Cd4* promoter (Aghajani et al. 2012), as well as *Rag2* knockout mice (*Rag2*$^{tm1.1Cgn}$/J) were purchased from Jackson Laboratories (Bar Harbor, ME). We bred *Tet2*$^{fl/fl}$ mice with CD4CreER^{T2} line to generate conditional inducible CD4 specific *Tet2* knockout mice. Age- and sex-matched male and female mice of each genotype were used in experiments in which different genotypes were compared. For drug treatment and tumor transplant studies, age-matched female mice were randomly assigned to different treatment groups. Animal experiments were conducted in compliance with all relevant ethical regulations. Animals were euthanized upon showing symptoms of clinically overt disease (do not feed, lack of activity, abnormal grooming behavior, hunch back posture) or excessive weight loss (20% body weight loss or 10-15% over a week).

Bone marrow transplantation

To analyze the oncogenic activity of *FYN-TRAF3IP2 in vivo* in both wild type and *Tet2*-inactivated CD4 T cells, we harvested bone marrow cells from the long bones of *Tet2*$^{fl/fl}$;CD4CreER^{T2} mice and isolated lineage negative cells using a magnetic bead-based, negative selection cell lineage depletion kit (Miltenyi Biotec #130-090-858) following manufacturer's guidelines. We transduced the isolated lineage negative cells with retroviral particles encoded by pMSCV IRES GFP containing *GFP* only; *TRAF3IP2-V5* and *GFP*; or *FYN-TRAF3IP2-V5* and *GFP*. We transplanted 1.75 x 10^5 GFP$^+$ lineage negative cells via retro-orbital injection into lethally irradiated 8 to 12 week-old isogenic C57BL/6 female mice. To induce *Tet2* deletion in CD4+ T cells of mice assigned to *Tet2*$^{-/-}$ group, we treated mice transplanted with the *Tet2*$^{fl/fl}$;CD4CreER^{T2} bone marrow progenitors with a single dose of tamoxifen (3 mg) at 8 weeks post-transplant, while administrating corn oil vehicle to the mice assigned to *Tet2*$^{fl/fl}$ group. To provide stimulatory signals to T cells and induce T cell proliferation, we immunized each mouse with 1×10^8 sheep red blood cells (SRBC) (Cocalico Biologicals #20-1334A) delivered by intraperitoneal injection every 4-5 weeks for 6 cycles.

At the end of follow up, one animal from *Tet2*$^{-/-}$ *TRAF3IP2-V5* group and one animal from *Tet2*$^{-/-}$ *FYN-TRAF3IP2-V5* developed non-transplant-derived GFP$^-$ disease and were excluded from the spleen weight analysis.

Histopathology and immunohistochemistry

Mouse tissues were dissected and fixed in 10% buffered formalin and paraffin-embedded at the Molecular Pathology Shared Resource of the Herbert Irving Comprehensive Cancer Center (HICCC) at Columbia University Medical Center. Tissue sections were subjected to hematoxylin-eosin staining using standard procedures. Immunostaining for Ki67 and cleaved caspase-3 was performed at HistoWiz, Inc. (Brooklyn, NY). Slides were scanned using a Leica SCN 400 scanner and photomicrographs were examined with Aperio ImageScope Software (Leica Biosystems).

Antibody staining for flow cytometry analysis

We stained single cell suspensions following standard procedures using fluorochrome-conjugated antibodies against CD4 (RM4-5 or GK1.5, BD biosciences), PD1 (J43, eBiosciences) and ICOS (7E.17G9, Biolegend).

For detection of CXCR5, we used purified anti-CXCR5 antibody (2G8) from BD Biosciences and followed a three-step staining protocol as previously described (Johnston et al. 2009). For intracellular detection of BCL6 and phospho-p65, we fixed and permeabilized the cells using Foxp3 / Transcription Factor Staining Buffer Set (eBiosciences 00-5523-00). Briefly, we FACS sorted $CD4^+$ GFP^+ *FYN-TRAF3IP2*-induced lymphoma cells, $CD4^+$ GFP^- matched non-tumor T cells of the lymphoma-bearing animals, or $CD4^+$ T cells from wild type C57BL/6 animals into 1x Fixation/Permeabilization buffer prepared according to the manufacturer's guidelines. We subsequently diluted the fixed cells in 1x permeabilization buffer as instructed by the manufacturer's protocol and labeled the protein of interest. For BCL6, we used fluorochrome-conjugated antibody against BCL6 (K112-91) from BD Biosciences. For phospho-p65, we used phospho-p65 antibody (93H1) followed by Alexa Fluor 647-conjugated secondary antibody (#4414), both supplied by Cell Signaling Technology.

We performed FACS sorting on SH800S cell sorter (SONY biotechnologies) using Sony Cell Sorter Software and acquired flow cytometry data using FACS Canto cytometer (BD Biosciences). We analyzed flow cytometry data using FlowJo software (TreeStar).

T cell receptor variable beta chain (TCR Vβ) repertoire analysis

We utilized flow cytometry to analyze the TCR Vβ repertoire of the $CD4^+$ GFP^+ lymphoma population using a panel of 14 monoclonal antibodies directed against the variable (V) region of the TCRβ chain: TCR Vβ2 (B20.6), TCR Vβ5.1/5.2 (MR9-4), TCR Vβ6 (RR4-7), TCR Vβ7 (TR310), TCR Vβ8.1/8.2 (MR5-2), TCR Vβ9 (MR10-2), TCR Vβ11 (RR3-15), TCR Vβ12 (MR11-1) and TCR Vβ13 (MR12-4) from Biolegend; TCR Vβ3 (KJ25), TCR Vβ4 (KT4), TCR Vβ 8.3 (1B3.3), TCR Vβ10b (B21.5) and TCR Vβ 14 (14-2) from BD Pharmigen. We assessed the clonal expansion by comparing of the TCR Vβ repertoire distribution in GFP^+ $CD4^+$ cells versus non-tumorigenic GFP-null $CD4^+$ T cells from the same sample.

In addition, TCR Vβ repertoire analysis of genomic DNA samples by TCR sequencing was performed at Adaptive Biotechnologies, (Seattle, USA) using the mouse immunoSEQ assay (Hsu et al. 2016). We analyzed TCR sequencing data using Adaptive Biotechnologies immunoSEQ analyzer proprietary software.

DNA and RNA isolation

We extracted genomic DNA and total RNA from FACS-sorted *FYN-TRAF3IP2*-induced mouse lymphoma cells using AllPrep DNA/RNA mini kit (Qiagen #80204). Briefly, we sorted $CD4^+$ GFP^+ lymphoma cells into appropriate volume of RLT plus buffer and isolated nucleic acid from the lysate according to the kit manufacturer's protocol.

We used RNeasy mini kit (Qiagen #74104) to extract total RNA in naïve $CD4^+$ T cells, isolated from wild type C57BL/6 mouse spleen via magnetic bead-based negative selection cell depletion (Miltenyi Biotec #130-104-453).

Tumor transplantation

We injected cell suspensions (1×10^8 cells) extracted from lymphoma-containing spleen of diseased mice intravenously into 6 to 8 week-old female isogenic C57BL/6 wild type or *Rag2* knockout immunodeficient mice.

RNAseq and gene expression profiling

RNAseq libraries were prepared and sequenced on Illumina HiSeq platform by GENEWIZ. Briefly, sequencing libraries were prepared using Illumina Nextera XT library from the full-length cDNA synthesized and amplified by SMART-Seq v4 Ultra Low Input Kit (Clontech, Mountain View, CA). Individual libraries were pooled at equimolar concentrations and sequenced to an average depth of 30 million, 150 base pair, paired-end reads per sample on an Illumina HiSeq 4000 instrument.

After trimming adapters from raw reads using Trim Galore (version 0.4.4), we aligned the reads to GRCm38.p5 with the Gencode vM16 feature annotation using STAR (version 2.7) (Dobin et al. 2013). We assigned the reads to Gencode vM16 features and computed raw counts at the gene-level using featureCounts (version 1.6.4) (Liao et al. 2014). We performed differential gene expression analysis using DESeq2 (version 1.24.0) (Love et al. 2014) in R (version 3.6.0), filtering out genes with fewer than 15 total fragments mapped and fitting a negative binomial GLM after estimating library size factors and gene count dispersions. We used the fitted GLM to test contrasts with Wald statistics and determine the log2 fold change. To plot heatmaps and visualize expression data, we used log transformed, size factor normalized gene counts.

Using javaGSEA and R, we performed Gene Set Enrichment Analysis (GSEA) (Subramanian et al. 2005) with gene sets available in Molecular Signatures Database (MSigDB), Dr. Thomas Gilmore's NF-κB target database (Boston University, Boston, MA) (http://www.bu.edu/nf-kb/gene-resources/target-genes/), and a previously published NF-κB signature identified in the context of B cell lymphoma (Saba et al. 2016).

***In vitro* cell viability and pharmacological treatment assays**

We measured cell growth and treatment responses of primary mouse tumors *in vitro* by measurement of the metabolic reduction of the tetrazolium salt MTT using the Cell Proliferation Kit I (Sigma Aldrich #11465007001) following the manufacturer's instructions. We analyzed drug treatment responses following 72 hour incubation with increasing concentrations of BMS-345541 or IKK-16. The dose response curves represented in the figures are representative technical triplicates of experiments on three independent mouse tumor samples.

Following 72 hour incubation with IC50 dose of the drugs, we quantified cell viability and apoptosis by flow cytometry with Annexin V-APC (BD Biosciences #550475) and 7-AAD markers (BD Biosciences #559925) and performed cell cycle analysis by flow cytometry after Propidium Iodide (Sigma Aldrich #P4864) DNA staining. The results represented in the figures are representative technical triplicates of at least three independent experiments.

***In vivo* pharmacological treatments**

For experimental therapeutics studies, we used *Tet2*$^{-/-}$ *FYN-TRAF3IP2* GFP^{+} PTCL, NOS tumor cells lentivirally infected with FUW-mCherry-Luc-puro to express luciferase. We transplanted luciferase-expressing lymphoma cells into *Rag2* knockout mice via retro-orbital injection and monitored tumor development by *in vivo* luminescence bioimaging with the IVIS Spectrum *In Vivo* Imaging System (Perkin Elmer).

For acute effect study, we administered vehicle only or BMS-345541 (first dose: 60 mg/kg; second dose 12 hours later: 100 mg/kg) intraperitoneally to animals presenting homogeneous tumor burden. We sacrificed the mice for analyses 6 hours after the last treatment.

For longitudinal studies we randomly assigned animals presenting homogeneous tumor burden at day 14 post-transplant to two treatment cohorts, vehicle only or BMS-345541 (n=10 animals/group). One mouse in treatment group died before the treatment started. Following baseline tumor load quantification, we intraperitoneally injected BMS-345541 (25 mg/kg) or vehicle only to mice every other day for the first four weeks first and dosed them two consecutive days with one day off thereafter. We assessed the effect of BMS-345541 on overall tumor burden by *in vivo* bioimaging 16 days after the start of the treatment schedule, before any lymphoma-caused mortality. We measured spleen weight and quantified spleen tumor burden at endpoint considering % of GFP^{+} cells and spleen weight. We collected and analyzed the i*n vivo* bioimaging data using Living Image software (Perkin Elmer).

Statistical Analyses

We conducted statistical analyses using Prism software v8.0 (GraphPad Software, La Jolla, CA, USA) and considered statistical significance at $P < 0.05$. We reported results as mean ± SD

(standard deviation), as indicated in the figure legends unless otherwise stated, with significance annotated by P value calculated using student's t-test assuming equal variance and normal distribution. For survival in mouse experiments, we represented the results as Kaplan-Meier curves and determined the significance using Log-rank test. Representative images correspond to experiments repeated at least twice.

References

(1997). "A clinical evaluation of the International Lymphoma Study Group classification of non-Hodgkin's lymphoma. The Non-Hodgkin's Lymphoma Classification Project." Blood **89**(11): 3909-3918.

Abate, F., A. C. da Silva-Almeida, S. Zairis, J. Robles-Valero, L. Couronne, H. Khiabanian, S. A. Quinn, M. Y. Kim, M. A. Laginestra, C. Kim, D. Fiore, G. Bhagat, M. A. Piris, E. Campo, I. S. Lossos, O. A. Bernard, G. Inghirami, S. Pileri, X. R. Bustelo, R. Rabadan, A. A. Ferrando and T. Palomero (2017). "Activating mutations and translocations in the guanine exchange factor VAV1 in peripheral T-cell lymphomas." Proc Natl Acad Sci U S A **114**(4): 764-769.

Abate, F., S. Zairis, E. Ficarra, A. Acquaviva, C. H. Wiggins, V. Frattini, A. Lasorella, A. Iavarone, G. Inghirami and R. Rabadan (2014). "Pegasus: a comprehensive annotation and prediction tool for detection of driver gene fusions in cancer." BMC Syst Biol **8**: 97.

Abouyabis, A. N., P. J. Shenoy, M. J. Lechowicz and C. R. Flowers (2008). "Incidence and outcomes of the peripheral T-cell lymphoma subtypes in the United States." Leuk Lymphoma **49**(11): 2099-2107.

Abouyabis, A. N., P. J. Shenoy, R. Sinha, C. R. Flowers and M. J. Lechowicz (2011). "A Systematic Review and Meta-Analysis of Front-line Anthracycline-Based Chemotherapy Regimens for Peripheral T-Cell Lymphoma." ISRN Hematol **2011**: 623924.

Adams, S. V., P. A. Newcomb and A. R. Shustov (2016). "Racial Patterns of Peripheral T-Cell Lymphoma Incidence and Survival in the United States." J Clin Oncol **34**(9): 963-971.

Advani, R., S. Horwitz, A. Zelenetz and S. J. Horning (2007). "Angioimmunoblastic T cell lymphoma: treatment experience with cyclosporine." Leuk Lymphoma **48**(3): 521-525.

Aghajani, K., S. Keerthivasan, Y. Yu and F. Gounari (2012). "Generation of CD4CreER(T(2)) transgenic mice to study development of peripheral CD4-T-cells." Genesis **50**(12): 908-913.

Akagi, T., M. Motegi, A. Tamura, R. Suzuki, Y. Hosokawa, H. Suzuki, H. Ota, S. Nakamura, Y. Morishima, M. Taniwaki and M. Seto (1999). "A novel gene, MALT1 at 18q21, is involved in t(11;18) (q21;q21) found in low-grade B-cell lymphoma of mucosa-associated lymphoid tissue." Oncogene **18**(42): 5785-5794.

Altmann, B., G. Wulf, L. Truemper, F. d'Amore, T. Relander, H. Toldbod, J. M. A. Delabie, A. Rosenwald, M. Ziepert and M. Loeffler (2018). "Alemtuzumab Added to CHOP for Treatment of Peripheral T-Cell Lymphoma (PTCL) in Previously Untreated Young and Elderly Patients: Pooled Analysis of the International ACT-1/2 Phase III Trials." Blood **132**(Suppl 1): 1622-1622.

Amatya, N., A. V. Garg and S. L. Gaffen (2017). "IL-17 Signaling: The Yin and the Yang." Trends Immunol **38**(5): 310-322.

Amrein, K. E., N. Flint, B. Panholzer and P. Burn (1992). "Ras GTPase-activating protein: a substrate and a potential binding protein of the protein-tyrosine kinase p56lck." Proc Natl Acad Sci U S A **89**(8): 3343-3346.

Anderson, J. R., J. O. Armitage and D. D. Weisenburger (1998). "Epidemiology of the non-Hodgkin's lymphomas: distributions of the major subtypes differ by geographic locations. Non-Hodgkin's Lymphoma Classification Project." Ann Oncol **9**(7): 717-720.

Annunziata, C. M., R. E. Davis, Y. Demchenko, W. Bellamy, A. Gabrea, F. Zhan, G. Lenz, I. Hanamura, G. Wright, W. Xiao, S. Dave, E. M. Hurt, B. Tan, H. Zhao, O. Stephens, M. Santra, D. R. Williams, L. Dang, B. Barlogie, J. D. Shaughnessy, Jr., W. M. Kuehl and L. M. Staudt (2007). "Frequent engagement of the classical and alternative NF-kappaB pathways by diverse genetic abnormalities in multiple myeloma." Cancer Cell **12**(2): 115-130.

Appleby, M. W., J. A. Gross, M. P. Cooke, S. D. Levin, X. Qian and R. M. Perlmutter (1992). "Defective T cell receptor signaling in mice lacking the thymic isoform of p59fyn." Cell **70**(5): 751-763.

Arber, D. A., L. M. Weiss, P. F. Albujar, Y. Y. Chen and E. S. Jaffe (1993). "Nasal lymphomas in Peru. High incidence of T-cell immunophenotype and Epstein-Barr virus infection." Am J Surg Pathol **17**(4): 392-399.

Atkinson, E. A., H. Ostergaard, K. Kane, M. J. Pinkoski, A. Caputo, M. W. Olszowy and R. C. Bleackley (1996). "A physical interaction between the cell death protein Fas and the tyrosine kinase p59fynT." J Biol Chem **271**(11): 5968-5971.

Au, W. Y., D. D. Weisenburger, T. Intragumtornchai, S. Nakamura, W. S. Kim, I. Sng, J. Vose, J. O. Armitage and R. Liang (2009). "Clinical differences between nasal and extranasal natural killer/T-cell lymphoma: a study of 136 cases from the International Peripheral T-Cell Lymphoma Project." Blood **113**(17): 3931-3937.

August, A. and B. Dupont (1996). "Association between mitogen-activated protein kinase and the zeta chain of the T cell receptor (TcR) with the SH2,3 domain of p56lck. Differential regulation by TcR cross-linking." J Biol Chem **271**(17): 10054-10059.

Awasthee, N., V. Rai, S. Chava, P. Nallasamy, A. B. Kunnumakkara, A. Bishayee, S. C. Chauhan, K. B. Challagundla and S. C. Gupta (2019). "Targeting IkappaappaB kinases for cancer therapy." Semin Cancer Biol **56**: 12-24.

Badour, K., J. Zhang, F. Shi, Y. Leng, M. Collins and K. A. Siminovitch (2004). "Fyn and PTP-PEST-mediated regulation of Wiskott-Aldrich syndrome protein (WASp) tyrosine phosphorylation is required for coupling T cell antigen receptor engagement to WASp effector function and T cell activation." J Exp Med **199**(1): 99-112.

Baens, M., S. Fevery, X. Sagaert, H. Noels, S. Hagens, V. Broeckx, A. D. Billiau, C. De Wolf-Peeters and P. Marynen (2006). "Selective expansion of marginal zone B cells in Emicro-API2-MALT1 mice is linked to enhanced IkappaB kinase gamma polyubiquitination." Cancer Res **66**(10): 5270-5277.

Ballester, B., O. Ramuz, C. Gisselbrecht, G. Doucet, L. Loi, B. Loriod, F. Bertucci, R. Bouabdallah, E. Devilard, N. Carbuccia, M. J. Mozziconacci, D. Birnbaum, P. Brousset, F. Berger, G. Salles, J. Briere, R. Houlgatte, P. Gaulard and L. Xerri (2006). "Gene expression profiling identifies molecular subgroups among nodal peripheral T-cell lymphomas." Oncogene **25**(10): 1560-1570.

Bargou, R. C., F. Emmerich, D. Krappmann, K. Bommert, M. Y. Mapara, W. Arnold, H. D. Royer, E. Grinstein, A. Greiner, C. Scheidereit and B. Dorken (1997). "Constitutive nuclear factor-kappaB-RelA activation is required for proliferation and survival of Hodgkin's disease tumor cells." J Clin Invest **100**(12): 2961-2969.

Bargou, R. C., C. Leng, D. Krappmann, F. Emmerich, M. Y. Mapara, K. Bommert, H. D. Royer, C. Scheidereit and B. Dorken (1996). "High-level nuclear NF-kappa B and Oct-2 is a common feature of cultured Hodgkin/Reed-Sternberg cells." Blood **87**(10): 4340-4347.

Beachy, S. H., M. Onozawa, Y. J. Chung, C. Slape, S. Bilke, P. Francis, M. Pineda, R. L. Walker, P. Meltzer and P. D. Aplan (2012). "Enforced expression of Lin28b leads to impaired T-cell development, release of inflammatory cytokines, and peripheral T-cell lymphoma." Blood **120**(5): 1048-1059.

Begalli, F., J. Bennett, D. Capece, D. Verzella, D. D'Andrea, L. Tornatore and G. Franzoso (2017). "Unlocking the NF-kappaB Conundrum: Embracing Complexity to Achieve Specificity." Biomedicines **5**(3).

Bejar, R., A. Lord, K. Stevenson, M. Bar-Natan, A. Perez-Ladaga, J. Zaneveld, H. Wang, B. Caughey, P. Stojanov, G. Getz, G. Garcia-Manero, H. Kantarjian, R. Chen, R. M. Stone, D. Neuberg, D. P. Steensma and B. L. Ebert (2014). "TET2 mutations predict response to hypomethylating agents in myelodysplastic syndrome patients." Blood **124**(17): 2705-2712.

Bennett, J., D. Capece, F. Begalli, D. Verzella, D. D'Andrea, L. Tornatore and G. Franzoso (2018). "NF-kappaB in the crosshairs: Rethinking an old riddle." Int J Biochem Cell Biol **95**: 108-112.

Beyers, A. D., L. L. Spruyt and A. F. Williams (1992). "Molecular associations between the T-lymphocyte antigen receptor complex and the surface antigens CD2, CD4, or CD8 and CD5." Proc Natl Acad Sci U S A **89**(7): 2945-2949.

Boddicker, R. L., G. L. Razidlo, S. Dasari, Y. Zeng, G. Hu, R. A. Knudson, P. T. Greipp, J. I. Davila, S. H. Johnson, J. C. Porcher, J. B. Smadbeck, B. W. Eckloff, D. D. Billadeau, P. J. Kurtin, M. A. McNiven, B. K. Link, S. M. Ansell, J. R. Cerhan, Y. W. Asmann, G. Vasmatzis and A. L. Feldman (2016). "Integrated mate-pair and RNA sequencing identifies novel, targetable gene fusions in peripheral T-cell lymphoma." Blood **128**(9): 1234-1245.

Burke, J. R., M. A. Pattoli, K. R. Gregor, P. J. Brassil, J. F. MacMaster, K. W. McIntyre, X. Yang, V. S. Iotzova, W. Clarke, J. Strnad, Y. Qiu and F. C. Zusi (2003). "BMS-345541 is a highly selective inhibitor of I kappa B kinase that binds at an allosteric site of the enzyme and blocks NF-kappa B-dependent transcription in mice." J Biol Chem **278**(3): 1450-1456.

Cabannes, E., G. Khan, F. Aillet, R. F. Jarrett and R. T. Hay (1999). "Mutations in the IkBa gene in Hodgkin's disease suggest a tumour suppressor role for IkappaBalpha." Oncogene **18**(20): 3063-3070.

Cairns, R. A., J. Iqbal, F. Lemonnier, C. Kucuk, L. de Leval, J. P. Jais, M. Parrens, A. Martin, L. Xerri, P. Brousset, L. C. Chan, W. C. Chan, P. Gaulard and T. W. Mak (2012). "IDH2 mutations are frequent in angioimmunoblastic T-cell lymphoma." Blood **119**(8): 1901-1903.

Calado, D. P., B. Zhang, L. Srinivasan, Y. Sasaki, J. Seagal, C. Unitt, S. Rodig, J. Kutok, A. Tarakhovsky, M. Schmidt-Supprian and K. Rajewsky (2010). "Constitutive canonical NF-kappaB activation cooperates with disruption of BLIMP1 in the pathogenesis of activated B cell-like diffuse large cell lymphoma." Cancer Cell **18**(6): 580-589.

Campo, E., S. Swerdlow, N. Harris, S. Pileri, H. Stein and E. Jaffe (2008). World Health Organization classification of tumors. Pathology and genetics of tumours of hematopoietic and lymphoid tissues, Lyon: IARC Press.

Carbone, A., A. Gloghini, H. J. Gruss and A. Pinto (1995). "CD40 ligand is constitutively expressed in a subset of T cell lymphomas and on the microenvironmental reactive T cells of follicular lymphomas and Hodgkin's disease." Am J Pathol **147**(4): 912-922.

Castro, I., J. A. Wright, B. Damdinsuren, K. L. Hoek, G. Carlesso, N. P. Shinners, R. M. Gerstein, R. T. Woodland, R. Sen and W. N. Khan (2009). "B cell receptor-mediated sustained c-Rel activation facilitates late transitional B cell survival through control of B cell activating factor receptor and NF-kappaB2." J Immunol **182**(12): 7729-7737.

Chakraborty, A. K. and A. Weiss (2014). "Insights into the initiation of TCR signaling." Nat Immunol **15**(9): 798-807.

Chang, S. H., H. Park and C. Dong (2006). "Act1 adaptor protein is an immediate and essential signaling component of interleukin-17 receptor." J Biol Chem **281**(47): 35603-35607.

Chapman, M. A., M. S. Lawrence, J. J. Keats, K. Cibulskis, C. Sougnez, A. C. Schinzel, C. L. Harview, J. P. Brunet, G. J. Ahmann, M. Adli, K. C. Anderson, K. G. Ardlie, D. Auclair, A. Baker, P. L. Bergsagel, B. E. Bernstein, Y. Drier, R. Fonseca, S. B. Gabriel, C. C. Hofmeister, S. Jagannath, A. J. Jakubowiak, A. Krishnan, J. Levy, T. Liefeld, S. Lonial, S. Mahan, B. Mfuko, S. Monti, L. M. Perkins, R. Onofrio, T. J. Pugh, S. V. Rajkumar, A. H. Ramos, D. S. Siegel, A. Sivachenko, A. K. Stewart, S. Trudel, R. Vij, D. Voet, W. Winckler, T. Zimmerman, J. Carpten, J. Trent, W. C. Hahn, L. A. Garraway, M. Meyerson, E. S. Lander, G. Getz and T. R. Golub (2011). "Initial genome sequencing and analysis of multiple myeloma." Nature **471**(7339): 467-472.

Chen, L. and D. B. Flies (2013). "Molecular mechanisms of T cell co-stimulation and co-inhibition." Nat Rev Immunol **13**(4): 227-242.

Chihara, D., H. Ito, T. Matsuda, A. Shibata, A. Katsumi, S. Nakamura, S. Tomotaka, L. M. Morton, D. D. Weisenburger and K. Matsuo (2014). "Differences in incidence and trends of haematological malignancies in Japan and the United States." Br J Haematol **164**(4): 536-545.

Chim, C. S., S. K. Kumar, R. Z. Orlowski, G. Cook, P. G. Richardson, M. A. Gertz, S. Giralt, M. V. Mateos, X. Leleu and K. C. Anderson (2018). "Management of relapsed and refractory multiple myeloma: novel agents, antibodies, immunotherapies and beyond." Leukemia **32**(2): 252-262.

Chng, W. J., S. Kumar, S. Vanwier, G. Ahmann, T. Price-Troska, K. Henderson, T. H. Chung, S. Kim, G. Mulligan, B. Bryant, J. Carpten, M. Gertz, S. V. Rajkumar, M. Lacy, A. Dispenzieri, R. Kyle, P. Greipp, P. L. Bergsagel and R. Fonseca (2007). "Molecular dissection of hyperdiploid multiple myeloma by gene expression profiling." Cancer Res **67**(7): 2982-2989.

Choi, Y. B., C. K. Kim and Y. Yun (1999). "Lad, an adapter protein interacting with the SH2 domain of p56lck, is required for T cell activation." J Immunol **163**(10): 5242-5249.

Chtanova, T., S. G. Tangye, R. Newton, N. Frank, M. R. Hodge, M. S. Rolph and C. R. Mackay (2004). "T follicular helper cells express a distinctive transcriptional profile, reflecting their role as non-Th1/Th2 effector cells that provide help for B cells." J Immunol **173**(1): 68-78.

Coiffier, B., B. Pro, H. M. Prince, F. Foss, L. Sokol, M. Greenwood, D. Caballero, F. Morschhauser, M. Wilhelm, L. Pinter-Brown, S. Padmanabhan Iyer, A. Shustov, T. Nielsen, J. Nichols, J. Wolfson, B. Balser and S. Horwitz (2014). "Romidepsin for the treatment of relapsed/refractory peripheral T-cell lymphoma: pivotal study update demonstrates durable responses." J Hematol Oncol **7**: 11.

Compagno, M., W. K. Lim, A. Grunn, S. V. Nandula, M. Brahmachary, Q. Shen, F. Bertoni, M. Ponzoni, M. Scandurra, A. Califano, G. Bhagat, A. Chadburn, R. Dalla-Favera and L. Pasqualucci (2009). "Mutations of multiple genes cause deregulation of NF-kappaB in diffuse large B-cell lymphoma." Nature **459**(7247): 717-721.

Coornaert, B., M. Baens, K. Heyninck, T. Bekaert, M. Haegman, J. Staal, L. Sun, Z. J. Chen, P. Marynen and R. Beyaert (2008). "T cell antigen receptor stimulation induces MALT1 paracaspase-mediated cleavage of the NF-kappaB inhibitor A20." Nat Immunol **9**(3): 263-271.

Corre, I., M. Gomez, S. Vielkind and D. A. Cantrell (2001). "Analysis of thymocyte development reveals that the GTPase RhoA is a positive regulator of T cell receptor responses in vivo." J Exp Med **194**(7): 903-914.

Cortes, J. R., A. Ambesi-Impiombato, L. Couronné, S. A. Quinn, C. S. Kim, A. C. da Silva Almeida, Z. West, L. Belver, M. S. Martin, L. Scourzic, G. Bhagat, O. A. Bernard, A. A. Ferrando and T. Palomero (2018). "RHOA G17V Induces T Follicular Helper Cell Specification and Promotes Lymphomagenesis." Cancer Cell **33**(2): 259-273.e257.

Cortés, J. R. and T. Palomero (2016). "The curious origins of angioimmunoblastic T-cell lymphoma." Curr Opin Hematol **23**(4): 434-443.

Couronne, L., C. Bastard and O. A. Bernard (2012). "TET2 and DNMT3A mutations in human T-cell lymphoma." N Engl J Med **366**(1): 95-96.

Crescenzo, R., F. Abate, E. Lasorsa, F. Tabbo, M. Gaudiano, N. Chiesa, F. Di Giacomo, E. Spaccarotella, L. Barbarossa, E. Ercole, M. Todaro, M. Boi, A. Acquaviva, E. Ficarra, D. Novero, A. Rinaldi, T. Tousseyn, A. Rosenwald, L. Kenner, L. Cerroni, A. Tzankov, M. Ponzoni, M. Paulli, D. Weisenburger, W. C. Chan, J. Iqbal, M. A. Piris, A. Zamo, C. Ciardullo, D. Rossi, G. Gaidano, S. Pileri, E. Tiacci, B. Falini, L. D. Shultz, L. Mevellec, J. E. Vialard, R. Piva, F. Bertoni, R. Rabadan and G. Inghirami (2015). "Convergent mutations and kinase fusions lead to oncogenic STAT3 activation in anaplastic large cell lymphoma." Cancer Cell **27**(4): 516-532.

d'Amore, F., T. Relander, G. F. Lauritzsen, E. Jantunen, H. Hagberg, H. Anderson, H. Holte, A. Osterborg, M. Merup, P. Brown, O. Kuittinen, M. Erlanson, B. Ostenstad, U. M. Fagerli, O. V. Gadeberg, C. Sundstrom, J. Delabie, E. Ralfkiaer, M. Vornanen and H. E. Toldbod (2012). "Up-front autologous stem-cell transplantation in peripheral T-cell lymphoma: NLG-T-01." J Clin Oncol **30**(25): 3093-3099.

Das, K. and P. Tan (2013). "Molecular cytogenetics: recent developments and applications in cancer." Clin Genet **84**(4): 315-325.

Davis, R. E., K. D. Brown, U. Siebenlist and L. M. Staudt (2001). "Constitutive nuclear factor kappaB activity is required for survival of activated B cell-like diffuse large B cell lymphoma cells." J Exp Med **194**(12): 1861-1874.

Davis, R. E., V. N. Ngo, G. Lenz, P. Tolar, R. M. Young, P. B. Romesser, H. Kohlhammer, L. Lamy, H. Zhao, Y. Yang, W. Xu, A. L. Shaffer, G. Wright, W. Xiao, J. Powell, J. K. Jiang, C. J. Thomas, A. Rosenwald, G. Ott, H. K. Muller-Hermelink, R. D. Gascoyne, J. M. Connors, N. A. Johnson, L. M. Rimsza, E. Campo, E. S. Jaffe, W. H. Wilson, J. Delabie, E. B. Smeland, R. I. Fisher, R. M. Braziel, R. R. Tubbs, J. R. Cook, D. D. Weisenburger, W. C. Chan, S. K. Pierce and L. M. Staudt (2010). "Chronic active B-cell-receptor signalling in diffuse large B-cell lymphoma." Nature **463**(7277): 88-92.

de Leval, L., D. S. Rickman, C. Thielen, A. Reynies, Y. L. Huang, G. Delsol, L. Lamant, K. Leroy, J. Briere, T. Molina, F. Berger, C. Gisselbrecht, L. Xerri and P. Gaulard (2007). "The gene expression profile of nodal peripheral T-cell lymphoma demonstrates a molecular link between angioimmunoblastic T-cell lymphoma (AITL) and follicular helper T (TFH) cells." Blood **109**(11): 4952-4963.

del Pozo, M. A., M. Vicente-Manzanares, R. Tejedor, J. M. Serrador and F. Sanchez-Madrid (1999). "Rho GTPases control migration and polarization of adhesion molecules and cytoskeletal ERM components in T lymphocytes." Eur J Immunol **29**(11): 3609-3620.

Derudder, E., E. J. Cadera, J. C. Vahl, J. Wang, C. J. Fox, S. Zha, G. van Loo, M. Pasparakis, M. S. Schlissel, M. Schmidt-Supprian and K. Rajewsky (2009). "Development of immunoglobulin lambda-chain-positive B cells, but not editing of immunoglobulin kappa-chain, depends on NF-kappaB signals." Nat Immunol **10**(6): 647-654.

Dierks, C., F. Adrian, P. Fisch, H. Ma, H. Maurer, D. Herchenbach, C. U. Forster, C. Sprissler, G. Liu, S. Rottmann, G. R. Guo, Z. Katja, H. Veelken and M. Warmuth (2010). "The ITK-SYK fusion oncogene induces a T-cell lymphoproliferative disease in mice mimicking human disease." Cancer Res **70**(15): 6193-6204.

Dierlamm, J., M. Baens, I. Wlodarska, M. Stefanova-Ouzounova, J. M. Hernandez, D. K. Hossfeld, C. De Wolf-Peeters, A. Hagemeijer, H. Van den Berghe and P. Marynen (1999). "The apoptosis inhibitor gene API2 and a novel 18q gene, MLT, are recurrently rearranged in the t(11;18)(q21;q21) associated with mucosa-associated lymphoid tissue lymphomas." Blood **93**(11): 3601-3609.

Dobin, A., C. A. Davis, F. Schlesinger, J. Drenkow, C. Zaleski, S. Jha, P. Batut, M. Chaisson and T. R. Gingeras (2013). "STAR: ultrafast universal RNA-seq aligner." Bioinformatics **29**(1): 15-21.

Duplay, P., M. Thome, F. Herve and O. Acuto (1994). "p56lck interacts via its src homology 2 domain with the ZAP-70 kinase." J Exp Med **179**(4): 1163-1172.

Dupuis, J., F. Morschhauser, H. Ghesquieres, H. Tilly, O. Casasnovas, C. Thieblemont, V. Ribrag, C. Bossard, F. Le Bras, E. Bachy, B. Hivert, E. Nicolas-Virelizier, F. Jardin, J. N. Bastie, S. Amorim, J. Lazarovici, A. Martin and B. Coiffier (2015). "Combination of romidepsin with cyclophosphamide, doxorubicin, vincristine, and prednisone in previously untreated patients with peripheral T-cell lymphoma: a non-randomised, phase 1b/2 study." Lancet Haematol **2**(4): e160-165.

Duyao, M. P., D. J. Kessler, D. B. Spicer, C. Bartholomew, J. L. Cleveland, M. Siekevitz and G. E. Sonenshein (1992). "Transactivation of the c-myc promoter by human T cell leukemia virus type 1 tax is mediated by NF kappa B." J Biol Chem **267**(23): 16288-16291.

Emmerich, F., M. Meiser, M. Hummel, G. Demel, H. D. Foss, F. Jundt, S. Mathas, D. Krappmann, C. Scheidereit, H. Stein and B. Dorken (1999). "Overexpression of I kappa B alpha without inhibition of NF-kappaB activity and mutations in the I kappa B alpha gene in Reed-Sternberg cells." Blood **94**(9): 3129-3134.

Emmerich, F., S. Theurich, M. Hummel, A. Haeffker, M. S. Vry, K. Dohner, K. Bommert, H. Stein and B. Dorken (2003). "Inactivating I kappa B epsilon mutations in Hodgkin/Reed-Sternberg cells." J Pathol **201**(3): 413-420.

Erikson, J. M., A. J. Valente, S. Mummidi, H. K. Kandikattu, V. G. DeMarco, S. B. Bender, W. P. Fay, U. Siebenlist and B. Chandrasekar (2017). "Targeting TRAF3IP2 by Genetic and Interventional Approaches Inhibits Ischemia/Reperfusion-induced Myocardial Injury and Adverse Remodeling." J Biol Chem **292**(6): 2345-2358.

Escalon, M. P., N. S. Liu, Y. Yang, M. Hess, P. L. Walker, T. L. Smith and N. H. Dang (2005). "Prognostic factors and treatment of patients with T-cell non-Hodgkin lymphoma: the M. D. Anderson Cancer Center experience." Cancer **103**(10): 2091-2098.

Fairfield, H., C. Falank, L. Avery and M. R. Reagan (2016). "Multiple myeloma in the marrow: pathogenesis and treatments." Ann N Y Acad Sci **1364**: 32-51.

Falchi, L., J. K. Lue, F. Montanari, E. Marchi, J. E. Amengual, A. Sawas, C. Deng, K. Khan, H. A. Kim, A. Rada, M. Malanga, M. F. Francescone, C. R. Soderquist, D. C. Park, G. Bhagat, L. Sokol, A. R. Shustov and O. A. O'Connor (2019). "TARGETING THE PERIPHERAL T-CELL LYMPHOMA (PTCL) EPIGENOME WITH ORAL 5-AZACYTIDINE AND ROMIDEPSIN: RESULTS AND CLINICAL-MOLECULAR CORRELATIONS FROM A PHASE 2 STUDY." Hematological Oncology **37**(S2): 178-179.

Federico, M., T. Rudiger, M. Bellei, B. N. Nathwani, S. Luminari, B. Coiffier, N. L. Harris, E. S. Jaffe, S. A. Pileri, K. J. Savage, D. D. Weisenburger, J. O. Armitage, N. Mounier and J. M. Vose (2013). "Clinicopathologic characteristics of angioimmunoblastic T-cell lymphoma: analysis of the international peripheral T-cell lymphoma project." J Clin Oncol **31**(2): 240-246.

Feldman, A. L., A. Dogan, D. I. Smith, M. E. Law, S. M. Ansell, S. H. Johnson, J. C. Porcher, N. Ozsan, E. D. Wieben, B. W. Eckloff and G. Vasmatzis (2011). "Discovery of recurrent t(6;7)(p25.3;q32.3) translocations in ALK-negative anaplastic large cell lymphomas by massively parallel genomic sequencing." Blood **117**(3): 915-919.

Feldman, A. L., G. Vasmatzis, Y. W. Asmann, J. Davila, S. Middha, B. W. Eckloff, S. H. Johnson, J. C. Porcher, S. M. Ansell and A. Caride (2013). "Novel TRAF1-ALK fusion identified by deep RNA sequencing of anaplastic large cell lymphoma." Genes Chromosomes Cancer **52**(11): 1097-1102.

Feller, A. C. and J. Diebold (2004). History of Lymphoma Classification. Histopathology of Nodal and Extranodal Non-Hodgkin's Lymphomas. Berlin, Heidelberg, Springer Berlin Heidelberg**:** 1-7.

Ferreri, A. J. and E. Zucca (2007). "Marginal-zone lymphoma." Crit Rev Oncol Hematol **63**(3): 245-256.

Fujiwara, S. I., Y. Yamashita, N. Nakamura, Y. L. Choi, T. Ueno, H. Watanabe, K. Kurashina, M. Soda, M. Enomoto, H. Hatanaka, S. Takada, M. Abe, K. Ozawa and H. Mano (2008). "High-resolution analysis of chromosome copy number alterations in angioimmunoblastic T-cell lymphoma and peripheral T-cell lymphoma, unspecified, with single nucleotide polymorphism-typing microarrays." Leukemia **22**(10): 1891-1898.

Fusaki, N., A. Iwamatsu, M. Iwashima and J. Fujisawa (1997). "Interaction between Sam68 and Src family tyrosine kinases, Fyn and Lck, in T cell receptor signaling." J Biol Chem **272**(10): 6214-6219.

Fusaki, N., S. Matsuda, H. Nishizumi, H. Umemori and T. Yamamoto (1996). "Physical and functional interactions of protein tyrosine kinases, p59fyn and ZAP-70, in T cell signaling." J Immunol **156**(4): 1369-1377.

Gaffen, S. L. (2009). "Structure and signalling in the IL-17 receptor family." Nature Reviews Immunology **9**: 556.

Gambacorti Passerini, C., F. Farina, A. Stasia, S. Redaelli, M. Ceccon, L. Mologni, C. Messa, L. Guerra, G. Giudici, E. Sala, L. Mussolin, D. Deeren, M. H. King, M. Steurer, R. Ordemann, A. M. Cohen, M. Grube, L. Bernard, G. Chiriano, L. Antolini and R. Piazza (2014). "Crizotinib in advanced, chemoresistant anaplastic lymphoma kinase-positive lymphoma patients." J Natl Cancer Inst **106**(2): djt378.

Gerondakis, S., T. S. Fulford, N. L. Messina and R. J. Grumont (2014). "NF-kappaB control of T cell development." Nat Immunol **15**(1): 15-25.

Gerondakis, S., R. Grumont, R. Gugasyan, L. Wong, I. Isomura, W. Ho and A. Banerjee (2006). "Unravelling the complexities of the NF-kappaB signalling pathway using mouse knockout and transgenic models." Oncogene **25**(51): 6781-6799.

Gong, Q., C. Wang, J. Rohr, A. L. Feldman, W. C. Chan and T. W. McKeithan (2016). "Comment on: Frequent CTLA4-CD28 gene fusion in diverse types of T-cell lymphoma, by Yoo et al." Haematologica **101**(6): e269-270.

Griner, E. M. and M. G. Kazanietz (2007). "Protein kinase C and other diacylglycerol effectors in cancer." Nat Rev Cancer **7**(4): 281-294.

Groen, K., N. van de Donk, C. Stege, S. Zweegman and I. S. Nijhof (2019). "Carfilzomib for relapsed and refractory multiple myeloma." Cancer Manag Res **11**: 2663-2675.

Groves, T., P. Smiley, M. P. Cooke, K. Forbush, R. M. Perlmutter and C. J. Guidos (1996). "Fyn can partially substitute for Lck in T lymphocyte development." Immunity **5**(5): 417-428.

Grumont, R., P. Lock, M. Mollinari, F. M. Shannon, A. Moore and S. Gerondakis (2004). "The mitogen-induced increase in T cell size involves PKC and NFAT activation of Rel/NF-kappaB-dependent c-myc expression." Immunity **21**(1): 19-30.

Gruss, H. J., D. Hirschstein, B. Wright, D. Ulrich, M. A. Caligiuri, M. Barcos, L. Strockbine, R. J. Armitage and S. K. Dower (1994). "Expression and function of CD40 on Hodgkin and Reed-Sternberg cells and the possible relevance for Hodgkin's disease." Blood **84**(7): 2305-2314.

Gu, C., L. Wu and X. Li (2013). "IL-17 family: cytokines, receptors and signaling." Cytokine **64**(2): 477-485.

Gyrd-Hansen, M., M. Darding, M. Miasari, M. M. Santoro, L. Zender, W. Xue, T. Tenev, P. C. da Fonseca, M. Zvelebil, J. M. Bujnicki, S. Lowe, J. Silke and P. Meier (2008). "IAPs contain an evolutionarily conserved ubiquitin-binding domain that regulates NF-kappaB as well as cell survival and oncogenesis." Nat Cell Biol **10**(11): 1309-1317.

Hacker, H. and M. Karin (2006). "Regulation and function of IKK and IKK-related kinases." Sci STKE **2006**(357): re13.

Hapgood, G. and K. J. Savage (2015). "The biology and management of systemic anaplastic large cell lymphoma." Blood **126**(1): 17-25.

Harris, N., E. Jaffe, H. Stein, P. Banks, J. Chan, M. Cleary, G. Delsol, C. De Wolf- Peeters, B. Falini and K. Gatter (1994). "A revised European-American classification of lymphoid neoplasms: a proposal from the International Lymphoma Study Group [see comments]." Blood **84**(5): 1361-1392.

Hatakeyama, M., T. Kono, N. Kobayashi, A. Kawahara, S. D. Levin, R. M. Perlmutter and T. Taniguchi (1991). "Interaction of the IL-2 receptor with the src-family kinase p56lck: identification of novel intermolecular association." Science **252**(5012): 1523-1528.

Hawash, I. Y., K. P. Kesavan, A. I. Magee, R. L. Geahlen and M. L. Harrison (2002). "The Lck SH3 domain negatively regulates localization to lipid rafts through an interaction with c-Cbl." J Biol Chem **277**(7): 5683-5691.

Hayden, M. S. and S. Ghosh (2008). "Shared principles in NF-kappaB signaling." Cell **132**(3): 344-362.

Hayden, M. S. and S. Ghosh (2012). "NF-kappaB, the first quarter-century: remarkable progress and outstanding questions." Genes Dev **26**(3): 203-234.

Heasman, S. J., L. M. Carlin, S. Cox, T. Ng and A. J. Ridley (2010). "Coordinated RhoA signaling at the leading edge and uropod is required for T cell transendothelial migration." J Cell Biol **190**(4): 553-563.

Hengeveld, P. J. and M. J. Kersten (2015). "B-cell activating factor in the pathophysiology of multiple myeloma: a target for therapy?" Blood Cancer J **5**: e282.

Hideshima, T., C. Mitsiades, G. Tonon, P. G. Richardson and K. C. Anderson (2007). "Understanding multiple myeloma pathogenesis in the bone marrow to identify new therapeutic targets." Nat Rev Cancer **7**(8): 585-598.

Hinz, M., D. Krappmann, A. Eichten, A. Heder, C. Scheidereit and M. Strauss (1999). "NF-kappaB function in growth control: regulation of cyclin D1 expression and G0/G1-to-S-phase transition." Mol Cell Biol **19**(4): 2690-2698.

Ho, A. W., F. Shen, H. R. Conti, N. Patel, E. E. Childs, A. C. Peterson, N. Hernandez-Santos, J. K. Kolls, L. P. Kane, W. Ouyang and S. L. Gaffen (2010). "IL-17RC is required for immune signaling via an extended SEF/IL-17R signaling domain in the cytoplasmic tail." J Immunol **185**(2): 1063-1070.

Hobbs, R. P., S. H. Smith and S. Getsios (2017). "Act1: A Psoriasis Susceptibility Gene Playing its Part in Keratinocytes." J Invest Dermatol **137**(7): 1410-1412.

Horwitz, S., O. A. O'Connor, B. Pro, T. Illidge, M. Fanale, R. Advani, N. L. Bartlett, J. H. Christensen, F. Morschhauser, E. Domingo-Domenech, G. Rossi, W. S. Kim, T. Feldman, A. Lennard, D. Belada, A. Illes, K. Tobinai, K. Tsukasaki, S. P. Yeh, A. Shustov, A. Huttmann, K. J. Savage, S. Yuen, S. Iyer, P. L. Zinzani, Z. Hua, M. Little, S. Rao, J. Woolery, T. Manley and L. Trumper (2019). "Brentuximab vedotin with chemotherapy for CD30-positive peripheral T-cell lymphoma (ECHELON-2): a global, double-blind, randomised, phase 3 trial." Lancet **393**(10168): 229-240.

Horwitz, S. M., R. Koch, P. Porcu, Y. Oki, A. Moskowitz, M. Perez, P. Myskowski, A. Officer, J. D. Jaffe, S. N. Morrow, K. Allen, M. Douglas, H. Stern, J. Sweeney, P. Kelly, V. Kelly, J. C. Aster, D. Weaver, F. M. Foss and D. M. Weinstock (2018a). "Activity of the PI3K-delta,gamma inhibitor duvelisib in a phase 1 trial and preclinical models of T-cell lymphoma." Blood **131**(8): 888-898.

Horwitz, S. M., A. J. Moskowitz, E. D. Jacobsen, N. Mehta-Shah, M. S. Khodadoust, D. C. Fisher, P. Myskowski, E. B. K. Wang, M. Tawa, T. Davey, W. Blouin, H. Hancock, N. Ganesan, N. Galasso, E. Marzouk, A. Bahgat, H. Jester, S. Fong, A. Butt, A. Dogan, Y. H. Kim and D. M. Weinstock (2018b). "The Combination of Duvelisib, a PI3K-δ,γ Inhibitor, and Romidepsin Is Highly Active in Relapsed/Refractory Peripheral T-Cell Lymphoma with Low Rates of Transaminitis: Results of Parallel Multicenter, Phase 1 Combination Studies with Expansion Cohorts." Blood **132**(Suppl 1): 683-683.

Hosokawa, Y., H. Suzuki, M. Nakagawa, T. H. Lee and M. Seto (2005). "API2-MALT1 fusion protein induces transcriptional activation of the API2 gene through NF-kappaB binding elements: evidence for a positive feed-back loop pathway resulting in unremitting NF-kappaB activation." Biochem Biophys Res Commun **334**(1): 51-60.

Hsi, E. D., S. M. Horwitz, K. R. Carson, L. C. Pinter-Brown, S. T. Rosen, B. Pro, M. Federico, C. Gisselbrecht, M. Schwartz, L. A. Bellm, M. Acosta, A. M. Collie, A. M. Gruver, B. J. Grzywacz, S. Turakhia, A. R. Shustov, R. H. Advani, T. Feldman, M. J. Lechowicz, S. M. Smith, F. Lansigan, A. Tulpule, M. D. Craig, J. P. Greer, B. S. Kahl, J. W. Leach, N. Morganstein, C. Casulo, S. I. Park and F. M. Foss (2017). "Analysis of Peripheral T-cell Lymphoma Diagnostic Workup in the United States." Clin Lymphoma Myeloma Leuk **17**(4): 193-200.

Hsu, M. S., S. Sedighim, T. Wang, J. P. Antonios, R. G. Everson, A. M. Tucker, L. Du, R. Emerson, E. Yusko, C. Sanders, H. S. Robins, W. H. Yong, T. B. Davidson, G. Li, L. M. Liau and R. M. Prins (2016). "TCR Sequencing Can Identify and Track Glioma-Infiltrating T Cells after DC Vaccination." Cancer Immunology Research **4**(5): 412.

Huang, Y., A. Moreau, J. Dupuis, B. Streubel, B. Petit, S. Le Gouill, N. Martin-Garcia, C. Copie-Bergman, F. Gaillard, M. Qubaja, B. Fabiani, G. Roncador, C. Haioun, M. H. Delfau-Larue, T. Marafioti, A. Chott and P. Gaulard (2009). "Peripheral T-cell lymphomas with a follicular growth pattern are derived from follicular helper T cells (TFH) and may show overlapping features with angioimmunoblastic T-cell lymphomas." Am J Surg Pathol **33**(5): 682-690.

Iqbal, J., D. D. Weisenburger, T. C. Greiner, J. M. Vose, T. McKeithan, C. Kucuk, H. Geng, K. Deffenbacher, L. Smith, K. Dybkaer, S. Nakamura, M. Seto, J. Delabie, F. Berger, F. Loong, W. Y. Au, Y. H. Ko, I. Sng, J. O. Armitage and W. C. Chan (2010). "Molecular signatures to improve diagnosis in peripheral T-cell lymphoma and prognostication in angioimmunoblastic T-cell lymphoma." Blood **115**(5): 1026-1036.

Iqbal, J., G. Wright, C. Wang, A. Rosenwald, R. D. Gascoyne, D. D. Weisenburger, T. C. Greiner, L. Smith, S. Guo, R. A. Wilcox, B. T. Teh, S. T. Lim, S. Y. Tan, L. M. Rimsza, E. S. Jaffe, E. Campo, A. Martinez, J. Delabie, R. M. Braziel, J. R. Cook, R. R. Tubbs, G. Ott, E. Geissinger, P. Gaulard, P. P. Piccaluga, S. A. Pileri, W. Y. Au, S. Nakamura, M. Seto, F. Berger, L. de Leval, J. M. Connors, J. Armitage, J. Vose, W. C. Chan and L. M. Staudt (2014). "Gene expression signatures delineate biological and prognostic subgroups in peripheral T-cell lymphoma." Blood **123**(19): 2915-2923.

Ishigame, H., S. Kakuta, T. Nagai, M. Kadoki, A. Nambu, Y. Komiyama, N. Fujikado, Y. Tanahashi, A. Akitsu, H. Kotaki, K. Sudo, S. Nakae, C. Sasakawa and Y. Iwakura (2009). "Differential roles of interleukin-17A and -17F in host defense against mucoepithelial bacterial infection and allergic responses." Immunity **30**(1): 108-119.

Ishitsuka, K. and K. Tamura (2014). "Human T-cell leukaemia virus type I and adult T-cell leukaemia-lymphoma." Lancet Oncol **15**(11): e517-526.

Iwanaga, M., T. Watanabe and K. Yamaguchi (2012). "Adult T-cell leukemia: a review of epidemiological evidence." Front Microbiol **3**: 322.

Iyer, M. K., A. M. Chinnaiyan and C. A. Maher (2011). "ChimeraScan: a tool for identifying chimeric transcription in sequencing data." Bioinformatics **27**(20): 2903-2904.

Jaffe, E. S., J. K. Chan, I. J. Su, G. Frizzera, S. Mori, A. C. Feller and F. C. Ho (1996). "Report of the Workshop on Nasal and Related Extranodal Angiocentric T/Natural Killer Cell Lymphomas. Definitions, differential diagnosis, and epidemiology." Am J Surg Pathol **20**(1): 103-111.

Jaffe, E. S., W. H. Organization and I. A. f. R. o. Cancer (2001). Pathology and Genetics of Tumours of Haematopoietic and Lymphoid Tissues, IARC Press.

Jiang, L., Z. H. Gu, Z. X. Yan, X. Zhao, Y. Y. Xie, Z. G. Zhang, C. M. Pan, Y. Hu, C. P. Cai, Y. Dong, J. Y. Huang, L. Wang, Y. Shen, G. Meng, J. F. Zhou, J. D. Hu, J. F. Wang, Y. H. Liu, L. H.

Yang, F. Zhang, J. M. Wang, Z. Wang, Z. G. Peng, F. Y. Chen, Z. M. Sun, H. Ding, J. M. Shi, J. Hou, J. S. Yan, J. Y. Shi, L. Xu, Y. Li, J. Lu, Z. Zheng, W. Xue, W. L. Zhao, Z. Chen and S. J. Chen (2015). "Exome sequencing identifies somatic mutations of DDX3X in natural killer/T-cell lymphoma." Nat Genet **47**(9): 1061-1066.

Jimi, E., R. J. Phillips, M. Rincon, R. Voll, H. Karasuyama, R. Flavell and S. Ghosh (2005). "Activation of NF-kappaB promotes the transition of large, CD43+ pre-B cells to small, CD43- pre-B cells." Int Immunol **17**(6): 815-825.

Johnston, R. J., A. C. Poholek, D. DiToro, I. Yusuf, D. Eto, B. Barnett, A. L. Dent, J. Craft and S. Crotty (2009). "Bcl6 and Blimp-1 are reciprocal and antagonistic regulators of T follicular helper cell differentiation." Science **325**(5943): 1006-1010.

Jones, R. G., S. D. Saibil, J. M. Pun, A. R. Elford, M. Bonnard, M. Pellegrini, S. Arya, M. E. Parsons, C. M. Krawczyk, S. Gerondakis, W. C. Yeh, J. R. Woodgett, M. R. Boothby and P. S. Ohashi (2005). "NF-kappaB couples protein kinase B/Akt signaling to distinct survival pathways and the regulation of lymphocyte homeostasis in vivo." J Immunol **175**(6): 3790-3799.

Jost, P. J. and J. Ruland (2007). "Aberrant NF-κB signaling in lymphoma: mechanisms, consequences, and therapeutic implications." Blood **109**(7): 2700-2707.

Jungnickel, B., A. Staratschek-Jox, A. Brauninger, T. Spieker, J. Wolf, V. Diehl, M. L. Hansmann, K. Rajewsky and R. Kuppers (2000). "Clonal deleterious mutations in the IkappaBalpha gene in the malignant cells in Hodgkin's lymphoma." J Exp Med **191**(2): 395-402.

Karin, M. and A. Lin (2002). "NF-kappaB at the crossroads of life and death." Nat Immunol **3**(3): 221-227.

Karin, M., Y. Yamamoto and Q. M. Wang (2004). "The IKK NF-kappa B system: a treasure trove for drug development." Nat Rev Drug Discov **3**(1): 17-26.

Kataoka, K., Y. Nagata, A. Kitanaka, Y. Shiraishi, T. Shimamura, J. Yasunaga, Y. Totoki, K. Chiba, A. Sato-Otsubo, G. Nagae, R. Ishii, S. Muto, S. Kotani, Y. Watatani, J. Takeda, M. Sanada, H. Tanaka, H. Suzuki, Y. Sato, Y. Shiozawa, T. Yoshizato, K. Yoshida, H. Makishima, M. Iwanaga, G. Ma, K. Nosaka, M. Hishizawa, H. Itonaga, Y. Imaizumi, W. Munakata, H. Ogasawara, T. Sato, K. Sasai, K. Muramoto, M. Penova, T. Kawaguchi, H. Nakamura, N. Hama, K. Shide, Y. Kubuki, T. Hidaka, T. Kameda, T. Nakamaki, K. Ishiyama, S. Miyawaki, S. S. Yoon, K. Tobinai, Y. Miyazaki, A. Takaori-Kondo, F. Matsuda, K. Takeuchi, O. Nureki, H. Aburatani, T. Watanabe, T. Shibata, M. Matsuoka, S. Miyano, K. Shimoda and S. Ogawa (2015). "Integrated molecular analysis of adult T cell leukemia/lymphoma." Nat Genet **47**(11): 1304-1315.

Kato, M., M. Sanada, I. Kato, Y. Sato, J. Takita, K. Takeuchi, A. Niwa, Y. Chen, K. Nakazaki, J. Nomoto, Y. Asakura, S. Muto, A. Tamura, M. Iio, Y. Akatsuka, Y. Hayashi, H. Mori, T. Igarashi, M. Kurokawa, S. Chiba, S. Mori, Y. Ishikawa, K. Okamoto, K. Tobinai, H. Nakagama, T. Nakahata, T. Yoshino, Y. Kobayashi and S. Ogawa (2009). "Frequent inactivation of A20 in B-cell lymphomas." Nature **459**(7247): 712-716.

Keats, J. J., R. Fonseca, M. Chesi, R. Schop, A. Baker, W. J. Chng, S. Van Wier, R. Tiedemann, C. X. Shi, M. Sebag, E. Braggio, T. Henry, Y. X. Zhu, H. Fogle, T. Price-Troska, G. Ahmann, C. Mancini, L. A. Brents, S. Kumar, P. Greipp, A. Dispenzieri, B. Bryant, G. Mulligan, L. Bruhn, M. Barrett, R. Valdez, J. Trent, A. K. Stewart, J. Carpten and P. L. Bergsagel (2007). "Promiscuous mutations activate the noncanonical NF-kappaB pathway in multiple myeloma." Cancer Cell **12**(2): 131-144.

Keusekotten, K., P. R. Elliott, L. Glockner, B. K. Fiil, R. B. Damgaard, Y. Kulathu, T. Wauer, M. K. Hospenthal, M. Gyrd-Hansen, D. Krappmann, K. Hofmann and D. Komander (2013). "OTULIN antagonizes LUBAC signaling by specifically hydrolyzing Met1-linked polyubiquitin." Cell **153**(6): 1312-1326.

Kim, C. S. and J. R. Cortés (unpublished). NF-κB signature in TET2 -/- RhoA G17V mAITL.

Kim, P. W., Z. Y. Sun, S. C. Blacklow, G. Wagner and M. J. Eck (2003). "A zinc clasp structure tethers Lck to T cell coreceptors CD4 and CD8." Science **301**(5640): 1725-1728.

Kimbrel, E. A., T. N. Davis, J. E. Bradner and A. L. Kung (2009). "In vivo pharmacodynamic imaging of proteasome inhibition." Mol Imaging **8**(3): 140-147.

Klein, U., S. Casola, G. Cattoretti, Q. Shen, M. Lia, T. Mo, T. Ludwig, K. Rajewsky and R. Dalla-Favera (2006). "Transcription factor IRF4 controls plasma cell differentiation and class-switch recombination." Nat Immunol **7**(7): 773-782.

Ko, M., H. S. Bandukwala, J. An, E. D. Lamperti, E. C. Thompson, R. Hastie, A. Tsangaratou, K. Rajewsky, S. B. Koralov and A. Rao (2011). "Ten-Eleven-Translocation 2 (TET2) negatively regulates homeostasis and differentiation of hematopoietic stem cells in mice." Proc Natl Acad Sci U S A **108**(35): 14566-14571.

Ko, M. and A. Rao (2011). "TET2: epigenetic safeguard for HSC." Blood **118**(17): 4501-4503.

Kobayashi, N., T. Kono, M. Hatakeyama, Y. Minami, T. Miyazaki, R. M. Perlmutter and T. Taniguchi (1993). "Functional coupling of the src-family protein tyrosine kinases p59fyn and p53/56lyn with the interleukin 2 receptor: implications for redundancy and pleiotropism in cytokine signal transduction." Proc Natl Acad Sci U S A **90**(9): 4201-4205.

Koh, K. P., A. Yabuuchi, S. Rao, Y. Huang, K. Cunniff, J. Nardone, A. Laiho, M. Tahiliani, C. A. Sommer, G. Mostoslavsky, R. Lahesmaa, S. H. Orkin, S. J. Rodig, G. Q. Daley and A. Rao (2011). "Tet1 and Tet2 regulate 5-hydroxymethylcytosine production and cell lineage specification in mouse embryonic stem cells." Cell Stem Cell **8**(2): 200-213.

Kontgen, F., R. J. Grumont, A. Strasser, D. Metcalf, R. Li, D. Tarlinton and S. Gerondakis (1995). "Mice lacking the c-rel proto-oncogene exhibit defects in lymphocyte proliferation, humoral immunity, and interleukin-2 expression." Genes Dev **9**(16): 1965-1977.

Koo, G. C., S. Y. Tan, T. Tang, S. L. Poon, G. E. Allen, L. Tan, S. C. Chong, W. S. Ong, K. Tay, M. Tao, R. Quek, S. Loong, K. W. Yeoh, S. P. Yap, K. A. Lee, L. C. Lim, D. Tan, C. Goh, I. Cutcutache, W. Yu, C. C. Ng, V. Rajasegaran, H. L. Heng, A. Gan, C. K. Ong, S. Rozen, P. Tan, B. T. Teh and S. T. Lim (2012). "Janus kinase 3-activating mutations identified in natural killer/T-cell lymphoma." Cancer Discov **2**(7): 591-597.

Kramer-Albers, E. M. and R. White (2011). "From axon-glial signalling to myelination: the integrating role of oligodendroglial Fyn kinase." Cell Mol Life Sci **68**(12): 2003-2012.

Ku, M., M. Wall, R. N. MacKinnon, C. R. Walkley, L. E. Purton, C. Tam, D. Izon, L. Campbell, H. C. Cheng and H. Nandurkar (2015). "Src family kinases and their role in hematological malignancies." Leuk Lymphoma **56**(3): 577-586.

Kucuk, C., B. Jiang, X. Hu, W. Zhang, J. K. Chan, W. Xiao, N. Lack, C. Alkan, J. C. Williams, K. N. Avery, P. Kavak, A. Scuto, E. Sen, P. Gaulard, L. Staudt, J. Iqbal, W. Zhang, A. Cornish, Q. Gong, Q. Yang, H. Sun, F. d'Amore, S. Leppa, W. Liu, K. Fu, L. de Leval, T. McKeithan and W.

C. Chan (2015). "Activating mutations of STAT5B and STAT3 in lymphomas derived from gammadelta-T or NK cells." Nat Commun **6**: 6025.

Kuestner, R. E., D. W. Taft, A. Haran, C. S. Brandt, T. Brender, K. Lum, B. Harder, S. Okada, C. D. Ostrander, J. L. Kreindler, S. J. Aujla, B. Reardon, M. Moore, P. Shea, R. Schreckhise, T. R. Bukowski, S. Presnell, P. Guerra-Lewis, J. Parrish-Novak, J. L. Ellsworth, S. Jaspers, K. E. Lewis, M. Appleby, J. K. Kolls, M. Rixon, J. W. West, Z. Gao and S. D. Levin (2007). "Identification of the IL-17 receptor related molecule IL-17RC as the receptor for IL-17F." J Immunol **179**(8): 5462-5473.

Kunimoto, H., Y. Fukuchi, M. Sakurai, K. Sadahira, Y. Ikeda, S. Okamoto and H. Nakajima (2012). "Tet2 disruption leads to enhanced self-renewal and altered differentiation of fetal liver hematopoietic stem cells." Sci Rep **2**: 273.

Lake, A., L. A. Shield, P. Cordano, D. T. Chui, J. Osborne, S. Crae, K. S. Wilson, S. Tosi, S. J. Knight, S. Gesk, R. Siebert, R. T. Hay and R. F. Jarrett (2009). "Mutations of NFKBIA, encoding IkappaB alpha, are a recurrent finding in classical Hodgkin lymphoma but are not a unifying feature of non-EBV-associated cases." Int J Cancer **125**(6): 1334-1342.

Lam, L. T., R. E. Davis, J. Pierce, M. Hepperle, Y. Xu, M. Hottelet, Y. Nong, D. Wen, J. Adams, L. Dang and L. M. Staudt (2005). "Small molecule inhibitors of IkappaB kinase are selectively toxic for subgroups of diffuse large B-cell lymphoma defined by gene expression profiling." Clin Cancer Res **11**(1): 28-40.

Lam, L. T., G. Wright, R. E. Davis, G. Lenz, P. Farinha, L. Dang, J. W. Chan, A. Rosenwald, R. D. Gascoyne and L. M. Staudt (2008). "Cooperative signaling through the signal transducer and activator of transcription 3 and nuclear factor-{kappa}B pathways in subtypes of diffuse large B-cell lymphoma." Blood **111**(7): 3701-3713.

Laurini, J. A., A. M. Perry, E. Boilesen, J. Diebold, K. A. Maclennan, H. K. Muller-Hermelink, B. N. Nathwani, J. O. Armitage and D. D. Weisenburger (2012). "Classification of non-Hodgkin lymphoma in Central and South America: a review of 1028 cases." Blood **120**(24): 4795-4801.

Layer, R. M., C. Chiang, A. R. Quinlan and I. M. Hall (2014). "LUMPY: a probabilistic framework for structural variant discovery." Genome Biol **15**(6): R84.

Lee, S. H., J. S. Kim, J. Kim, S. J. Kim, W. S. Kim, S. Lee, Y. H. Ko and H. Y. Yoo (2015). "A highly recurrent novel missense mutation in CD28 among angioimmunoblastic T-cell lymphoma patients." Haematologica **100**(12): e505-507.

Lemonnier, F., L. Couronne, M. Parrens, J. P. Jais, M. Travert, L. Lamant, O. Tournillac, T. Rousset, B. Fabiani, R. A. Cairns, T. Mak, C. Bastard, O. A. Bernard, L. de Leval and P. Gaulard (2012). "Recurrent TET2 mutations in peripheral T-cell lymphomas correlate with TFH-like features and adverse clinical parameters." Blood **120**(7): 1466-1469.

Lemonnier, F., J. Dupuis, P. Sujobert, O. Tournillhac, M. Cheminant, C. Sarkozy, L. Pelletier, A. Marcais, C. Robe, V. Fataccioli, C. Haioun, O. Hermine, P. Gaulard and R. Delarue (2018). "Treatment with 5-azacytidine induces a sustained response in patients with angioimmunoblastic T-cell lymphoma." Blood **132**(21): 2305-2309.

Lenardo, M., J. W. Pierce and D. Baltimore (1987). "Protein-binding sites in Ig gene enhancers determine transcriptional activity and inducibility." Science **236**(4808): 1573-1577.

Lenz, G., R. E. Davis, V. N. Ngo, L. Lam, T. C. George, G. W. Wright, S. S. Dave, H. Zhao, W. Xu, A. Rosenwald, G. Ott, H. K. Muller-Hermelink, R. D. Gascoyne, J. M. Connors, L. M. Rimsza,

E. Campo, E. S. Jaffe, J. Delabie, E. B. Smeland, R. I. Fisher, W. C. Chan and L. M. Staudt (2008). "Oncogenic CARD11 mutations in human diffuse large B cell lymphoma." Science **319**(5870): 1676-1679.

Li, X., M. Commane, H. Nie, X. Hua, M. Chatterjee-Kishore, D. Wald, M. Haag and G. R. Stark (2000). "Act1, an NF-kappa B-activating protein." Proc Natl Acad Sci U S A **97**(19): 10489-10493.

Li, Z., X. Cai, C. L. Cai, J. Wang, W. Zhang, B. E. Petersen, F. C. Yang and M. Xu (2011). "Deletion of Tet2 in mice leads to dysregulated hematopoietic stem cells and subsequent development of myeloid malignancies." Blood **118**(17): 4509-4518.

Li, Z., H. Wang, L. Xue, D. M. Shin, D. Roopenian, W. Xu, C. F. Qi, M. Y. Sangster, C. J. Orihuela, E. Tuomanen, J. E. Rehg, X. Cui, Q. Zhang, H. C. Morse, 3rd and S. W. Morris (2009). "Emu-BCL10 mice exhibit constitutive activation of both canonical and noncanonical NF-kappaB pathways generating marginal zone (MZ) B-cell expansion as a precursor to splenic MZ lymphoma." Blood **114**(19): 4158-4168.

Liao, Y., G. K. Smyth and W. Shi (2014). "featureCounts: an efficient general purpose program for assigning sequence reads to genomic features." Bioinformatics **30**(7): 923-930.

Liberzon, A., C. Birger, H. Thorvaldsdóttir, M. Ghandi, Jill P. Mesirov and P. Tamayo (2015). "The Molecular Signatures Database Hallmark Gene Set Collection." Cell Systems **1**(6): 417-425.

Lin, K., N. S. Longo, X. Wang, J. A. Hewitt and K. M. Abraham (2000). "Lck domains differentially contribute to pre-T cell receptor (TCR)- and TCR-alpha/beta-regulated developmental transitions." J Exp Med **191**(4): 703-716.

Liu, C., W. Qian, Y. Qian, N. V. Giltiay, Y. Lu, S. Swaidani, S. Misra, L. Deng, Z. J. Chen and X. Li (2009). "Act1, a U-box E3 ubiquitin ligase for IL-17 signaling." Sci Signal **2**(92): ra63.

Lohr, J. G., P. Stojanov, S. L. Carter, P. Cruz-Gordillo, M. S. Lawrence, D. Auclair, C. Sougnez, B. Knoechel, J. Gould, G. Saksena, K. Cibulskis, A. McKenna, M. A. Chapman, R. Straussman, J. Levy, L. M. Perkins, J. J. Keats, S. E. Schumacher, M. Rosenberg, G. Getz and T. R. Golub (2014). "Widespread genetic heterogeneity in multiple myeloma: implications for targeted therapy." Cancer Cell **25**(1): 91-101.

Lork, M., J. Staal and R. Beyaert (2019). "Ubiquitination and phosphorylation of the CARD11-BCL10-MALT1 signalosome in T cells." Cell Immunol **340**: 103877.

Love, M. I., W. Huber and S. Anders (2014). "Moderated estimation of fold change and dispersion for RNA-seq data with DESeq2." Genome Biol **15**(12): 550.

Lucas, P. C., P. Kuffa, S. Gu, D. Kohrt, D. S. Kim, K. Siu, X. Jin, J. Swenson and L. M. McAllister-Lucas (2007). "A dual role for the API2 moiety in API2-MALT1-dependent NF-kappaB activation: heterotypic oligomerization and TRAF2 recruitment." Oncogene **26**(38): 5643-5654.

Lucas, P. C., M. Yonezumi, N. Inohara, L. M. McAllister-Lucas, M. E. Abazeed, F. F. Chen, S. Yamaoka, M. Seto and G. Nunez (2001). "Bcl10 and MALT1, independent targets of chromosomal translocation in malt lymphoma, cooperate in a novel NF-kappa B signaling pathway." J Biol Chem **276**(22): 19012-19019.

Lukes, R. J. and R. D. Collins (1974). "Immunologic characterization of human malignant lymphomas." Cancer **34**(4 Suppl): suppl:1488-1503.

Manasanch, E. E. and R. Z. Orlowski (2017). "Proteasome inhibitors in cancer therapy." Nat Rev Clin Oncol **14**(7): 417-433.

Mandelbaum, J., G. Bhagat, H. Tang, T. Mo, M. Brahmachary, Q. Shen, A. Chadburn, K. Rajewsky, A. Tarakhovsky, L. Pasqualucci and R. Dalla-Favera (2010). "BLIMP1 is a tumor suppressor gene frequently disrupted in activated B cell-like diffuse large B cell lymphoma." Cancer Cell **18**(6): 568-579.

Manis, J. P., M. Tian and F. W. Alt (2002). "Mechanism and control of class-switch recombination." Trends Immunol **23**(1): 31-39.

Manso, R., M. Sanchez-Beato, S. Monsalvo, S. Gomez, L. Cereceda, P. Llamas, F. Rojo, M. Mollejo, J. Menarguez, J. Alves, M. Garcia-Cosio, M. A. Piris and S. M. Rodriguez-Pinilla (2014). "The RHOA G17V gene mutation occurs frequently in peripheral T-cell lymphoma and is associated with a characteristic molecular signature." Blood **123**(18): 2893-2894.

Marie-Cardine, A., L. R. Hendricks-Taylor, N. J. Boerth, H. Zhao, B. Schraven and G. A. Koretzky (1998). "Molecular interaction between the Fyn-associated protein SKAP55 and the SLP-76-associated phosphoprotein SLAP-130." J Biol Chem **273**(40): 25789-25795.

Martin, G. S. (2001). "The hunting of the Src." Nat Rev Mol Cell Biol **2**(6): 467-475.

Martinez-Delgado, B., M. Cuadros, E. Honrado, A. Ruiz de la Parte, G. Roncador, J. Alves, J. M. Castrillo, C. Rivas and J. Benitez (2005). "Differential expression of NF-kappaB pathway genes among peripheral T-cell lymphomas." Leukemia **19**(12): 2254-2263.

Martinez-Delgado, B., B. Melendez, M. Cuadros, J. Alvarez, J. M. Castrillo, A. Ruiz De La Parte, M. Mollejo, C. Bellas, R. Diaz, L. Lombardia, F. Al-Shahrour, O. Dominguez, A. Cascon, M. Robledo, C. Rivas and J. Benitez (2004). "Expression profiling of T-cell lymphomas differentiates peripheral and lymphoblastic lymphomas and defines survival related genes." Clin Cancer Res **10**(15): 4971-4982.

Mauro, C., P. Vito, S. Mellone, F. Pacifico, A. Chariot, S. Formisano and A. Leonardi (2003). "Role of the adaptor protein CIKS in the activation of the IKK complex." Biochem Biophys Res Commun **309**(1): 84-90.

Mehta-Shah, N., A. J. Moskowitz, M. Lunning, P. Lynch, M. Scheuerman, A. Kumar, J. F. Gerecitano, A. D. Zelenetz, P. A. Hamlin, Jr., A. Noy, M. J. Matasar, M. L. Palomba, A. Younes, W. Schaffer, R. Grewal, J. Rademaker, C. S. Sauter, P. B. Dahi, P. Myskowski, M. Kheterpal, A. Dogan, M. Pulitzer, L. Tang, A. Ni and S. M. Horwitz (2016). "A Phase Ib/IIa Trial of the Combination of Romidepsin, Lenalidomide and Carfilzomib in Patients with Relapsed/Refractory Lymphoma Shows Complete Responses in Relapsed and Refractory T-Cell Lymphomas." Blood **128**(22): 2991-2991.

Meininger, I. and D. Krappmann (2016). "Lymphocyte signaling and activation by the CARMA1-BCL10-MALT1 signalosome." Biol Chem **397**(12): 1315-1333.

Molin, D., A. Edstrom, I. Glimelius, B. Glimelius, G. Nilsson, C. Sundstrom and G. Enblad (2002). "Mast cell infiltration correlates with poor prognosis in Hodgkin's lymphoma." Br J Haematol **119**(1): 122-124.

Molina, T. J., K. Kishihara, D. P. Siderovski, W. van Ewijk, A. Narendran, E. Timms, A. Wakeham, C. J. Paige, K. U. Hartmann, A. Veillette and et al. (1992). "Profound block in thymocyte development in mice lacking p56lck." Nature **357**(6374): 161-164.

Mondragon, L., R. Mhaidly, G. M. De Donatis, M. Tosolini, P. Dao, A. R. Martin, C. Pons, J. Chiche, M. Jacquin, V. Imbert, E. Proics, L. Boyer, A. Doye, F. Luciano, J. G. Neels, F. Coutant, N. Fabien, L. Sormani, C. Rubio-Patino, J. P. Bossowski, F. Muller, S. Marchetti, E. Villa, J. F. Peyron, P. Gaulard, F. Lemonnier, V. Asnafi, L. Genestier, R. Benhida, J. J. Fournie, T. Passeron, J. E. Ricci and E. Verhoeyen (2019). "GAPDH Overexpression in the T Cell Lineage Promotes Angioimmunoblastic T Cell Lymphoma through an NF-kappaB-Dependent Mechanism." Cancer Cell **36**(3): 268-287.e210.

Monin, L. and S. L. Gaffen (2018). "Interleukin 17 Family Cytokines: Signaling Mechanisms, Biological Activities, and Therapeutic Implications." Cold Spring Harb Perspect Biol **10**(4).

Moran-Crusio, K., L. Reavie, A. Shih, O. Abdel-Wahab, D. Ndiaye-Lobry, C. Lobry, M. E. Figueroa, A. Vasanthakumar, J. Patel, X. Zhao, F. Perna, S. Pandey, J. Madzo, C. Song, Q. Dai, C. He, S. Ibrahim, M. Beran, J. Zavadil, S. D. Nimer, A. Melnick, L. A. Godley, I. Aifantis and R. L. Levine (2011). "Tet2 loss leads to increased hematopoietic stem cell self-renewal and myeloid transformation." Cancer Cell **20**(1): 11-24.

Moreaux, J., E. Legouffe, E. Jourdan, P. Quittet, T. Reme, C. Lugagne, P. Moine, J. F. Rossi, B. Klein and K. Tarte (2004). "BAFF and APRIL protect myeloma cells from apoptosis induced by interleukin 6 deprivation and dexamethasone." Blood **103**(8): 3148-3157.

Morgan, J. A., Y. Yin, A. D. Borowsky, F. Kuo, N. Nourmand, J. I. Koontz, C. Reynolds, L. Soreng, C. A. Griffin, F. Graeme-Cook, N. L. Harris, D. Weisenburger, G. S. Pinkus, J. A. Fletcher and J. Sklar (1999). "Breakpoints of the t(11;18)(q21;q21) in mucosa-associated lymphoid tissue (MALT) lymphoma lie within or near the previously undescribed gene MALT1 in chromosome 18." Cancer Res **59**(24): 6205-6213.

Mori, N., M. Fujii, S. Ikeda, Y. Yamada, M. Tomonaga, D. W. Ballard and N. Yamamoto (1999). "Constitutive activation of NF-kappaB in primary adult T-cell leukemia cells." Blood **93**(7): 2360-2368.

Morris, S., M. Kirstein, M. Valentine, K. Dittmer, D. Shapiro, D. Saltman and A. Look (1994). "Fusion of a kinase gene, ALK, to a nucleolar protein gene, NPM, in non-Hodgkin's lymphoma." Science **263**(5151): 1281-1284.

Mou, F., M. Praskova, F. Xia, D. Van Buren, H. Hock, J. Avruch and D. Zhou (2012). "The Mst1 and Mst2 kinases control activation of rho family GTPases and thymic egress of mature thymocytes." J Exp Med **209**(4): 741-759.

Ng, D. H., J. D. Watts, R. Aebersold and P. Johnson (1996). "Demonstration of a direct interaction between p56lck and the cytoplasmic domain of CD45 in vitro." J Biol Chem **271**(3): 1295-1300.

Ng, S. Y., L. Brown, K. Stevenson, T. deSouza, J. C. Aster, A. Louissaint, Jr. and D. M. Weinstock (2018). "RhoA G17V is sufficient to induce autoimmunity and promotes T-cell lymphomagenesis in mice." Blood **132**(9): 935-947.

Ngo, V. N., R. M. Young, R. Schmitz, S. Jhavar, W. Xiao, K. H. Lim, H. Kohlhammer, W. Xu, Y. Yang, H. Zhao, A. L. Shaffer, P. Romesser, G. Wright, J. Powell, A. Rosenwald, H. K. Muller-Hermelink, G. Ott, R. D. Gascoyne, J. M. Connors, L. M. Rimsza, E. Campo, E. S. Jaffe, J. Delabie, E. B. Smeland, R. I. Fisher, R. M. Braziel, R. R. Tubbs, J. R. Cook, D. D. Weisenburger, W. C. Chan and L. M. Staudt (2011). "Oncogenically active MYD88 mutations in human lymphoma." Nature **470**(7332): 115-119.

Noels, H., G. van Loo, S. Hagens, V. Broeckx, R. Beyaert, P. Marynen and M. Baens (2007). "A Novel TRAF6 binding site in MALT1 defines distinct mechanisms of NF-kappaB activation by API2middle dotMALT1 fusions." J Biol Chem **282**(14): 10180-10189.

Novatchkova, M., A. Leibbrandt, J. Werzowa, A. Neubuser and F. Eisenhaber (2003). "The STIR-domain superfamily in signal transduction, development and immunity." Trends Biochem Sci **28**(5): 226-229.

O'Connor, O. A., L. Falchi, J. K. Lue, E. Marchi, C. Kinahan, A. Sawas, C. Deng, F. Montanari, J. E. Amengual, H. A. Kim, A. M. Rada, K. Khan, A. T. Jacob, M. Malanga, M. Francescone, R. Nandakumar, C. Soderquist, D. C. Park, G. Bhagat, B. Cheng, A. Risueno, D. Menezes, A. R. Shustov, L. Sokol and L. Scotto (2019a). "ORAL 5-AZACYTIDINE AND ROMIDEPSIN EXHIBIT MARKED ACTIVITY IN PATIENTS WITH PTCL: A MULTICENTER PHASE I STUDY." Blood.

O'Connor, O. A., S. Horwitz, T. Masszi, A. Van Hoof, P. Brown, J. Doorduijn, G. Hess, W. Jurczak, P. Knoblauch, S. Chawla, G. Bhat, M. R. Choi, J. Walewski, K. Savage, F. Foss, L. F. Allen and A. Shustov (2015). "Belinostat in Patients With Relapsed or Refractory Peripheral T-Cell Lymphoma: Results of the Pivotal Phase II BELIEF (CLN-19) Study." J Clin Oncol **33**(23): 2492-2499.

O'Connor, O. A., M. Ozcan, E. D. Jacobsen, J. M. Roncero, J. Trotman, J. Demeter, T. Masszi, J. Pereira, R. Ramchandren, A. Beaven, D. Caballero, S. M. Horwitz, A. Lennard, M. Turgut, N. Hamerschlak, F. A. d'Amore, F. Foss, W. S. Kim, J. P. Leonard, P. L. Zinzani, C. S. Chiattone, E. D. Hsi, L. Trumper, H. Liu, E. Sheldon-Waniga, C. D. Ullmann, K. Venkatakrishnan, E. J. Leonard and A. R. Shustov (2019b). "Randomized Phase III Study of Alisertib or Investigator's Choice (Selected Single Agent) in Patients With Relapsed or Refractory Peripheral T-Cell Lymphoma." J Clin Oncol **37**(8): 613-623.

O'Connor, O. A., B. Pro, L. Pinter-Brown, N. Bartlett, L. Popplewell, B. Coiffier, M. J. Lechowicz, K. J. Savage, A. R. Shustov, C. Gisselbrecht, E. Jacobsen, P. L. Zinzani, R. Furman, A. Goy, C. Haioun, M. Crump, J. M. Zain, E. Hsi, A. Boyd and S. Horwitz (2011). "Pralatrexate in patients with relapsed or refractory peripheral T-cell lymphoma: results from the pivotal PROPEL study." J Clin Oncol **29**(9): 1182-1189.

Odqvist, L., M. Sanchez-Beato, S. Montes-Moreno, E. Martin-Sanchez, R. Pajares, L. Sanchez-Verde, P. L. Ortiz-Romero, J. Rodriguez, S. M. Rodriguez-Pinilla, F. Iniesta-Martinez, J. C. Solera-Arroyo, R. Ramos-Asensio, T. Flores, J. M. Palanca, F. G. Bragado, P. D. Franjo and M. A. Piris (2013). "NIK controls classical and alternative NF-kappaB activation and is necessary for the survival of human T-cell lymphoma cells." Clin Cancer Res **19**(9): 2319-2330.

Oh, H. and S. Ghosh (2013). "NF-kappaB: roles and regulation in different CD4(+) T-cell subsets." Immunol Rev **252**(1): 41-51.

Okada, S., A. Puel, J. L. Casanova and M. Kobayashi (2016). "Chronic mucocutaneous candidiasis disease associated with inborn errors of IL-17 immunity." Clin Transl Immunology **5**(12): e114.

Ondrejka, S. L., B. Grzywacz, J. Bodo, H. Makishima, C. Polprasert, J. W. Said, B. Przychodzen, J. P. Maciejewski and E. D. Hsi (2016). "Angioimmunoblastic T-cell Lymphomas With the RHOA p.Gly17Val Mutation Have Classic Clinical and Pathologic Features." Am J Surg Pathol **40**(3): 335-341.

Osman, N., H. Turner, S. Lucas, K. Reif and D. A. Cantrell (1996). "The protein interactions of the immunoglobulin receptor family tyrosine-based activation motifs present in the T cell receptor zeta subunits and the CD3 gamma, delta and epsilon chains." Eur J Immunol **26**(5): 1063-1068.

Palacios, E. H. and A. Weiss (2004). "Function of the Src-family kinases, Lck and Fyn, in T-cell development and activation." Oncogene **23**(48): 7990-8000.

Palomero, T., L. Couronne, H. Khiabanian, M. Y. Kim, A. Ambesi-Impiombato, A. Perez-Garcia, Z. Carpenter, F. Abate, M. Allegretta, J. E. Haydu, X. Jiang, I. S. Lossos, C. Nicolas, M. Balbin, C. Bastard, G. Bhagat, M. A. Piris, E. Campo, O. A. Bernard, R. Rabadan and A. A. Ferrando (2014). "Recurrent mutations in epigenetic regulators, RHOA and FYN kinase in peripheral T cell lymphomas." Nat Genet **46**(2): 166-170.

Parker, S. J. and C. M. Metallo (2015). "Metabolic consequences of oncogenic IDH mutations." Pharmacol Ther **152**: 54-62.

Parravicini, V., M. Gadina, M. Kovarova, S. Odom, C. Gonzalez-Espinosa, Y. Furumoto, S. Saitoh, L. E. Samelson, J. J. O'Shea and J. Rivera (2002). "Fyn kinase initiates complementary signals required for IgE-dependent mast cell degranulation." Nat Immunol **3**(8): 741-748.

Pasqualucci, L., V. Trifonov, G. Fabbri, J. Ma, D. Rossi, A. Chiarenza, V. A. Wells, A. Grunn, M. Messina, O. Elliot, J. Chan, G. Bhagat, A. Chadburn, G. Gaidano, C. G. Mullighan, R. Rabadan and R. Dalla-Favera (2011). "Analysis of the coding genome of diffuse large B-cell lymphoma." Nat Genet **43**(9): 830-837.

Pathan, N. I., C. L. Ashendel, R. L. Geahlen and M. L. Harrison (1996). "Activation of T cell Raf-1 at mitosis requires the protein-tyrosine kinase Lck." J Biol Chem **271**(48): 30315-30317.

Pechloff, K., J. Holch, U. Ferch, M. Schweneker, K. Brunner, M. Kremer, T. Sparwasser, L. Quintanilla-Martinez, U. Zimber-Strobl, B. Streubel, A. Gewies, C. Peschel and J. Ruland (2010). "The fusion kinase ITK-SYK mimics a T cell receptor signal and drives oncogenesis in conditional mouse models of peripheral T cell lymphoma." J Exp Med **207**(5): 1031-1044.

Phelan, J. D., R. M. Young, D. E. Webster, S. Roulland, G. W. Wright, M. Kasbekar, A. L. Shaffer, 3rd, M. Ceribelli, J. Q. Wang, R. Schmitz, M. Nakagawa, E. Bachy, D. W. Huang, Y. Ji, L. Chen, Y. Yang, H. Zhao, X. Yu, W. Xu, M. M. Palisoc, R. R. Valadez, T. Davies-Hill, W. H. Wilson, W. C. Chan, E. S. Jaffe, R. D. Gascoyne, E. Campo, A. Rosenwald, G. Ott, J. Delabie, L. M. Rimsza, F. J. Rodriguez, F. Estephan, M. Holdhoff, M. J. Kruhlak, S. M. Hewitt, C. J. Thomas, S. Pittaluga, T. Oellerich and L. M. Staudt (2018). "A multiprotein supercomplex controlling oncogenic signalling in lymphoma." Nature **560**(7718): 387-391.

Piccaluga, P. P., C. Agostinelli, A. Califano, A. Carbone, L. Fantoni, S. Ferrari, A. Gazzola, A. Gloghini, S. Righi, M. Rossi, E. Tagliafico, P. L. Zinzani, S. Zupo, M. Baccarani and S. A. Pileri (2007). "Gene expression analysis of angioimmunoblastic lymphoma indicates derivation from T follicular helper cells and vascular endothelial growth factor deregulation." Cancer Res **67**(22): 10703-10710.

Piccaluga, P. P., F. Fuligni, A. De Leo, C. Bertuzzi, M. Rossi, F. Bacci, E. Sabattini, C. Agostinelli, A. Gazzola, M. A. Laginestra, C. Mannu, M. R. Sapienza, S. Hartmann, M. L. Hansmann, R. Piva, J. Iqbal, J. C. Chan, D. Weisenburger, J. M. Vose, M. Bellei, M. Federico, G. Inghirami, P. L. Zinzani and S. A. Pileri (2013). "Molecular profiling improves classification and prognostication of nodal peripheral T-cell lymphomas: results of a phase III diagnostic accuracy study." J Clin Oncol **31**(24): 3019-3025.

Piekarz, R. L., R. Frye, H. M. Prince, M. H. Kirschbaum, J. Zain, S. L. Allen, E. S. Jaffe, A. Ling, M. Turner, C. J. Peer, W. D. Figg, S. M. Steinberg, S. Smith, D. Joske, I. Lewis, L. Hutchins, M. Craig, A. T. Fojo, J. J. Wright and S. E. Bates (2011). "Phase 2 trial of romidepsin in patients with peripheral T-cell lymphoma." Blood **117**(22): 5827-5834.

Pinto, A., D. Aldinucci, A. Gloghini, V. Zagonel, M. Degan, S. Improta, S. Juzbasic, M. Todesco, V. Perin, V. Gattei, F. Herrmann, H. J. Gruss and A. Carbone (1996). "Human eosinophils express functional CD30 ligand and stimulate proliferation of a Hodgkin's disease cell line." Blood **88**(9): 3299-3305.

Piva, R., L. Agnelli, E. Pellegrino, K. Todoerti, V. Grosso, I. Tamagno, A. Fornari, B. Martinoglio, E. Medico, A. Zamo, F. Facchetti, M. Ponzoni, E. Geissinger, A. Rosenwald, H. K. Muller-Hermelink, C. De Wolf-Peeters, P. P. Piccaluga, S. Pileri, A. Neri and G. Inghirami (2010). "Gene expression profiling uncovers molecular classifiers for the recognition of anaplastic large-cell lymphoma within peripheral T-cell neoplasms." J Clin Oncol **28**(9): 1583-1590.

Prescott, J. A. and S. J. Cook (2018). "Targeting IKKβ in Cancer: Challenges and Opportunities for the Therapeutic Utilisation of IKKβ Inhibitors." Cells **7**(9).

Pro, B., R. Advani, P. Brice, N. L. Bartlett, J. D. Rosenblatt, T. Illidge, J. Matous, R. Ramchandren, M. Fanale, J. M. Connors, Y. Yang, E. L. Sievers, D. A. Kennedy and A. Shustov (2012). "Brentuximab vedotin (SGN-35) in patients with relapsed or refractory systemic anaplastic large-cell lymphoma: results of a phase II study." J Clin Oncol **30**(18): 2190-2196.

Qian, D., S. Lev, N. S. van Oers, I. Dikic, J. Schlessinger and A. Weiss (1997). "Tyrosine phosphorylation of Pyk2 is selectively regulated by Fyn during TCR signaling." J Exp Med **185**(7): 1253-1259.

Qian, Y., C. Liu, J. Hartupee, C. Z. Altuntas, M. F. Gulen, D. Jane-Wit, J. Xiao, Y. Lu, N. Giltiay, J. Liu, T. Kordula, Q. W. Zhang, B. Vallance, S. Swaidani, M. Aronica, V. K. Tuohy, T. Hamilton and X. Li (2007). "The adaptor Act1 is required for interleukin 17-dependent signaling associated with autoimmune and inflammatory disease." Nat Immunol **8**(3): 247-256.

Qian, Y., J. Qin, G. Cui, M. Naramura, E. C. Snow, C. F. Ware, R. L. Fairchild, S. A. Omori, R. C. Rickert, M. Scott, B. L. Kotzin and X. Li (2004). "Act1, a negative regulator in CD40- and BAFF-mediated B cell survival." Immunity **21**(4): 575-587.

Quach, H., D. Ritchie, A. K. Stewart, P. Neeson, S. Harrison, M. J. Smyth and H. M. Prince (2010). "Mechanism of action of immunomodulatory drugs (IMiDS) in multiple myeloma." Leukemia **24**(1): 22-32.

Quivoron, C., L. Couronne, V. Della Valle, C. K. Lopez, I. Plo, O. Wagner-Ballon, M. Do Cruzeiro, F. Delhommeau, B. Arnulf, M. H. Stern, L. Godley, P. Opolon, H. Tilly, E. Solary, Y. Duffourd, P. Dessen, H. Merle-Beral, F. Nguyen-Khac, M. Fontenay, W. Vainchenker, C. Bastard, T. Mercher and O. A. Bernard (2011). "TET2 inactivation results in pleiotropic hematopoietic abnormalities in mouse and is a recurrent event during human lymphomagenesis." Cancer Cell **20**(1): 25-38.

Rawat, A. and R. Nagaraj (2010). "Determinants of membrane association in the SH4 domain of Fyn: roles of N-terminus myristoylation and side-chain thioacylation." Biochim Biophys Acta **1798**(10): 1854-1863.

Reimer, P., T. Rudiger, E. Geissinger, F. Weissinger, C. Nerl, N. Schmitz, A. Engert, H. Einsele, H. K. Muller-Hermelink and M. Wilhelm (2009). "Autologous stem-cell transplantation as first-line therapy in peripheral T-cell lymphomas: results of a prospective multicenter study." J Clin Oncol **27**(1): 106-113.

Richardson, P. G., C. Mitsiades, T. Hideshima and K. C. Anderson (2006). "Bortezomib: proteasome inhibition as an effective anticancer therapy." Annu Rev Med **57**: 33-47.

Richardson, P. G., S. Zweegman, E. K. O'Donnell, J. P. Laubach, N. Raje, P. Voorhees, R. H. Ferrari, T. Skacel, S. K. Kumar and S. Lonial (2018). "Ixazomib for the treatment of multiple myeloma." Expert Opin Pharmacother **19**(17): 1949-1968.

Rimokh, R., J. P. Magaud, F. Berger, J. Samarut, B. Coiffier, D. Germain and D. Y. Mason (1989). "A translocation involving a specific breakpoint (q35) on chromosome 5 is characteristic of anaplastic large cell lymphoma ('Ki-1 lymphoma')." Br J Haematol **71**(1): 31-36.

Rohr, J., S. Guo, J. Huo, A. Bouska, C. Lachel, Y. Li, P. D. Simone, W. Zhang, Q. Gong, C. Wang, A. Cannon, T. Heavican, A. Mottok, S. Hung, A. Rosenwald, R. Gascoyne, K. Fu, T. C. Greiner, D. D. Weisenburger, J. M. Vose, L. M. Staudt, W. Xiao, G. E. Borgstahl, S. Davis, C. Steidl, T. McKeithan, J. Iqbal and W. C. Chan (2016). "Recurrent activating mutations of CD28 in peripheral T-cell lymphomas." Leukemia **30**(5): 1062-1070.

Romashkova, J. A. and S. S. Makarov (1999). "NF-kappaB is a target of AKT in anti-apoptotic PDGF signalling." Nature **401**(6748): 86-90.

Rosebeck, S., L. Madden, X. Jin, S. Gu, I. J. Apel, A. Appert, R. A. Hamoudi, H. Noels, X. Sagaert, P. Van Loo, M. Baens, M. Q. Du, P. C. Lucas and L. M. McAllister-Lucas (2011). "Cleavage of NIK by the API2-MALT1 fusion oncoprotein leads to noncanonical NF-kappaB activation." Science **331**(6016): 468-472.

Rosenwald, A., G. Wright, K. Leroy, X. Yu, P. Gaulard, R. D. Gascoyne, W. C. Chan, T. Zhao, C. Haioun, T. C. Greiner, D. D. Weisenburger, J. C. Lynch, J. Vose, J. O. Armitage, E. B. Smeland, S. Kvaloy, H. Holte, J. Delabie, E. Campo, E. Montserrat, A. Lopez-Guillermo, G. Ott, H. K. Muller-Hermelink, J. M. Connors, R. Braziel, T. M. Grogan, R. I. Fisher, T. P. Miller, M. LeBlanc, M. Chiorazzi, H. Zhao, L. Yang, J. Powell, W. H. Wilson, E. S. Jaffe, R. Simon, R. D. Klausner and L. M. Staudt (2003). "Molecular diagnosis of primary mediastinal B cell lymphoma identifies a clinically favorable subgroup of diffuse large B cell lymphoma related to Hodgkin lymphoma." J Exp Med **198**(6): 851-862.

Ruland, J. and L. Hartjes (2019). "CARD-BCL-10-MALT1 signalling in protective and pathological immunity." Nat Rev Immunol **19**(2): 118-134.

Ryzhakov, G., K. Blazek and I. A. Udalova (2011). "Evolution of vertebrate immunity: sequence and functional analysis of the SEFIR domain family member Act1." J Mol Evol **72**(5-6): 521-530.

Saba, N. S., D. Liu, S. E. Herman, C. Underbayev, X. Tian, D. Behrend, M. A. Weniger, M. Skarzynski, J. Gyamfi, L. Fontan, A. Melnick, C. Grant, M. Roschewski, A. Navarro, S. Beà, S. Pittaluga, K. Dunleavy, W. H. Wilson and A. Wiestner (2016). "Pathogenic role of B-cell receptor signaling and canonical NF-κB activation in mantle cell lymphoma." Blood **128**(1): 82-92.

Saitoh, Y., N. Yamamoto, M. Z. Dewan, H. Sugimoto, V. J. Martinez Bruyn, Y. Iwasaki, K. Matsubara, X. Qi, T. Saitoh, I. Imoto, J. Inazawa, A. Utsunomiya, T. Watanabe, T. Masuda, N. Yamamoto and S. Yamaoka (2008). "Overexpressed NF-kappaB-inducing kinase contributes to the tumorigenesis of adult T-cell leukemia and Hodgkin Reed-Sternberg cells." Blood **111**(10): 5118-5129.

Sakata-Yanagimoto, M., T. Enami, K. Yoshida, Y. Shiraishi, R. Ishii, Y. Miyake, H. Muto, N. Tsuyama, A. Sato-Otsubo, Y. Okuno, S. Sakata, Y. Kamada, R. Nakamoto-Matsubara, N. B. Tran, K. Izutsu, Y. Sato, Y. Ohta, J. Furuta, S. Shimizu, T. Komeno, Y. Sato, T. Ito, M. Noguchi, E. Noguchi, M. Sanada, K. Chiba, H. Tanaka, K. Suzukawa, T. Nanmoku, Y. Hasegawa, O. Nureki, S. Miyano, N. Nakamura, K. Takeuchi, S. Ogawa and S. Chiba (2014). "Somatic RHOA mutation in angioimmunoblastic T cell lymphoma." Nat Genet **46**(2): 171-175.

Salmond, R. J., A. Filby, I. Qureshi, S. Caserta and R. Zamoyska (2009). "T-cell receptor proximal signaling via the Src-family kinases, Lck and Fyn, influences T-cell activation, differentiation, and tolerance." Immunol Rev **228**(1): 9-22.

Samelson, L. E., A. F. Phillips, E. T. Luong and R. D. Klausner (1990). "Association of the fyn protein-tyrosine kinase with the T-cell antigen receptor." Proc Natl Acad Sci U S A **87**(11): 4358-4362.

Sanchez-Izquierdo, D., G. Buchonnet, R. Siebert, R. D. Gascoyne, J. Climent, L. Karran, M. Marin, D. Blesa, D. Horsman, A. Rosenwald, L. M. Staudt, D. G. Albertson, M. Q. Du, H. Ye, P. Marynen, J. Garcia-Conde, D. Pinkel, M. J. Dyer and J. A. Martinez-Climent (2003). "MALT1 is deregulated by both chromosomal translocation and amplification in B-cell non-Hodgkin lymphoma." Blood **101**(11): 4539-4546.

Sato, I., Y. Obata, K. Kasahara, Y. Nakayama, Y. Fukumoto, T. Yamasaki, K. K. Yokoyama, T. Saito and N. Yamaguchi (2009). "Differential trafficking of Src, Lyn, Yes and Fyn is specified by the state of palmitoylation in the SH4 domain." J Cell Sci **122**(Pt 7): 965-975.

Savage, K. J., N. L. Harris, J. M. Vose, F. Ullrich, E. S. Jaffe, J. M. Connors, L. Rimsza, S. A. Pileri, M. Chhanabhai, R. D. Gascoyne, J. O. Armitage and D. D. Weisenburger (2008). "ALK-anaplastic large-cell lymphoma is clinically and immunophenotypically different from both ALK+ ALCL and peripheral T-cell lymphoma, not otherwise specified: report from the International Peripheral T-Cell Lymphoma Project." Blood **111**(12): 5496-5504.

Savage, K. J., S. Monti, J. L. Kutok, G. Cattoretti, D. Neuberg, L. De Leval, P. Kurtin, P. Dal Cin, C. Ladd, F. Feuerhake, R. C. Aguiar, S. Li, G. Salles, F. Berger, W. Jing, G. S. Pinkus, T. Habermann, R. Dalla-Favera, N. L. Harris, J. C. Aster, T. R. Golub and M. A. Shipp (2003). "The molecular signature of mediastinal large B-cell lymphoma differs from that of other diffuse large B-cell lymphomas and shares features with classical Hodgkin lymphoma." Blood **102**(12): 3871-3879.

Scarfo, I., E. Pellegrino, E. Mereu, I. Kwee, L. Agnelli, E. Bergaggio, G. Garaffo, N. Vitale, M. Caputo, R. Machiorlatti, P. Circosta, F. Abate, A. Barreca, D. Novero, S. Mathew, A. Rinaldi, E. Tiacci, S. Serra, S. Deaglio, A. Neri, B. Falini, R. Rabadan, F. Bertoni, G. Inghirami and R. Piva (2016). "Identification of a new subclass of ALK-negative ALCL expressing aberrant levels of ERBB4 transcripts." Blood **127**(2): 221-232.

Schlottmann, K. E., E. Gulbins, S. M. Lau and K. M. Coggeshall (1996). "Activation of Src-family tyrosine kinases during Fas-induced apoptosis." J Leukoc Biol **60**(4): 546-554.

Schmidlin, H., S. A. Diehl, M. Nagasawa, F. A. Scheeren, R. Schotte, C. H. Uittenbogaart, H. Spits and B. Blom (2008). "Spi-B inhibits human plasma cell differentiation by repressing BLIMP1 and XBP-1 expression." Blood **112**(5): 1804-1812.

Schmiedel, B. J., C. A. Scheible, T. Nuebling, H. G. Kopp, S. Wirths, M. Azuma, P. Schneider, G. Jung, L. Grosse-Hovest and H. R. Salih (2013). "RANKL expression, function, and therapeutic targeting in multiple myeloma and chronic lymphocytic leukemia." Cancer Res **73**(2): 683-694.

Schmitz, R., M. L. Hansmann, V. Bohle, J. I. Martin-Subero, S. Hartmann, G. Mechtersheimer, W. Klapper, I. Vater, M. Giefing, S. Gesk, J. Stanelle, R. Siebert and R. Kuppers (2009). "TNFAIP3 (A20) is a tumor suppressor gene in Hodgkin lymphoma and primary mediastinal B cell lymphoma." J Exp Med **206**(5): 981-989.

Schraven, B., H. Kirchgessner, B. Gaber, Y. Samstag and S. Meuer (1991). "A functional complex is formed in human T lymphocytes between the protein tyrosine phosphatase CD45, the

protein tyrosine kinase p56lck and pp32, a possible common substrate." Eur J Immunol **21**(10): 2469-2477.

Schwab, U., H. Stein, J. Gerdes, H. Lemke, H. Kirchner, M. Schaadt and V. Diehl (1982). "Production of a monoclonal antibody specific for Hodgkin and Sternberg-Reed cells of Hodgkin's disease and a subset of normal lymphoid cells." Nature **299**(5878): 65-67.

Sciammas, R., A. L. Shaffer, J. H. Schatz, H. Zhao, L. M. Staudt and H. Singh (2006). "Graded expression of interferon regulatory factor-4 coordinates isotype switching with plasma cell differentiation." Immunity **25**(2): 225-236.

Sen, R. and D. Baltimore (1986). "Multiple nuclear factors interact with the immunoglobulin enhancer sequences." Cell **46**(5): 705-716.

Shaffer, A. L., N. C. Emre, L. Lamy, V. N. Ngo, G. Wright, W. Xiao, J. Powell, S. Dave, X. Yu, H. Zhao, Y. Zeng, B. Chen, J. Epstein and L. M. Staudt (2008). "IRF4 addiction in multiple myeloma." Nature **454**(7201): 226-231.

Shaw, A. T., D. W. Kim, K. Nakagawa, T. Seto, L. Crino, M. J. Ahn, T. De Pas, B. Besse, B. J. Solomon, F. Blackhall, Y. L. Wu, M. Thomas, K. J. O'Byrne, D. Moro-Sibilot, D. R. Camidge, T. Mok, V. Hirsh, G. J. Riely, S. Iyer, V. Tassell, A. Polli, K. D. Wilner and P. A. Janne (2013). "Crizotinib versus chemotherapy in advanced ALK-positive lung cancer." N Engl J Med **368**(25): 2385-2394.

Shen, F., Z. Hu, J. Goswami and S. L. Gaffen (2006). "Identification of common transcriptional regulatory elements in interleukin-17 target genes." J Biol Chem **281**(34): 24138-24148.

Shide, K., T. Kameda, H. Shimoda, T. Yamaji, H. Abe, A. Kamiunten, M. Sekine, T. Hidaka, K. Katayose, Y. Kubuki, S. Yamamoto, T. Miike, H. Iwakiri, S. Hasuike, K. Nagata, K. Marutsuka, A. Iwama, T. Matsuda, A. Kitanaka and K. Shimoda (2012). "TET2 is essential for survival and hematopoietic stem cell homeostasis." Leukemia **26**(10): 2216-2223.

Simon, A., M. Peoch, P. Casassus, E. Deconinck, P. Colombat, B. Desablens, O. Tournilhac, H. Eghbali, C. Foussard, J. Jaubert, J. P. Vilque, J. F. Rossi, V. Lucas, V. Delwail, A. Thyss, F. Maloisel, N. Milpied, S. le Gouill, T. Lamy and R. Gressin (2010). "Upfront VIP-reinforced-ABVD (VIP-rABVD) is not superior to CHOP/21 in newly diagnosed peripheral T cell lymphoma. Results of the randomized phase III trial GOELAMS-LTP95." Br J Haematol **151**(2): 159-166.

Smale, S. T. (2012). "Dimer-specific regulatory mechanisms within the NF-kappaB family of transcription factors." Immunol Rev **246**(1): 193-204.

Smith-Garvin, J. E., G. A. Koretzky and M. S. Jordan (2009). "T cell activation." Annu Rev Immunol **27**: 591-619.

Sonder, S. U., S. Saret, W. Tang, D. E. Sturdevant, S. F. Porcella and U. Siebenlist (2011). "IL-17-induced NF-kappaB activation via CIKS/Act1: physiologic significance and signaling mechanisms." J Biol Chem **286**(15): 12881-12890.

Staal, J., Y. Driege, T. Bekaert, A. Demeyer, D. Muyllaert, P. Van Damme, K. Gevaert and R. Beyaert (2011). "T-cell receptor-induced JNK activation requires proteolytic inactivation of CYLD by MALT1." Embo j **30**(9): 1742-1752.

Staudt, L. M. and S. Dave (2005). "The biology of human lymphoid malignancies revealed by gene expression profiling." Adv Immunol **87**: 163-208.

Stein, P. L., H. M. Lee, S. Rich and P. Soriano (1992). "pp59fyn mutant mice display differential signaling in thymocytes and peripheral T cells." Cell **70**(5): 741-750.

Steiner, A., C. R. Harapas, S. L. Masters and S. Davidson (2018). "An Update on Autoinflammatory Diseases: Relopathies." Curr Rheumatol Rep **20**(7): 39.

Streubel, B., I. Simonitsch-Klupp, L. Mullauer, A. Lamprecht, D. Huber, R. Siebert, M. Stolte, F. Trautinger, J. Lukas, A. Puspok, M. Formanek, T. Assanasen, H. K. Muller-Hermelink, L. Cerroni, M. Raderer and A. Chott (2004). "Variable frequencies of MALT lymphoma-associated genetic aberrations in MALT lymphomas of different sites." Leukemia **18**(10): 1722-1726.

Streubel, B., U. Vinatzer, M. Willheim, M. Raderer and A. Chott (2006). "Novel t(5;9)(q33;q22) fuses ITK to SYK in unspecified peripheral T-cell lymphoma." Leukemia **20**(2): 313-318.

Subramanian, A., P. Tamayo, V. K. Mootha, S. Mukherjee, B. L. Ebert, M. A. Gillette, A. Paulovich, S. L. Pomeroy, T. R. Golub, E. S. Lander and J. P. Mesirov (2005). "Gene set enrichment analysis: A knowledge-based approach for interpreting genome-wide expression profiles." Proceedings of the National Academy of Sciences **102**(43): 15545.

Sun, L., L. Deng, C. K. Ea, Z. P. Xia and Z. J. Chen (2004). "The TRAF6 ubiquitin ligase and TAK1 kinase mediate IKK activation by BCL10 and MALT1 in T lymphocytes." Mol Cell **14**(3): 289-301.

Sun, S. C. (2008). "Deubiquitylation and regulation of the immune response." Nat Rev Immunol **8**(7): 501-511.

Susa, M., D. Rohner and S. Bichsel (1996). "Differences in binding of PI 3-kinase to the src-homology domains 2 and 3 of p56 lck and p59 fyn tyrosine kinases." Biochem Biophys Res Commun **220**(3): 729-734.

Swerdlow, S. H., E. Campo, N. L. Harris and S. A. Pileri (2017). WHO Classification of Tumours of Haematopoietic and Lymphoid Tissues, International Agency for Research on Cancer.

Swerdlow, S. H., E. Campo, S. A. Pileri, N. L. Harris, H. Stein, R. Siebert, R. Advani, M. Ghielmini, G. A. Salles, A. D. Zelenetz and E. S. Jaffe (2016). "The 2016 revision of the World Health Organization classification of lymphoid neoplasms." Blood **127**(20): 2375-2390.

Tai, Y. T., C. Acharya, G. An, M. Moschetta, M. Y. Zhong, X. Feng, M. Cea, A. Cagnetta, K. Wen, H. van Eenennaam, A. van Elsas, L. Qiu, P. Richardson, N. Munshi and K. C. Anderson (2016). "APRIL and BCMA promote human multiple myeloma growth and immunosuppression in the bone marrow microenvironment." Blood **127**(25): 3225-3236.

Tam, W., M. Gomez, A. Chadburn, J. W. Lee, W. C. Chan and D. M. Knowles (2006). "Mutational analysis of PRDM1 indicates a tumor-suppressor role in diffuse large B-cell lymphomas." Blood **107**(10): 4090-4100.

Tan, B. T., R. A. Warnke and D. A. Arber (2006). "The frequency of B- and T-cell gene rearrangements and epstein-barr virus in T-cell lymphomas: a comparison between angioimmunoblastic T-cell lymphoma and peripheral T-cell lymphoma, unspecified with and without associated B-cell proliferations." J Mol Diagn **8**(4): 466-475; quiz 527.

Thome, M. and J. Tschopp (2001). "Regulation of lymphocyte proliferation and death by FLIP." Nat Rev Immunol **1**(1): 50-58.

Thompson, P. A., J. S. Gutkind, K. C. Robbins, J. A. Ledbetter and J. B. Bolen (1992). "Identification of distinct populations of PI-3 kinase activity following T-cell activation." Oncogene **7**(4): 719-725.

Timson Gauen, L. K., A. N. Kong, L. E. Samelson and A. S. Shaw (1992). "p59fyn tyrosine kinase associates with multiple T-cell receptor subunits through its unique amino-terminal domain." Mol Cell Biol **12**(12): 5438-5446.

Timson Gauen, L. K., M. E. Linder and A. S. Shaw (1996). "Multiple features of the p59fyn src homology 4 domain define a motif for immune-receptor tyrosine-based activation motif (ITAM) binding and for plasma membrane localization." J Cell Biol **133**(5): 1007-1015.

Toth, C. R., R. F. Hostutler, A. S. Baldwin, Jr. and T. P. Bender (1995). "Members of the nuclear factor kappa B family transactivate the murine c-myb gene." J Biol Chem **270**(13): 7661-7671.

Touzeau, C., P. Maciag, M. Amiot and P. Moreau (2018). "Targeting Bcl-2 for the treatment of multiple myeloma." Leukemia **32**(9): 1899-1907.

Troppan, K., S. Hofer, K. Wenzl, M. Lassnig, B. Pursche, E. Steinbauer, M. Wiltgen, B. Zulus, W. Renner, C. Beham-Schmid, A. Deutsch and P. Neumeister (2015). "Frequent down regulation of the tumor suppressor gene a20 in multiple myeloma." PLoS One **10**(4): e0123922.

Tsygankov, A. Y., S. Mahajan, J. E. Fincke and J. B. Bolen (1996). "Specific association of tyrosine-phosphorylated c-Cbl with Fyn tyrosine kinase in T cells." J Biol Chem **271**(43): 27130-27137.

Turner, J. M., M. H. Brodsky, B. A. Irving, S. D. Levin, R. M. Perlmutter and D. R. Littman (1990). "Interaction of the unique N-terminal region of tyrosine kinase p56lck with cytoplasmic domains of CD4 and CD8 is mediated by cysteine motifs." Cell **60**(5): 755-765.

Vallabhapurapu, S. and M. Karin (2009). "Regulation and function of NF-kappaB transcription factors in the immune system." Annu Rev Immunol **27**: 693-733.

Vallois, D., M. P. D. Dobay, R. D. Morin, F. Lemonnier, E. Missiaglia, M. Juilland, J. Iwaszkiewicz, V. Fataccioli, B. Bisig, A. Roberti, J. Grewal, J. Bruneau, B. Fabiani, A. Martin, C. Bonnet, O. Michielin, J.-P. Jais, M. Figeac, O. A. Bernard, M. Delorenzi, C. Haioun, O. Tournilhac, M. Thome, R. D. Gascoyne, P. Gaulard and L. de Leval (2016). "Activating mutations in genes related to TCR signaling in angioimmunoblastic and other follicular helper T-cell–derived lymphomas." Blood **128**(11): 1490-1502.

Vallois, D., A. Dupuy, F. Lemonnier, G. Allen, E. Missiaglia, V. Fataccioli, N. Ortonne, A. Clavert, R. Delarue, M. C. Rousselet, B. Fabiani, F. Llamas-Gutierrez, S. Ogawa, M. Thome, Y. H. Ko, K. Kataoka, P. Gaulard and L. de Leval (2018). "RNA fusions involving CD28 are rare in peripheral T-cell lymphomas and concentrate mainly in those derived from follicular helper T cells." Haematologica **103**(8): e360-e363.

van Oers, N. S., B. Lowin-Kropf, D. Finlay, K. Connolly and A. Weiss (1996). "alpha beta T cell development is abolished in mice lacking both Lck and Fyn protein tyrosine kinases." Immunity **5**(5): 429-436.

Vasmatzis, G., S. H. Johnson, R. A. Knudson, R. P. Ketterling, E. Braggio, R. Fonseca, D. S. Viswanatha, M. E. Law, N. S. Kip, N. Ozsan, S. K. Grebe, L. A. Frederick, B. W. Eckloff, E. A. Thompson, M. E. Kadin, D. Milosevic, J. C. Porcher, Y. W. Asmann, D. I. Smith, I. V. Kovtun, S. M. Ansell, A. Dogan and A. L. Feldman (2012). "Genome-wide analysis reveals recurrent

structural abnormalities of TP63 and other p53-related genes in peripheral T-cell lymphomas." Blood **120**(11): 2280-2289.

Vose, J., J. Armitage and D. Weisenburger (2008). "International peripheral T-cell and natural killer/T-cell lymphoma study: pathology findings and clinical outcomes." J Clin Oncol **26**(25): 4124-4130.

Waelchli, R., B. Bollbuck, C. Bruns, T. Buhl, J. Eder, R. Feifel, R. Hersperger, P. Janser, L. Revesz, H. G. Zerwes and A. Schlapbach (2006). "Design and preparation of 2-benzamido-pyrimidines as inhibitors of IKK." Bioorg Med Chem Lett **16**(1): 108-112.

Walker, B. A., E. M. Boyle, C. P. Wardell, A. Murison, D. B. Begum, N. M. Dahir, P. Z. Proszek, D. C. Johnson, M. F. Kaiser, L. Melchor, L. I. Aronson, M. Scales, C. Pawlyn, F. Mirabella, J. R. Jones, A. Brioli, A. Mikulasova, D. A. Cairns, W. M. Gregory, A. Quartilho, M. T. Drayson, N. Russell, G. Cook, G. H. Jackson, X. Leleu, F. E. Davies and G. J. Morgan (2015). "Mutational Spectrum, Copy Number Changes, and Outcome: Results of a Sequencing Study of Patients With Newly Diagnosed Myeloma." J Clin Oncol **33**(33): 3911-3920.

Walsh, M. C., J. Lee and Y. Choi (2015). "Tumor necrosis factor receptor- associated factor 6 (TRAF6) regulation of development, function, and homeostasis of the immune system." Immunol Rev **266**(1): 72-92.

Wang, C., T. W. McKeithan, Q. Gong, W. Zhang, A. Bouska, A. Rosenwald, R. D. Gascoyne, X. Wu, J. Wang, Z. Muhammad, B. Jiang, J. Rohr, A. Cannon, C. Steidl, K. Fu, Y. Li, S. Hung, D. D. Weisenburger, T. C. Greiner, L. Smith, G. Ott, E. G. Rogan, L. M. Staudt, J. Vose, J. Iqbal and W. C. Chan (2015). "IDH2R172 mutations define a unique subgroup of patients with angioimmunoblastic T-cell lymphoma." Blood **126**(15): 1741-1752.

Wang, D., Y. You, S. M. Case, L. M. McAllister-Lucas, L. Wang, P. S. DiStefano, G. Nunez, J. Bertin and X. Lin (2002). "A requirement for CARMA1 in TCR-induced NF-kappa B activation." Nat Immunol **3**(9): 830-835.

Wang, T., A. L. Feldman, D. A. Wada, Y. Lu, A. Polk, R. Briski, K. Ristow, T. M. Habermann, D. Thomas, S. C. Ziesmer, L. E. Wellik, T. M. Lanigan, T. E. Witzig, M. R. Pittelkow, N. G. Bailey, A. C. Hristov, M. S. Lim, S. M. Ansell and R. A. Wilcox (2014). "GATA-3 expression identifies a high-risk subset of PTCL, NOS with distinct molecular and clinical features." Blood **123**(19): 3007-3015.

Wang, X., M. B. Werneck, B. G. Wilson, H. J. Kim, M. J. Kluk, C. S. Thom, J. W. Wischhusen, J. A. Evans, J. L. Jesneck, P. Nguyen, C. G. Sansam, H. Cantor and C. W. Roberts (2011). "TCR-dependent transformation of mature memory phenotype T cells in mice." J Clin Invest **121**(10): 3834-3845.

Wang, Y., N. Wu, D. Liu and Y. Jin (2017). "Recurrent Fusion Genes in Leukemia: An Attractive Target for Diagnosis and Treatment." Curr Genomics **18**(5): 378-384.

Wary, K. K., A. Mariotti, C. Zurzolo and F. G. Giancotti (1998). "A requirement for caveolin-1 and associated kinase Fyn in integrin signaling and anchorage-dependent cell growth." Cell **94**(5): 625-634.

Watatani, Y., Y. Sato, H. Miyoshi, K. Sakamoto, K. Nishida, Y. Gion, Y. Nagata, Y. Shiraishi, K. Chiba, H. Tanaka, L. Zhao, Y. Ochi, Y. Takeuchi, J. Takeda, H. Ueno, Y. Kogure, Y. Shiozawa, N. Kakiuchi, T. Yoshizato, M. M. Nakagawa, Y. Nanya, K. Yoshida, H. Makishima, M. Sanada, M. Sakata-Yanagimoto, S. Chiba, R. Matsuoka, M. Noguchi, N. Hiramoto, T. Ishikawa, J. Kitagawa, N. Nakamura, H. Tsurumi, T. Miyazaki, Y. Kito, S. Miyano, K. Shimoda, K. Takeuchi, K. Ohshima,

T. Yoshino, S. Ogawa and K. Kataoka (2019). "Molecular heterogeneity in peripheral T-cell lymphoma, not otherwise specified revealed by comprehensive genetic profiling." Leukemia.

Weisenburger, D. D., K. J. Savage, N. L. Harris, R. D. Gascoyne, E. S. Jaffe, K. A. MacLennan, T. Rüdiger, S. Pileri, S. Nakamura, B. Nathwani, E. Campo, F. Berger, B. Coiffier, W.-S. Kim, H. Holte, M. Federico, W. Y. Au, K. Tobinai, J. O. Armitage and J. M. Vose (2011a). "Peripheral T-cell lymphoma, not otherwise specified: a report of 340 cases from the International Peripheral T-cell Lymphoma Project." Blood **117**(12): 3402-3408.

Weisenburger, D. D., K. J. Savage, N. L. Harris, R. D. Gascoyne, E. S. Jaffe, K. A. MacLennan, T. Rudiger, S. Pileri, S. Nakamura, B. Nathwani, E. Campo, F. Berger, B. Coiffier, W. S. Kim, H. Holte, M. Federico, W. Y. Au, K. Tobinai, J. O. Armitage and J. M. Vose (2011b). "Peripheral T-cell lymphoma, not otherwise specified: a report of 340 cases from the International Peripheral T-cell Lymphoma Project." Blood **117**(12): 3402-3408.

Wilcox, R. A. (2016). "A three-signal model of T-cell lymphoma pathogenesis." Am J Hematol **91**(1): 113-122.

Willis, T. G., D. M. Jadayel, M. Q. Du, H. Peng, A. R. Perry, M. Abdul-Rauf, H. Price, L. Karran, O. Majekodunmi, I. Wlodarska, L. Pan, T. Crook, R. Hamoudi, P. G. Isaacson and M. J. Dyer (1999). "Bcl10 is involved in t(1;14)(p22;q32) of MALT B cell lymphoma and mutated in multiple tumor types." Cell **96**(1): 35-45.

Wilson, W. H., R. M. Young, R. Schmitz, Y. Yang, S. Pittaluga, G. Wright, C. J. Lih, P. M. Williams, A. L. Shaffer, J. Gerecitano, S. de Vos, A. Goy, V. P. Kenkre, P. M. Barr, K. A. Blum, A. Shustov, R. Advani, N. H. Fowler, J. M. Vose, R. L. Elstrom, T. M. Habermann, J. C. Barrientos, J. McGreivy, M. Fardis, B. Y. Chang, F. Clow, B. Munneke, D. Moussa, D. M. Beaupre and L. M. Staudt (2015). "Targeting B cell receptor signaling with ibrutinib in diffuse large B cell lymphoma." Nat Med **21**(8): 922-926.

Wolven, A., H. Okamura, Y. Rosenblatt and M. D. Resh (1997). "Palmitoylation of p59fyn is reversible and sufficient for plasma membrane association." Mol Biol Cell **8**(6): 1159-1173.

Wotherspoon, A. C., C. Doglioni, T. C. Diss, L. Pan, A. Moschini, M. de Boni and P. G. Isaacson (1993). "Regression of primary low-grade B-cell gastric lymphoma of mucosa-associated lymphoid tissue type after eradication of Helicobacter pylori." Lancet **342**(8871): 575-577.

Xie, M., C. Lu, J. Wang, M. D. McLellan, K. J. Johnson, M. C. Wendl, J. F. McMichael, H. K. Schmidt, V. Yellapantula, C. A. Miller, B. A. Ozenberger, J. S. Welch, D. C. Link, M. J. Walter, E. R. Mardis, J. F. Dipersio, F. Chen, R. K. Wilson, T. J. Ley and L. Ding (2014). "Age-related mutations associated with clonal hematopoietic expansion and malignancies." Nat Med **20**(12): 1472-1478.

Yamagishi, M., K. Nakano, A. Miyake, T. Yamochi, Y. Kagami, A. Tsutsumi, Y. Matsuda, A. Sato-Otsubo, S. Muto, A. Utsunomiya, K. Yamaguchi, K. Uchimaru, S. Ogawa and T. Watanabe (2012). "Polycomb-mediated loss of miR-31 activates NIK-dependent NF-kappaB pathway in adult T cell leukemia and other cancers." Cancer Cell **21**(1): 121-135.

Yang, J., X. Liao, M. K. Agarwal, L. Barnes, P. E. Auron and G. R. Stark (2007). "Unphosphorylated STAT3 accumulates in response to IL-6 and activates transcription by binding to NFkappaB." Genes Dev **21**(11): 1396-1408.

Yoo, H. Y., P. Kim, W. S. Kim, S. H. Lee, S. Kim, S. Y. Kang, H. Y. Jang, J. E. Lee, J. Kim, S. J. Kim, Y. H. Ko and S. Lee (2016a). "Author reply to Comment on: Frequent CTLA4-CD28 gene fusion in diverse types of T-cell lymphoma, by Yoo et al." Haematologica **101**(6): e271.

Yoo, H. Y., P. Kim, W. S. Kim, S. H. Lee, S. Kim, S. Y. Kang, H. Y. Jang, J. E. Lee, J. Kim, S. J. Kim, Y. H. Ko and S. Lee (2016b). "Frequent CTLA4-CD28 gene fusion in diverse types of T-cell lymphoma." Haematologica **101**(6): 757-763.

Yoo, H. Y., M. K. Sung, S. H. Lee, S. Kim, H. Lee, S. Park, S. C. Kim, B. Lee, K. Rho, J. E. Lee, K. H. Cho, W. Kim, H. Ju, J. Kim, S. J. Kim, W. S. Kim, S. Lee and Y. H. Ko (2014). "A recurrent inactivating mutation in RHOA GTPase in angioimmunoblastic T cell lymphoma." Nat Genet **46**(4): 371-375.

Young, R. M., A. L. Shaffer, 3rd, J. D. Phelan and L. M. Staudt (2015). "B-cell receptor signaling in diffuse large B-cell lymphoma." Semin Hematol **52**(2): 77-85.

Zamoyska, R., A. Basson, A. Filby, G. Legname, M. Lovatt and B. Seddon (2003). "The influence of the src-family kinases, Lck and Fyn, on T cell differentiation, survival and activation." Immunol Rev **191**: 107-118.

Zhang, B., C. Liu, W. Qian, Y. Han, X. Li and J. Deng (2013). "Crystal structure of IL-17 receptor B SEFIR domain." J Immunol **190**(5): 2320-2326.

Zhang, L. L., J. Y. Wei, L. Wang, S. L. Huang and J. L. Chen (2017a). "Human T-cell lymphotropic virus type 1 and its oncogenesis." Acta Pharmacol Sin **38**(8): 1093-1103.

Zhang, Q., M. J. Lenardo and D. Baltimore (2017b). "30 Years of NF-κB: A Blossoming of Relevance to Human Pathobiology." Cell **168**(1-2): 37-57.

Zhang, Q., R. Siebert, M. Yan, B. Hinzmann, X. Cui, L. Xue, K. M. Rakestraw, C. W. Naeve, G. Beckmann, D. D. Weisenburger, W. G. Sanger, H. Nowotny, M. Vesely, E. Callet-Bauchu, G. Salles, V. M. Dixit, A. Rosenthal, B. Schlegelberger and S. W. Morris (1999). "Inactivating mutations and overexpression of BCL10, a caspase recruitment domain-containing gene, in MALT lymphoma with t(1;14)(p22;q32)." Nat Genet **22**(1): 63-68.

Zhang, S. and D. Yu (2012). "Targeting Src family kinases in anti-cancer therapies: turning promise into triumph." Trends Pharmacol Sci **33**(3): 122-128.

Zhou, H., M. Q. Du and V. M. Dixit (2005). "Constitutive NF-kappaB activation by the t(11;18)(q21;q21) product in MALT lymphoma is linked to deregulated ubiquitin ligase activity." Cancer Cell **7**(5): 425-431.

Zhou, H., I. Wertz, K. O'Rourke, M. Ultsch, S. Seshagiri, M. Eby, W. Xiao and V. M. Dixit (2004). "Bcl10 activates the NF-kappaB pathway through ubiquitination of NEMO." Nature **427**(6970): 167-171.

Zing, N. P. C., T. Fischer, J. Zain, M. Federico and S. T. Rosen (2018). "Peripheral T-Cell Lymphomas: Incorporating New Developments in Diagnostics, Prognostication, and Treatment Into Clinical Practice-PART 1: PTCL-NOS, FTCL, AITL, ALCL." Oncology (Williston Park) **32**(7): e74-e82.

zur Hausen, J. D., P. Burn and K. E. Amrein (1997). "Co-localization of Fyn with CD3 complex, CD45 or CD28 depends on different mechanisms." Eur J Immunol **27**(10): 2643-2649.